

Dissertation zur Erlangung des Doktorgrades
der Fakultät für Chemie und Pharmazie
der Ludwig-Maximilians-Universität München



"Acid-labile surface modification of
four-arm oligoaminoamide pDNA polyplexes
balances shielding and gene transfer activity
in vitro and *in vivo*"

Linda Beckert
aus
Dresden, Deutschland

2016

Erklärung

Diese Dissertation wurde im Sinne von § 7 der Promotionsordnung vom 28. November 2011 von Herrn Prof. Dr. Ernst Wagner betreut.

Eidesstattliche Versicherung

Diese Dissertation wurde eigenständig und ohne unerlaubte Hilfe erarbeitet.

München, 05.07.2016

.....
Linda Beckert

Dissertation eingereicht am: 05.07.2016

1. Gutachter: Prof. Dr. Ernst Wagner

2. Gutachter: Prof. Dr. Olivia Merkel

Mündliche Prüfung am: 19.01.2017

Meiner Familie

Table of content

1. Introduction	11
1.1. Gene therapy.....	11
1.2. Challenges in DNA delivery via non-viral carriers.....	12
1.3. Design of bioresponsive non-viral carriers for gene delivery	15
1.3.1. Bioresponsive stability of non-viral carriers	15
1.3.2. Bioresponsive shielding of the surface of non-viral carriers	19
1.3.3. Targeting of non-viral carriers	22
1.4. Aims of the thesis	24
2. Materials and Methods.....	26
2.1. Materials.....	26
2.1.1. Reagents and Solvents	26
2.1.2. Equipment for solid-phase assisted peptide synthesis (SPPS)	30
2.1.3. Cell culture	30
2.1.4. Nucleic acids	31
2.2. Methods.....	31
2.2.1. Synthesis of 3-(azidomethyl)-4-methyl-2,5-furandione (AzMMMan)	31
2.2.2. Synthesis of Fmoc/Boc-protected succinyl-pentaethylene hexamine (Fmoc/Boc-Sph).....	32
2.2.3. Solid-phase assisted peptide synthesis	32
2.2.3.1. Loading of resins	33
2.2.3.2. General procedure of SPPS	34
2.2.3.3. Cleavage of oligomers and targeting ligand.....	35
2.2.3.4. Kaiser Test.....	36
2.2.4. Synthesis of shielding polymers	36
2.2.4.1. Synthesis of monovalent AzMMMan-PEG(5000)-MeO.....	36

2.2.4.2. Synthesis of bifunctional FoIA-PEG(5000)-AzMMMan and bifunctional FoIA-PEG(5000)-NHS via FoIA-PEG ₆ -cysteamine	36
2.2.4.3. Synthesis of bifunctional FoIA-PEG(5000)-AzMMMan and bifunctional FoIA-PEG(5000)-NHS via NHS-FoIA.....	37
2.2.4.4. Synthesis of monovalent pHPMA-AzMMMan and monovalent pHPMA-TT	38
2.2.4.5. Synthesis of multivalent pHPMA-AzMMMan and multivalent pHPMA-TT	38
2.2.4.6. Polyplex formation	38
2.2.4.7. Measurement of particle size and zeta potential.....	39
2.2.4.8. Agarose gel shift assay.....	39
2.2.4.9. Ethidium bromide exclusion assay (EtBr assay)	39
2.2.4.10. Oligomer buffering capacity	39
2.2.4.11. Cell culture.....	40
2.2.4.12. Luciferase gene expression	40
2.2.4.13. Cell viability assay (MTT).....	41
2.2.4.14. Cellular uptake: flow cytometry studies.....	41
2.2.4.15. Intracellular localization: laser scanning microscopy (LSM).....	42
2.2.4.16. <i>In vivo</i> delivery and expression.....	42
2.2.4.17. Statistical analysis.....	42
3. Results.....	43
3.1. Designing new sequence-defined oligomers: evaluation of stabilizing effects of lysine residues on DNA polyplexes	43
3.1.1. Biophysical characterization of oligomers concerning DNA binding ability, particle size, zeta potential and buffering capacity	47
3.1.2. <i>In vitro</i> characterization of DNA polyplexes.....	52
3.2. Design and biophysical characterization of shielded polyplexes	54
3.2.1. Biophysical characterization of shielded polyplexes.....	55
3.2.2. <i>In vitro</i> characterization of shielded polyplexes	62

3.2.3. <i>In vivo</i> evaluation of shielded polyplexes	66
3.3. FcA receptor-directed pCMVL/784 polyplexes for gene transfer <i>in vitro</i>	68
3.3.1. Synthesis of the post-PEGylation reagents FcA-PEG(5000)-AzMMMan and FcA-PEG(5000)-NHS	69
3.3.2. Biophysical characterization of FcA-targeted, stably or pH-sensitively shielded pCMVL/784 polyplexes	74
3.3.3. <i>In vitro</i> characterization of FcA-targeted, stably or pH-sensitively shielded pCMVL/784 polyplexes	77
4. Discussion.....	80
4.1. Evaluation of new sequence-defined oligomers concerning stabilizing effects of lysine residues on DNA polyplexes	80
4.2. Evaluation of pH-sensitively or stably modified PEG or pHPMA-shielded DNA polyplexes	83
4.3. Evaluation of FcA-targeted pH-sensitively or stably PEGylated DNA polyplexes	86
5. Summary.....	90
6. References.....	92
7. Appendix	105
7.1. Abbreviations.....	105
7.2. Analytical data	107
7.3. Summarized spectral data.....	108
7.4. Publication	110
7.5. Poster presentation	110
8. Acknowledgements.....	111

Introduction

1. Introduction

1.1. Gene therapy

Gene therapy is a fast-growing field of medical research aiming at the introduction of therapeutic genes in the human body to repair malfunctions. In this concept, a disease-causing gene is silenced or restored making gene therapy an interesting alternative for the treatment of gene-associated defects like cancer or inflammatory diseases [1-3]. Genes are carriers of the genetic information, which provide the biological code that determines the specific functions of a cell. The origins of gene therapy can be traced back to the science of genetics. Researchers like Francis Crick established this branch of biology upon the realization that: "Almost all aspects of life are engineered at the molecular level, and without understanding molecules we can only have a very sketchy understanding of life itself." Consequently, major milestones in understanding the basis of life were the elucidation of the mechanisms of genetic transmission [4], the identification of the genetic material as DNA [5] and the clarification of the DNA structure [6]. Those findings enabled the first concept of gene therapy proposed by Friedman and Roblin in 1972 [7]. It was preceded by the development of new sequencing technologies and the deciphering of the human genome [8-10] that enabled the identification of different gene-associated diseases [11-13]. However, it took more than 16 years and several drawbacks for the approval of the first gene therapy trial in 1990 by the US Food and Drugs Administration (FDA) [14, 15]. This trial focused on the treatment of the severe combined immune deficiency (SCID), a monogenetic disorder characterized by adenosine deaminase deficiency [16]. Four years later cancer gene therapy was introduced into the clinical research. The first FDA-approved cancer trial was performed with a carrier expressing antisense IGF-I RNA aiming at the treatment of glioblastoma multiform. This strategy was efficient due to a strong immune and apoptotic reaction as a result of the anti-tumor mechanism of IGF-I antisense [17]. However, gene therapy research was halted in the USA and EU owing to an excessive immune reaction in one patient causing his death in 1999 [15] and the development of leukemia-like illness of two other patients in 2002 [18].

Nevertheless, the first gene medicine was authorized by the European Commission in 2012. The launch of Glybera® (alipogene tiparvovec) marked the first breakthrough for a successful application of therapeutic genes as medical agent [19].

Introduction

Irrespective of the great potential, the main challenge for the implementation of gene therapeutics from bench to bedside is the achievement of highly efficient, safe and target-specific gene delivery carriers [20]. Regarding efficiency and specificity, nature offers a good example, i.e. viruses. Currently viral carriers are the most investigated gene delivery systems, resulting in more than 1800 clinical trials worldwide within 20 years since the first approved trial in 1990 [21-24]. As an alternative to virus-based carriers, non-viral gene carriers have been developed [25]. Non-viral approaches include physical methods such as microinjection [26], electroporation [27, 28], gene gun [29] or magnetofection [30] as well as chemical methods enabling "lipoplex" or "polyplex" formation [31]. In case of chemical methods, complex formation is facilitated by electrostatic interaction between the negatively charged nucleic acid and positively charged lipids or polymers. When designing non-viral gene carriers a high structure flexibility is ensured beyond the limitation of natural occurring building blocks offering the opportunity of tailor-made properties. Moreover, those carriers can be produced in large scale at low cost. Together with the lack of immunogenicity and the lower toxicity compared to the viral counterparts, non-viral vectors represent an attractive alternative for gene delivery. Nevertheless, non-viral carriers are generally considered as less efficient in gene transfer with gene expression levels beyond clinical relevance. In order to refine non-viral carriers significant efforts should be made in the clarification of the delivery pathway as well as in the elucidation of individual obstacles faced by the carrier.

1.2. Challenges in DNA delivery via non-viral carriers

Non-viral gene delivery still finds itself hampered by the lack of high efficiency and specific targeting, in particular in therapeutic treatment regimen that do not cope with local administration. When considering chemical methods, such as polyplexes (Fig. 1.1.A), numerous extracellular (Fig. 1.1.B) and intracellular (Fig. 1.1.C) barriers need to be overcome until the therapeutic nucleic acid reaches its target.

Introduction

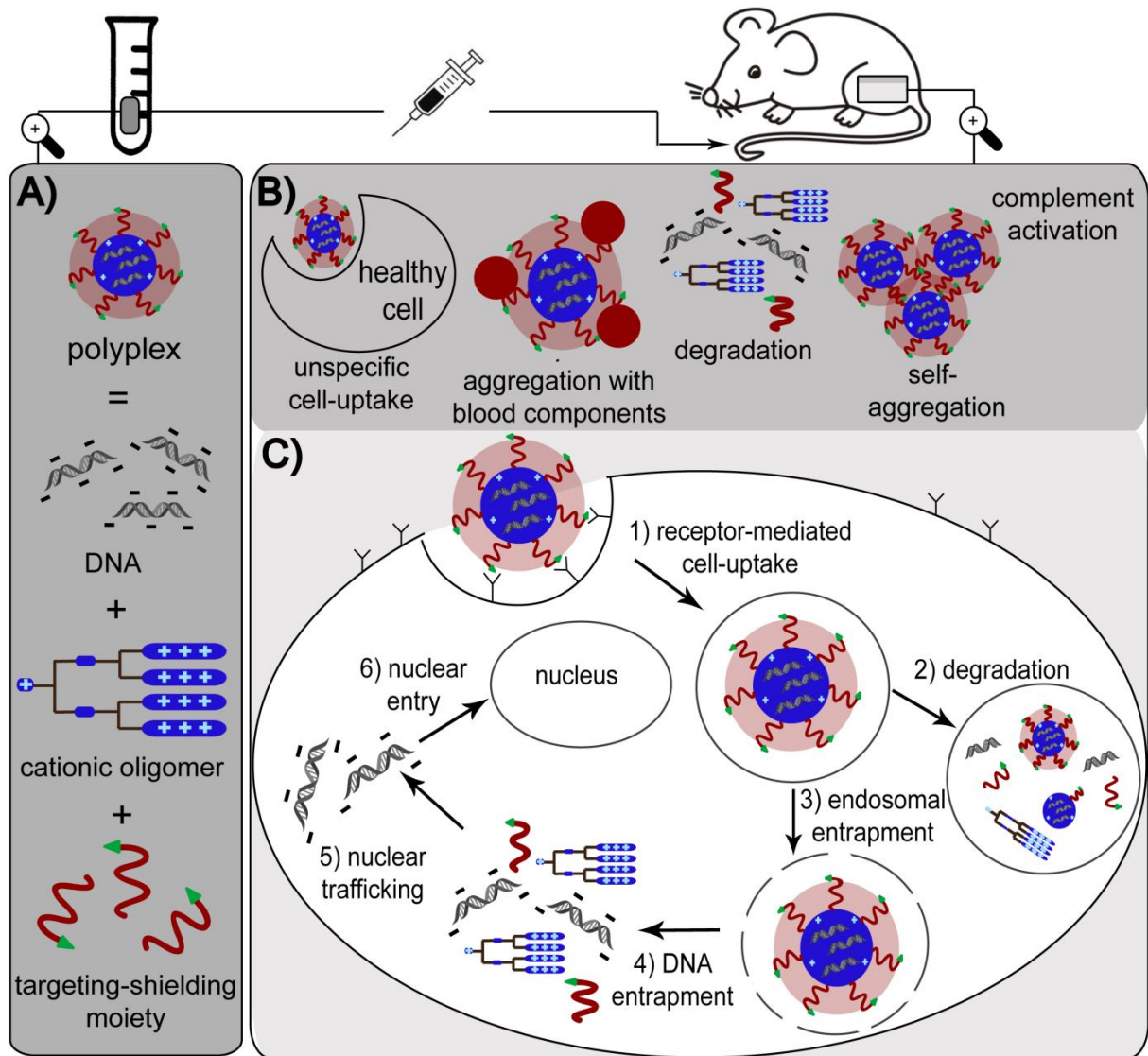


Figure 1.1. Illustration of major barriers faced by non-viral DNA-based gene delivery carriers. A) DNA is condensed by a polycation, to form stable polyplexes. Additionally, the surface of the polyplexes is modified by a targeting-shielding moiety. B) After *i.v.* administration the polyplex faces various extracellular barriers such as unspecific cell-uptake, aggregation by blood components, degradation, self-aggregation and complement activation. C) After cellular uptake via receptor-mediated endocytosis, polyplexes have to overcome various intracellular barriers such as degradation, endosomal entrapment, DNA entrapment within the polyplex, nuclear trafficking and nuclear entry to accumulate in the nucleus.

Only in rare cases the direct delivery of naked nucleic acids without a carrier can be applied with reasonable efficiency such as genetic vaccines [32, 33]. Most likely the anionic charge together with the large size and vulnerability toward nucleases restricts successful naked nucleic acid transfer. In this regard, non-viral carriers were

Introduction

developed in order to protect the nucleic acid in the extracellular environment and facilitate the transport within the intracellular space to its target. Figure 1.1.A illustrates the formation of polyplexes comprising of a positively charged polymer, also referred as polycation, a negatively charged DNA and a shielding-targeting moiety attached to the surface of the formed polyplexes.

Up to date, nearly two thirds of gene therapy clinical trials worldwide have addressed several types of cancer inter alia gliomas [34], liver [35] and pancreatic [36] cancer. The success in cancer gene therapy strongly depends on polyplex properties such as size and charge, which have a significant influence on the pharmacokinetics, biodistribution and intratumoral penetration of polyplexes after intravenous (*i.v.*) administration. For instance polyplexes with a mean size of 10-100nm are of particular interest for tumor specific targeting. The small size enables particle passage through capillary gaps within tumor vasculatures. As a consequence of the fast tumor cell growth, the newly formed tumor cells differ in their anatomical and pathophysiological characteristics from normal tissue. Thus, vascular permeability is enhanced facilitating an increased transport rate and accumulation of polyplexes into tumor tissue. This phenomenon is referred to as "enhanced permeability and retention (EPR) effect" of polyplexes in solid tumors [37].

The positive surface charge of the polyplexes facilitates cellular uptake but also mediates self-aggregation of the polyplexes, unspecific cell-uptake and binding to extracellular components such as the complement system [38-40]. As a part of the immune system the complement system enhances the clearance of pathogens from the organism. As a consequence of the activation of the complement system by polyplexes, the opsonization of latter by the C3 complement promotes the clearance by the reticuloendothelial system (RES) [38]. Additionally, the positive surface charge can lead to aggregation of polyplexes with blood components as well as degradation by enzymes (Fig. 1.1.B).

Once the polyplex has reached its target cell, it faces several obstacles: crossing the plasma membrane, degradation within the endolysosomal vesicles, endosomal entrapment, nuclear trafficking and the mediation of nuclear entry of the payload (Fig. 1.1.C). Successful gene delivery strongly depends on the ability of non-viral carriers to enable efficient cell-uptake. On the one hand, this can be achieved by the positive surface charge of the polyplexes mediating the association with the negatively

Introduction

charged plasma membrane. On the other hand, cell entry can be enabled by specific interactions between ligands and receptors. In particular, receptor-mediated endocytosis is the major cell entry pathway [41, 42]. Thus, after the polyplex was taken up via endocytosis, it then has to circumvent endosomal entrapment before it is degraded within the endolysosomal vesicles. This degradation is caused by the progressively acidification of polyplexes during the endocytic pathway [43-45]. Therefore, carriers have been designed with a strong buffering capacity within the pH range from 5.0 to 7.4 enabling endosomal release also referred to as "proton sponge" effect [46]. Here, the protonation of the basic polymer leads to an influx of chloride counter-ions followed by water, which triggers the swelling of the endosome and causes the rupture of the endosomal membrane.

After the polyplex has been successfully released into the cytoplasm, nuclear trafficking presents another barrier to successful gene delivery. On the one hand, nucleases present in the cytoplasm are a threat to the integrity of polyplexes. On the other hand, the decreased mobility of macromolecules and the arbitrary release from the endosome within the cytoplasm hinders polyplex diffusion toward the nucleus [47]. In addition, the nucleic acid has yet to be released from the non-viral carrier. In most cases it remains unclear whether this is achieved just after endosomal release or just before the nucleic acid enters the nucleus [48].

Eventually, the nuclear envelope is the last barrier that has to be overcome by the DNA. The nuclear envelope consists of two chemically distinct lipid bilayers, the inner and outer nuclear membrane, separated by the perinuclear space. Nuclear pore complexes stretch the nuclear envelope and enable active transport of macromolecules from the cytoplasm to the nucleus. However, the upper size limit of nuclear pores (around 25nm) makes it unlikely that standard carriers such as polyethylenimine (PEI), which forms polyplexes in a size range between 50-100nm, are able to cross the nuclear envelope. Consequently, only 1-10% of DNA is found within the nucleus depending on applied DNA dose, cell type or detection method. It is assumed that passive nuclear uptake in proliferating cells is the main administration route of DNA into the nucleus enabled by the breakdown of the nuclear envelope [47].

Considering the multistep delivery process and the described barriers hampering efficient gene transfer, specific strategies have to be developed to enhance gene

Introduction

delivery efficiency. Ideally, the carrier is suitable for transporting different types of nucleic acids and able to self-assemble with the nucleic acid. Additionally, it exhibits sufficient polyplex stability and solubility. Moreover, the carrier should have few toxic properties and induces no immune response. Therefore, non-viral carriers capable of changing their properties e.g. charge and conformation, upon environmental changes in a dynamic bioresponsive behavior have been designed. Additionally, shielding agents are incorporated within the polyplex surface to reduce unspecific interactions and nucleic acid degradation during blood circulation. Furthermore, targeting ligands are attached to polyplexes mediating efficient cell targeting and intracellular uptake. Moreover, linker molecules sensitive to changes of environmental parameters such as pH [49, 50], enzymatic activity [51, 52] or redox potential [53] are introduced between the shielding moiety and the surface of the polyplex to enable membrane fusion and endosomal release, respectively. Those strategies have shown reasonable success in preventing particle aggregation, lowering carrier toxicity, increasing polyplex circulation time and improving systemic targeted gene transfer. However, future developments should focus on further optimization of non-viral gene delivery carriers to achieve gene expression levels comparable of those obtained by the use of their viral counterparts. The following sections present an overview of different strategies for the design of functional polymers for polyplex formation with a focus on three key functions: polyplex stability, polyplex surface shielding and targeting ligands.

1.3. Design of bioresponsive non-viral carriers for gene delivery

1.3.1. Bioresponsive stability of non-viral carriers

Successful gene delivery requires stable binding of nucleic acid molecules to non-viral carriers to avoid degradation and premature release within the extracellular environment. Moreover, cellular uptake is only possible if the polyplex remains stable and intact during the passage through the extracellular space. However, as the polyplex reaches its site of action stability should be weakened to an extent that nucleic acid is released. In literature this conflicting effect of polyplex stability is referred to as “package and release dilemma” [54]. Thus, it still remains an enormous challenge to design non-viral carriers, which provide sufficient protection and efficient nucleic acid release. While the optimization of carrier properties like charge density

Introduction

and molecular weight has shown to increase polyplex stability, it did not solve the "release dilemma". Therefore, the controlled dissociation of polyplexes triggered by changes in the microenvironmental parameters such as pH, redox potential, light or temperature have shown to be promising approaches. Various barriers in the polyplex delivery pathway have been elucidated enabling structure-activity relationship studies. This in turn provides valuable information for the design of non-viral carriers that achieve an optimal balance between nucleic acid protection and release.

Based on those findings, we have developed and established a library of sequence-defined nucleic acid carriers comprising natural and artificial amino acids. Standard solid-phase assisted peptide synthesis (SPPS) was applied for the assembly of the carriers. This precise synthesis strategy offers the opportunity to produce carriers of defined architectures and different incorporated modules and functionalities. Using this library, detailed structure-activity relationship studies were performed, identifying essential structural requirements for non-viral carriers for enhanced gene transfer efficiency. For instance, Salcher *et al.* synthesized sequence-defined carriers comprising different artificial amino acids within a four-arm structure. The carriers were evaluated regarding sufficient polyplex stability and efficient nucleic acid release after reaching its target. In particular, the diaminoethane units of the artificial amino acids showed to increase nucleic acid binding and trigger endosomal release. To find a compromise between nucleic acid protection and release, the effect of variations within the molecular weight and length of the building blocks has been evaluated. In this regard, three different building blocks containing either a triethylene tetramine (Gtt), a tetraethylene pentamine (Stp) or a pentaethylene hexamine (Sph) are introduced within the sequence. Each building block consists of two terminal amide linked nitrogens and two (Gtt), three (Stp) or four (Sph) protonable secondary amine nitrogens. In addition, the effect of 2-5 building blocks per oligomer chain is considered. Here, oligomers beyond three building blocks per oligomer chain differed only slight in their ability to bind DNA and mediate efficient transfection efficiency. However, DNA binding ability and transfection efficiency is enhanced in case of building blocks comprised of a higher number of protonable secondary amine nitrogens. Thus, building blocks can be ranked concerning their ability to bind DNA and form stable polyplexes in the distinct order Sph>Stp>Gtt [55]. Furthermore the impact of the different building blocks on mediating sufficient endosomal release was

Introduction

evaluated. Consequently, carriers with a strong buffering capacity within the pH range from 5.0 to 7.4 have been shown to overcome the endosomal entrapment by the "proton sponge" effect. Oligomers containing building blocks of even-numbered protonable secondary amines like Gtt and Sph mediated significantly higher endosomal buffering compared to the odd-numbered building block Stp [56].

In addition, polyplex stability has shown to increase after a hydrophobic dioleic motif, cysteine residue(s) and/or an oligotyrosine motif were incorporated within the sequence of the carrier. For instance, the introduction of fatty acids in a t-shaped oligomer exhibit higher polyplexes stability due to hydrophobic interactions [57, 58]. Another study showed, that the incorporation of a oligotyrosine motif and the combination with another stabilizing component increased DNA polyplex stability and transfection efficiency by 100-fold [59]. Moreover, the introduction of cysteines within the structure of a sequence-defined oligomer led to the formation of cross-linkages. As a consequence, the rather small size of the synthesized oligomer ($M_w \leq 3100\text{Da}$) is compensated and premature nucleic acid release into serum is avoided.

However, at its target site, the polyplex has to disassemble to release nucleic acid. This can be triggered by the degradation of the oligomer [60], competitive displacement of nucleic acids by other polyanions such as intracellular RNA [61] or reduction of cleavable bonds between the nucleic acid and the oligomer [62]. Consequently, non-viral carriers have been developed containing disulfide bonds to enable a redox-responsive controlled release of nucleic acid. Those carriers are capable of distinguishing between extra- and intracellular cytosolic locations based on differences in the respective redox potentials. Hence, the increased polyplex stability provided by cross-links due to disulfide formation is beneficial during extracellular delivery phase and intracellular uptake. After entering the cytosolic environment disulfide bonds are reduced facilitating efficient cargo release [63, 64]. Additionally, the oligocationic carrier is disassembled into smaller, usually non-toxic fragments.

In sum, non-viral carriers with an improved balance of polyplex stability and the ability to disassemble at the target site are favorable for efficient *in vitro* and *in vivo* gene delivery.

Introduction

1.3.2. Bioresponsive shielding of the surface of non-viral carriers

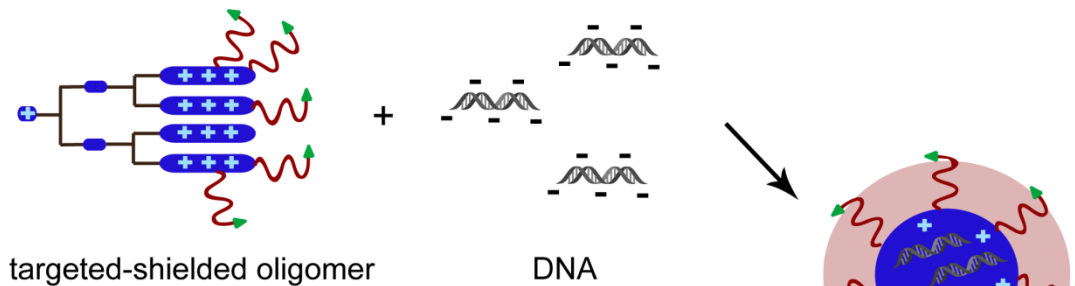
The formation of highly positively charged polyplexes prevents on one the hand particle aggregation, but on the other it causes non-specific interactions with negatively charged groups of plasma proteins, vessel endothelium and blood cells after intravenous administration. Adsorption of blood components to the polyplex surface leads to the formation of large aggregates which primarily accumulate in the lung [65] due to the physical retention of large aggregates in narrow pulmonary capillaries. Additionally, those complexes are recognized by the immune system and are rapidly eliminated through RES [66, 67]. These facts including significant toxicity limit the use and efficiency of simple polycationic polyplexes, and herein steric stabilization and protection of the complexes is mandatory for systemic application. In this regard, a technical breakthrough was the modification of the particle surface with hydrophilic polymers. Those polymers function as 'shielding agents' to mask surface charge and provide steric protection of the delivery system resulting in a prolonged blood circulation [68]. Moreover, unspecific cell-uptake is reduced and polyplex accumulation within solid tumors is increased due to the EPR effect [69]. Additionally, the surface modification of polyplexes by shielding agents significantly decreases particle-particle interaction and promotes complex stability [70].

The most prominent example of a shielding polymer is polyethylene glycol (PEG) which has been attached to several FDA-approved pharmaceuticals to improve the delivery profile [71]. The broad scope of application is based on its low toxicity as well as its non-immunogenicity. PEG is a highly hydrophilic, uncharged, widely soluble polymer and has been used in different structures (branched, star, comb, linear) and sizes. Regarding non-viral gene delivery, PEG has been successfully attached to multiple carriers demonstrating enhanced gene delivery efficiency *in vitro* and *in vivo* [72, 73]. Similar findings were made for poly(N-(2-hydroxypropyl)methacryl-amide) (pHPMA) after the attachment to the surface of non-viral gene carriers to mask surface charge [74, 75]. Likewise, pHPMA is a highly hydrophilic, non-toxic, non-immunogenic polymer available in different sizes and structures (monovalent and multivalent). Despite the fact, that several formulations have entered clinical trials, up to date no FDA-approved pHPMA based pharmaceutical has launched the market [76].

Introduction

A common concept for the attachment of the shielding polymer to the polyplex surface is the "pre-PEGylation" concept (Fig. 1.2.A) [77]. It relies on the modification of a cationic carrier with the shielding polymer before nucleic acid complex formation. "Post-PEGylation" is another concept applied for the formation of shielded polyplexes. Thereby, DNA polyplexes are formed prior to the addition of the shielding polymer (Fig. 1.2.B) [78].

A) Pre-PEGylation



B) Post-PEGylation

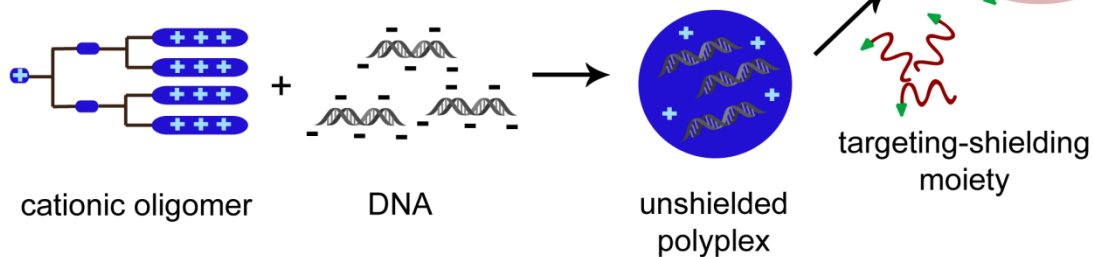


Figure 1.2. Illustration of A) pre-PEGylation and B) post-PEGylation approach applied for polyplex surface shielding. In the "pre-PEGylation" concept the shielding polymer is attached to the polycation prior to nucleic acid complexation, whereas in the "post-PEGylation" approach polyplexes are formed prior to the attachment of the shielding polymer.

Despite several significant advantages, the introduction of a shielding moiety affects cellular uptake and endosomal release as a consequence of the reduced interactions between the delivery system and the cell and endosomal membranes, respectively. Various attempts have been made to overcome this paradoxical effect of shielding referred as "PEG dilemma" by the development of bioresponsive deshielding strategies after reaching the target tissue [79-81]. This deshielding process is mediated by changes of environmental parameters such as pH [49, 50], enzymatic activity [51] or redox potential [53]. Hence, the cleavage of the PEG shield only

Introduction

occurs in presence of the stimuli. However in absence, the PEG shield remains intact in order to prolong blood circulation and avoid particle-particle aggregation or unspecific cell-uptake. Exploiting pH changes within the tumor tissue or endosomes acid-labile linkers, such as acetals [82-84], dialkylmaleic acids [50] or pyridylhydrazones [78, 85], have been introduced between the shielding moiety and the surface of the polyplex. These surface-modified delivery systems are intended to remain shielded during circulation, i.e. at physiological pH. However, the pH-labile bond is cleaved after the polyplex has entered a slightly acidic environment such as in tumor tissue or in an intracellular endosomal vesicle. Thus, the delivery system with its original endosomolytic capability is restored enabling membrane fusion or disruption to accomplish endosomal release. Previous studies have shown an up to 100-fold enhanced gene transfer by introducing a pH-sensitive hydrazone linker into PEG/PEI/DNA polyplexes *in vitro* and *in vivo* [78, 85].

In addition, enzymatic cleavable linkers attached between the polyplex surface and the shielding polymer presents an attractive tool to mediate location-specific cleavage of the PEG shield. In this respect, attention has recently turned to matrix metalloproteinases (MMPs) due to their over-expression within tumor tissues facilitating tumor site-specific cleavage of the PEG shield [86]. In healthy tissues the level of MMPs is rather low and therefore the PEG shield remains attached to the surface of the polyplex. To demonstrate the feasibility of this strategy PEG-cleavable polyplex micelles based on MMP-cleavable peptide-linked block copolymers have been synthesized [87]. Here, PAsp(DET) (poly(aspartamide)) with a flanking N-(2-aminoethyl)-2-aminoethyl group is bound via a MMPs cleavable peptide linker (GPLGVRG) to PEG. In the presence of matrix metalloproteinase-2 the PEG layer is efficiently cleaved and the initial positive surface charge of the carrier re-exposed. Consequently, polyplexes show a higher cellular uptake, an improved endosomal escape and a high-efficiency in gene transfection. The original purpose of PEG, to prolong blood circulation, still remains.

Alternatively, different location-specific changes such as disulfide reducing potential have been applied to cleave the PEG shield. In this regard, a pH-sensitive polymer (poly(methacryloyl sulfadimethoxine) (PSD)-block-PEG) with sharp transitions around physiological pH was evaluated. Hereby, the pH-sensitive PSD-*b*-PEG moiety is attached to PEI/DNA polyplexes enabling efficient surface shielding against

Introduction

unspecific cell interactions at pH 7.4. However, after polyplexes have entered the extracellular tumor environment or endosomes, the pH changes to approximately pH 6.6 resulting in sulfonamide protonation and release from the nanoparticles. Therefore, the initial positive surface charge of PEI is restored, which enables sufficient interactions with cell membranes and cellular uptake [49].

Together, these studies indicate that polyplexes designed to respond to different location-specific changes such as disulfide reducing potential, pH or enzyme concentrations represents a feasible strategy to overcome the PEG dilemma.

1.3.3.Targeting of non-viral carriers

Specific *in vivo* targeting to malignant cells by therapeutic genes presents an attractive concept to accomplish delivery tasks. In most cases, cell-specific targeting is enabled by specific interactions between a ligand, attached to the polyplex surface, and a receptor, exposed on the cell surface. However, cell-specific targeting is a key property that promotes nucleic acid transfer from the site of administration to the surface of the target cells and promotes cell-internalization. Additionally, side effects arising from toxicities toward mammalian cells are shown to be decreased by targeting malignant cells specifically. Furthermore, the receptor-ligand interaction stimulates the receptor-mediated endocytosis of target-specific polyplexes, which is known to be more efficient compared to adsorptive endocytosis [41, 42]. Various ligands are suitable for targeted gene delivery. Those can be categorized into several classes e.g. small molecules like folic acid (FolA), proteins such as transferrin (Tf) or epidermal growth factor (EGF) or asialoglycoproteins as well as peptides like CMBP1 or sugar derivatives such as N-acetylgalactosamine. When designing a target-specific carrier several aspects must be taken into account including the level of receptor expression, tissue specificity of ligands, ligand internalization, binding affinity, surface charge or degree of interaction with e.g. proteins. Thus, it is essential to select an appropriate ligand for successful application of a targeted non-viral carrier. Almost 30 years ago Wu *et al.* pioneered liver-cell specific targeting by an asialoglycoprotein targeted non-viral gene delivery system *in vitro* and *in vivo* [88, 89]. Meanwhile, various ligands have been incorporated within non-viral gene delivery systems and many studies have demonstrated successful cell-type specific *in vivo* gene delivery [90-95].

Introduction

A commonly used ligand for targeted gene delivery to a wide variety of cell types is the iron-transporting serum glycoprotein transferrin (Tf). The interaction of Tf with the transferrin receptor (TfR) triggers the cellular iron uptake. TfR as a biological target is of special interest since it is over-expressed on the surface of many human cancers. Therefore, Tf has been conjugated to various non-viral carriers such as PEI [77, 96], polypropylenimine (PPI) dendrimers [97], polyamidoamine (PAMAM) dendrimers [98] or poly-L-lysine (PLL) [99, 100] in order to achieve TfR-targeted gene delivery in cancer cells *in vitro* and *in vivo*.

The epidermal growth factor (EGF) is another promising ligand for tumor cell-specific targeting because it binds with high affinity and specificity to the epidermal growth factor receptor (EGFR). In several tumors including glioblastoma, epithelial tumors and lung cancers as well as hepatocellular carcinoma EGFR is upregulated or overactivated due to mutations resulting in uncontrolled proliferation. Thus, various EGFR-targeting molecules including recombinant EGF proteins, EGFR-binding peptides and antibodies are conjugated to gene delivery systems, to analyze the targeting efficiency and subsequently the gene expression levels. In this regard, using EGF-targeted PEI-based polyplexes, high-level transgene expression was found *in vitro* [42, 101]. For example, after systemic administration of EGF-targeted polyplexes a 50-fold increased transgene expression in hepatocellular carcinomas compared to normal liver tissue was reported [102].

Recently, a c-Met binding ligand cMBP2 was pioneered in terms of non-viral gene delivery. The over-expressed receptor tyrosine kinase HGFR/c-Met found in epithelial derived tumors serves as binding site for the natural ligand hepatocyte growth factor (HGF) as well as the c-Met binding peptide cMBP2, activating different cell-signaling pathways including those involved in tumor progression. In this regard, the activation of c-Met signaling presents an interesting target for cancer treatment. This has been successfully demonstrated by Kos *et al.* showing an enhanced selective gene transfer to hepatocarcinoma cells by targeting the c-Met receptor by cMBP2 *in vitro* and *in vivo* [103].

Introduction

1.4. Aims of the thesis

The successful implementation of nucleic acids as medical agents depends on the delivery efficiency of the non-viral carrier. While polymer-based gene carriers are promising due to the high-level of flexibility in structural design, overall efficiency is still several magnitudes lower in comparison to viral gene carriers. Whereas viruses have developed distinct mechanisms to transport DNA successfully into mammalian cells, most non-viral carriers are still unable to deliver DNA over extra- and intracellular barriers. To compensate for this disadvantage many research groups focus on the identification of structure-function relationships of DNA delivery carriers. We have generated a library of well-defined oligomer-based carriers with different architectures and functionalities, to identify individual structural requirements to the carrier. Based on this, this thesis focused on the optimization of polyplex stability and biological properties of a four-arm structured benchmark oligomer (compound ID: 606) to improve DNA delivery.

First, a small library of eight oligomers was to be synthesized via the solid-phase approach. In the sequence of these oligomers lysine residues had to be introduced at different sites to assess the influence of the incorporated lysine residues on polyplex stability in comparison to the benchmark oligomer 606. Additionally, the biophysical and biological properties of these stabilized particles had to be evaluated to identify the best oligomer.

Second, the polyplex surface ought to be modified with hydrophilic shielding polymers, monovalent PEG or monovalent and multivalent pHPMA (kindly provided by our collaboration partner Dr. Libor Kostka from the Centre for Biomacromolecular and Bioanalogous Systems, Department of Biomedical Polymers, Institute of Macromolecular Chemistry Academy of Sciences CR, v.v.i., Heyrovského sq. 2, Prague, Czech Republic), to investigate the effect on surface charge masking, providence of steric protection and prolongation of blood circulation of the delivery system. In order to overcome the "PEG dilemma" the aim was to develop a pH-sensitive deshielding strategy based on the introduction of the acid-labile linker azidomethyl-methylmaleic anhydride (AzMMMan) between the shielding moiety and the surface of the polyplex. The well-established "post-coating" approach was to be applied to attach the shielding material subsequently after polyplex formation to the particle surface via reactive groups [101, 104]. In this concept, the primary amines of

Introduction

the lysine residues within the oligomeric structure serve as attachment points for the shielding material. Two of the most commonly used shielding polymers, monovalent PEG (5kDa) or monovalent and multivalent pHPMA (10kDa, 20kDa, 30kDa), should be studied in parallel. The effect of shielding polymer chain length and architecture on polyplex shielding was to be evaluated. Furthermore, the shielding ability of pHPMA and PEG ought to be compared. To test the utility of such acid-labile carriers, the delivery efficiency was to be compared to that of acid-stably shielded polyplexes containing N-hydroxysuccinimide (NHS) groups in case of PEG and carbonylthiazolidine-2-thione (TT) groups in case of pHPMA. A detailed physicochemical, *in vitro* and *in vivo* analysis was to be performed to evaluate the effect of the pH-sensitive shielding compared to the analogous stable shielding on transfection efficiency.

Finally, the aim was to modify pH-sensitive and stable PEG-shielded particles with the targeting ligand folate (FolA) to assess the effect on specific receptor-mediated uptake. After the establishment of a suitable synthesis route for the targeting ligand FolA, DNA polyplexes were to be surface-modified. Specific receptor-mediated cell-uptake, cellular internalization and gene expression of FolA-targeted pH-sensitive or stable-modified PEG-shielded polyplexes was to be evaluated.

Material and Methods

2. Materials and Methods

2.1. Materials

2.1.1. Reagents and Solvents

All reagents and solvents used for experiments described in this thesis are summarized in Table 2.1. and Table 2.2.

Table 2.1. Reagents with CAS numbers, sources of supply and abbreviation (abbr.) used for experimental procedures.

	Reagents	CAS-No.	Supplier	Abbr.
Resins	Fmoc-L-Lys(Boc)-Wang resin		Sigma-Aldrich (München, Germany)	
	1-amino-ethane-2-thiol(cysteamine)-2-chlorotrityl resin		Iris Biotech (Marktredewitz, Germany)	
	Fmoc-Ala-Wang		Sigma-Aldrich (München, Germany)	
Amino acids	Boc-L-Cys(Trt)-OH	21947-98-8		
	Fmoc-L-Glu-OtBu	84793-07-7		
	Fmoc-L-His(Trt)-OH	109425-51-6	Iris Biotech	
	Fmoc-L-Lys(Boc)-OH	71989-26-9		
	Fmoc-L-Lys(Fmoc)-OH	78081-87-5		
SPPS	Acetic anhydride	108-24-7	Sigma-Aldrich	
	Benzotriazol-1-yl-oxytripyrrolidinophosphonium-hexafluorophosphate	128625-52-5	Multisyntech GmbH (Witten, Germany)	PyBOP
	1,8-diazabicyclo[5.4.0]undec-7-en	6674-22-2	Sigma-Aldrich	
	Diisopropylethylamin	7087-68-5	Iris Biotech	DIPEA
	Di- <i>tert</i> -butyldicarbonate	24424-99-5	Sigma-Aldrich	
	Ethyl trifluoroacetate	383-63-1	Sigma-Aldrich	
	Fmoc-OSu	82911-69-1	Iris Biotech	
	2-(1H-benzotriazol-1-yl)-1,1,3,3-tetramethyluronium-hexafluorophosphate	94790-37-1	Multisyntech GmbH	HBTU
	1-hydroxybenzotriazole hydrate	123333-53-9	Sigma-Aldrich	HOBt
	Hydrochloric acid	7647-01-0	Sigma-Aldrich	HCl
Ninhydrin	485-47-2	Sigma-Aldrich		

Material and Methods

	Pentaethylene hexamine	4067-16-7	Sigma-Aldrich	PEHA
	Phenol	108-95-2	Sigma-Aldrich	
	Piperidine	110-89-4	Iris Biotech	
	Potassium cyanide	151-50-8	Sigma-Aldrich	
	Pyridine	110-86-1	Sigma-Aldrich	
	Sephadex® G-10	9050-68-4	GE Healthcare (Freiburg, Germany)	
	Sodium bicarbonate	144-55-8	Sigma-Aldrich	
	Sodium chloride	7647-14-5	Sigma-Aldrich	NaCl
	Sodium hydroxide (anhydrous)	1310-73-2	Sigma-Aldrich	NaOH
	Succinic anhydride	108-30-5	Sigma-Aldrich	
	Triethylamine	121-44-8	Sigma-Aldrich	
	Trifluoroacetic acid	76-05-1	Iris Biotech	TFA
	Triisopropylsilane	6485-79-6	Sigma-Aldrich	TIS
	Trisodium citrate dihydrate	6132-04-3	Sigma-Aldrich	
	Triton™ X-100	9002-93-1	Sigma-Aldrich	
AzMMMan	Benzoyl peroxide	94-36-0	Sigma-Aldrich	
	2,3-dimethylmaleic anhydride	766-39-2	Sigma-Aldrich	DMMAn
	<i>N</i> -Bromosuccinimide	128-08-5	Sigma-Aldrich	NBS
	Sephadex LH 20	9041-37-6	Sigma-Aldrich	
	Sodium azide	26628-22-8	Acros Organics (Geel, Belgien)	
	Sodium sulfate NHS-C ₃ -Azide	7757-82-6	Sigma-Aldrich baseclick (Tutzingen, Germany)	Na ₂ SO ₄
PEG reagents	DBCO-PEG(5000)-MeO		Jena Bioscience (Jena, Germany)	
	MeO-PEG(5000)-NHS		RAPP Polymere (Tübingen, Germany)	
	OPSS-PEG(5000)-NHS		RAPP Polymere	
	NHS-PEG(5000)-SH		RAPP Polymere	
	NH ₂ -PEG ₄ -DBCO	1255942-06-3	Sigma-Aldrich	
	Mal-PEG ₄ -DBCO		Sigma-Aldrich	
FoIA reagents	Fmoc-N-amido-dPEG ₆ - acid	882847-34-9	Iris Biotech	
	Folic acid	59-30-3	Sigma-Aldrich	FoIA
	<i>N,N</i> -Dicyclohexyl- carbodiimide	538-75-0	Sigma-Aldrich	
	<i>N</i> -Hydroxysuccinimide	6066-82-6	Sigma-Aldrich	NHS
	<i>N</i> ¹⁰ -(Trifluoroacetyl) pterotic acid	37793-53-6	Iris Biotech	

Material and Methods

	Adenosine-5`-triphosphate	56-65-5	Roche Diagnostics (Basel, Schweiz)	
	Agarose NEEO Ultra-Qualität	9012-36-6	Carl Roth GmbH (Karlsruhe, Germany)	
	Ammonium persulfate	7727-54-0	Sigma-Aldrich	APS
	Barium chloride dihydrate	10326-27-9	Sigma-Aldrich	
	Boric acid	10043-35-3	Sigma-Aldrich	
	Bromophenol blue	115-39-9	Sigma-Aldrich	
	Coenzym A		Sigma-Aldrich	
	Coomassie® Blue Staining		Fisher Scientific (Schwerte, Germany)	
	DL-Dithiothreitol	578517	Sigma-Aldrich	
	Ethylenediaminetetra-acetic acid disodium salt dihydrate	6381-92-6	Sigma-Aldrich	EDTA
	GelRed		Biotium Inc. (Hayward, USA)	
Other	Glycylglycine	556-50-3	Roche Diagnostics	
	Ethidium bromide solution	1239-45-8	Sigma-Aldrich	EtBr
	Linear polyethylenimine	9002-98-6	In house synthesis	LPEI
	Magnesium chloride	7786-30-3	Sigma-Aldrich	
	<i>N,N,N',N'</i> -Tetramethylethylenediamine	110-18-9	Sigma-Aldrich	TEMED
	Potassium chloride	7447-40-7	Sigma-Aldrich	
	Potassium dihydrogen phosphate	7778-77-0	Sigma-Aldrich	
	Potassium iodide	7681-11-0	Sigma-Aldrich	
	Propane-1,2,3-triol	56-81-5	Sigma-Aldrich	
	Rotiphorese® Gel 30		Carl Roth GmbH	
	Sodium dodecyl sulfate	151-21-3	Sigma-Aldrich	SDS
	Sodium hydrogen phosphate	7558-79-4	Sigma-Aldrich	
	Tris(hydroxymethyl)amimomethane	77-86-1	Sigma-Aldrich	Tris
	Trizma® base	77-86-1	Sigma-Aldrich	

Material and Methods

Table 2.2. Solvents with CAS-numbers, sources of supply and abbreviation used for experimental procedures.

Solvent	CAS-No.	Supplier	Abbreviation
Acetone ⁴⁾	67-64-1	Sigma-Aldrich	
Acetonitrile ¹⁾	75-05-8	VWR Int. (Darmstadt, Germany)	ACN
Carbon tetrachloride ⁴⁾	56-23-5	Acros Organics	
Chloroform ²⁾	67-66-3	VWR Int.	
Chloroform-d ³⁾	865-49-6	Euriso-Top (Saint-Aubin Cedex, France)	
Deuterium oxide ³⁾	7789-20-0	Euriso-Top	
Dichloromethane ^{2) 4)}	75-09-2	VWR Int. ²⁾ Bernd Kraft (Duisburg, Germany) ⁴⁾	DCM
Dichloromethane-d ³⁾	1665-00-5	Euriso-Top	
Diethyl ether ⁴⁾	60-29-7	Bernd Kraft	
<i>N,N</i> -Dimethylformamide ⁵⁾	68-12-2	Iris Biotech	DMF
Dimethyl sulfoxide ¹⁰⁾	67-68-5	Sigma-Aldrich	DMSO
Ethanol absolute ⁴⁾	64-17-5	VWR Int.	EtOH
Ethyl acetate ⁷⁾	141-78-6	Staub & Co. (Nürnberg, Germany)	
n-Heptane ⁸⁾	142-82-5	Grüssing (Filsum, Germany)	
n-Hexane ⁸⁾	110-54-3	Brenntag (Mülheim/Ruhr, Germany)	
Methanol ¹⁾	67-56-1	Fisher Scientific	MeOH
2-Methylpentane ⁷⁾	107-83-5	Sigma-Aldrich	
<i>N</i> -Methyl-2-pyrrolidone ⁵⁾	872-50-4	Iris Biotech	NMP
Methyl- <i>tert</i> -butyl ether ²⁾	1634-04-4	Brenntag	MTBE
2-Propanol ⁹⁾	67-63-0	Sigma-Aldrich	
Tetrahydrofuran ⁵⁾	109-99-9	Fisher Scientific	
Water ⁶⁾		In house purification	H ₂ O

1) HPLC grade; 2) DAB grade, distilled before use; 3) NMR grade (>99.9%); 4) analytical grade; 5) peptide grade; 6) purified, deionized; 7) purum, distilled before use; 8) purissimum; 9) DAB grade; 10) anhydrous

Material and Methods

2.1.2. Equipment for solid-phase assisted peptide synthesis (SPPS)

Disposable polypropylene syringe microreactors were purchased from Multisyntech. Those reactors were equipped with polytetrafluoroethylene filters in case of the use in the automated single peptide synthesis. For manual peptide synthesis microreactors were equipped with polyethylene filters.

2.1.3. Cell culture

All cell culture consumables (well plates, flasks, dishes) were purchased from NUNC (Langensfeld, Germany) or TPP (Trasadingen, Switzerland).

Table 2.3. Reagents and media with CAS numbers, sources of supply and abbreviation (Abbr.) used for *in vitro* experiments.

	Reagents	CAS-No.	Supplier	Abbr.
Reagents	Chloroquine diphosphate	50-63-5	Sigma-Aldrich	
	Collagen A	9007-34-5	Merck Millipore (Darmstadt, Germany)	
	D(+) glucose monohydrate	14431-43-7	Merck Millipore	
	4',6-Diamidino-2-phenylindole	28718-90-3	Sigma-Aldrich	DAPI
	3-(4,5-Dimethyl-2-thiazolyl)-2,5-diphenyl-2H-tetrazolium bromide	298-93-1	Sigma-Aldrich	MTT
	D-luciferin	2591-17-5	Promega (Mannheim, Germany)	
	HEPES	7365-45-9	Biomol GmbH (Hamburg, Germany)	
	Fetal calf serum		Invitrogen (Karlsruhe, Germany)	FCS
	Heparin-Na 25000		Ratiopharm (Ulm, Germany)	
	Luciferase cell culture 5x lysis buffer		Promega	
	Penicillin/ Streptomycin		Biochrom GmbH (Berlin, Germany)	
	Paraformaldehyde	30525-89-4	Sigma-Aldrich	
	Rhodamine phalloidin		Fisher Scientific	
	Sodium chloride	7647-14-5	Prolabo (Haasrode, Belgien)	NaCl
	Trypsin/EDTA solution (10x)		Biochrom GmbH	

Material and Methods

Medium	Dulbecco's Modified Eagle's Medium- low glucose RPMI 1640 (1x)	Sigma-Aldrich Life Technologies GmbH (Darmstadt, Germany)	DMEM
	Dulbecco's Modified Eagle's medium 50:50 mixture with Ham's F12	Sigma-Aldrich	

Table 2.4. Summary of used cell lines.

Cell line	Cell type	Medium
Neuro-2a	Mouse neuroblastoma	DMEM (low glucose)
KB	Human cervix carcinoma	Folate-free RPMI 1640
HUH7	Human hepatocellular carcinoma	DMEM (low glucose)/Ham's F12 1:1

2.1.4. Nucleic acids

pCMVL, encoding for firefly luciferase under control of the CMV promoter, was purchased from PlasmidFactory (Bielefeld, Germany). Cy5-labeling kit for pCMVL labeling was obtained by Mirus Bio (Madison, USA).

2.2. Methods

2.2.1. Synthesis of 3-(azidomethyl)-4-methyl-2,5-furandione (AzMMMan)

AzMMMan was synthesized according to the literature [105, 106] with modifications.

Firstly, dimethylmaleic anhydride [DMMan (5.04g, 39.97mmol)], N-bromosuccinimide [NBS (4.56g, 25.62mmol)], and benzoyl peroxide (64mg, 0.36mmol) were dissolved in 250mL carbon tetrachloride (dried over molecular sieve UOP Type 3A). The reaction mixture was gently heated under reflux in an inert atmosphere at 110-120°C for 5h in a 500mL round-bottom flask. Once the mixture was cooled to room temperature an additional amount of benzoyl peroxide (64mg, 0.36mmol) was added and boiling under reflux was continued for 5h. After the mixture was cooled to room temperature again, the residue was filtered and washed two times with 25mL carbon

Material and Methods

tetrachloride. Subsequently, the organic phase was washed twice with water (100mL) and once with brine (100mL). Thereafter, the organic layer was dried over Na_2SO_4 and concentrated in vacuum to form a yellow oil. Benzoyl peroxide was removed by silica gel flash chromatography using a mixture of 2-methylpentane/ethyl acetate (8:2) as eluent. The residue was subsequently distilled with the help of a kugelrohr apparatus under vacuum. DMMan fraction was removed at 110-120°C, 7mbar. 3-(Bromomethyl)-4-methyl-2,5-furandione (BrMMan) was isolated at 140°C, 7mbar (1.8g, yield 22%). 3,4-bis(bromomethyl)furan-2,5-dione remained in the still pot.

Secondly, BrMMan (310.5mg, 1.5mmol) was dissolved in 10mL acetone (dried over molecular sieve UOP Type 3A) and sodium azide (97.5mg, 1.5mmol) was added. The mixture was stirred for 24h at 37°C. After filtering the solvent was evaporated. The remaining oil was resolved in ethyl acetate (20mL) and washed two times with water (20mL) and one time with brine (20mL). The organic layer was dried over Na_2SO_4 . The liquid was concentrated in vacuum to result in a brown oil (222mg, yield 88%).

2.2.2.Synthesis of Fmoc/Boc-protected succinyl-pentaethylene hexamine (Fmoc/Boc-Sph)

Sph was prepared following an adapted procedure of Salcher et al. [55, 107]. Prior to synthesis, pentaethylene hexamine (PEHA) was purified according to Jonassen and Westerman [108]. Fractions of 25mL PEHA were distilled with a kugelrohr apparatus. The second fraction (210-225°C, 0.01bar) was collected and used for Sph synthesis. The first (200°C, 0.01bar) and the third fraction (> 230°C, 0.01bar) were discarded.

2.2.3.Solid-phase assisted peptide synthesis

Oligomer synthesis was performed together with Dr. Libor Kostka, visiting postdoctoral scientist at LMU.

Material and Methods

2.2.3.1. Loading of resins

All polycationic carriers and the targeting ligand were synthesized using preloaded resins. For the synthesis of oligomer 784, 785 and 797 a Fmoc-L-Lys(Boc)-Wang resin with a load of 0,76mmol/g was used. Oligomer 606 was synthesized using Fmoc-Ala-Wang resin with a load of 0.32mmol/g according to Lächelt et al. [56]. The same resin was used for the synthesis of oligomer 748 and 749. The loading of the resins was decreased to 0.15-0.2mmol/g enabling successful coupling of amino acids (AA) to the four arm branching core (A/KK(HK)₂). The appropriate amount of resin was pre-swollen in DCM (10mL/g resin) for 30min before loading was decreased. Afterwards, the Fmoc protecting group was removed by treating the resin two times 5min and two times 10min with deprotection solution [20% piperidine in DMF (v/v)]. Subsequently, the resin was washed three times with DMF and DCM and afterwards Kaiser test was performed. An equimolar amount of Fmoc-L-Lys(Fmoc)-OH, 1-hydroxybenzotriazole hydrate (HOBt) and benzotriazol-1-yl-oxytripyrrolidinophosphoniumhexafluorophosphate (PyBOP) as well as a twofold molar amount of diisopropylethylamine (DIPEA) were dissolved in DCM/DMF [1/1 (v/v); 10mL/g resin] and added to the resin for 1h. After coupling, the reaction solvent was drained and the resin was washed three times with DMF and DCM. Unreacted groups were capped with a mixture of 20eq acetic anhydride and 40eq DIPEA dissolved in DCM/DMF [1/1 v/v); 10mL/g resin]. Afterwards, solvents were drained, the resin was washed three times with DMF and DCM and Kaiser test was performed. According to the individual oligomer sequence coupling of further amino acids was performed as stated above.

The targeting ligand Fola-PEG₆-cysteamine was synthesized using an 1-aminoethane-2-thiol(cysteamine)-2-chlorotriyl resin with a load of 0,95mmol/g. The resin was pre-swollen in anhydrous DCM for 30min and loading was decreased to 0.4-0.5mmol/g. 1eq Fmoc-N-amido-dPEG₆-acid, 1eq HOBt, 1eq PyBOP and 2eq DIPEA were dissolved in anhydrous DCM/DMF [1/1 (v/v); 10mL/g resin] and added to the resin. The reactor was agitated until Kaiser test indicated complete conversion. After Fmoc cleavage, Fmoc-Glu(OH)-tBu and N¹⁰-(Trifluoroacetyl)pteroic acid were attached in additional separate steps. Afterwards, solvents were drained, the resin was washed three times with DMF followed by three times washing with DCM before the TFA group was removed by incubating the resin four times 30min with 1M ammonium hydroxide/DMF [1/1 (v/v)]. In between the cleavage steps the resin was washed three times with DMF followed by three times with DCM. Finally, the

Material and Methods

targeting ligand was cleaved off the resin according 2.2.3.3. "cleavage of oligomers and targeting ligand".

The loading of the resins was determined as following: around two times 5mg of the resin were separated, washed twice with DCM and n-hexane and dried under vacuum. An exact amount of resin was treated with 1mL deprotection solution for 1h, diluted in DMF and UV absorption was measured at 301nm. The loading was calculated according to the equation:

$$\text{resin load [mmol/g]} = (A \cdot 1000) / (m [\text{mg}] \cdot 7800 \cdot \text{df}) \text{ with df as dilution factor}$$

The residual resin was treated two times 5min and two times 10min with deprotection solution, washed three times with DMF and three times with DCM and dried under vacuum. Reaction progress was monitored by Kaiser test (chapter 2.2.3.4.).

2.2.3.2. General procedure of SPPS

SPPS was carried out according to standard Fmoc/tBu protecting group strategy first published by Merrifield et al. [109]. Synthesis was performed either by an automated microwave-based system (Biotage AB, Uppsala, Sweden) or manually. For automated synthesis the pre-loaded resin was pre-swollen in a syringe reactor for 20min in NMP and for manual synthesis in DCM. The general synthesis procedure was performed as described in Table 2.5. (automated synthesis) and Table 2.6. (manual synthesis). After reaction and washing steps, solvents and non-reacted reagents were removed.

Table 2.5. General protocol for automated synthesis.

Synthesis step	Reagents	Reaction time	Volume [mL/g resin]
Coupling	AA/PyBOP/HBTU/DIPEA	3x/5x alternating	10
	[4eq/4eq/4eq/8eq]	10min, 60°C and	
	in DMF/NMP [1/1 (v/v)]	5min, RT	
Washing	3xDMF	1min	10
Deprotection	20% piperidine in DMF ³⁾ (v/v)	5x5min, RT	10
Washing	3xDMF	1min	10
Kaiser Test	Kaiser test solution ^{1); 2)}	positive	

Material and Methods

Table 2.6. General protocol for manual synthesis.

Synthesis step	Reagents	Reaction time	Volume [mL/g resin]
Coupling	AA/PyBOP/HOBT/DIPEA [4eq/4eq/4eq/8eq] in DMF/DCM [1/1 (v/v)]	60-90min shaking	10
Washing	3xDMF/ 3xDCM	1min	10
Kaiser test	Kaiser test solution ¹⁾	negative	
Deprotection	20% piperidine in DMF ³⁾ (v/v)	2x5min and 2x10min, RT	10
Washing	3xDMF/ 3xDCM	1min	10
Kaiser Test	Kaiser test solution ^{1); 2)}	positive	

1) according 2.2.3.4.

2) not during synthesis, only last step

3) if needed addition of 2% 1,8-diazabicyclo[5.4.0] undec-7-en and 1% Triton

2.2.3.3. Cleavage of oligomers and targeting ligand

The oligomer was cleaved off the resin by treatment with a cleavage solution containing TFA/TIS/H₂O [95/2.5/2.5 (v/v)] for 1.5h. After washing the resin two times with trifluoroacetic acid (TFA) and DCM all solutions were combined, concentrated and precipitated by dropwise addition to a mixture of ice-cold MTBE/n-hexane [1/1 (v/v)] and cooled to -20°C. The resulting precipitate was centrifuged (10min; 4000rpm) and dried under vacuum. The resulting precipitate of the targeting ligand was dissolved in 50% (v/v) acetonitrile in water and lyophilized. In case of an oligomer precipitate, the pellet was re-suspended in size exclusion buffer [10mM HCl, 30% ACN, 70% H₂O (v/v)]. The oligomer was purified by size exclusion chromatography using a self-packed Sephadex® G-10 column connected to an Äkta basic system (GE Healthcare, München, Germany) detecting at 214nm, 250nm and 280nm. Isocratic elution at a flow rate of 2mL/min was applied. The product fractions were pooled, frozen in liquid nitrogen and lyophilized.

Material and Methods

2.2.3.4. Kaiser Test

Kaiser test was used as a control to monitor the coupling and deprotection efficiency by detection of free amino groups. Due to the linkage of the chain to the resin via its C-terminus, the N-terminus is extending off. Ninhydrin is used to detect free amines (in case of deprotected resin) by color change. In case of a protected N-terminus the test gives a yellow result. The test was carried out after each coupling and deprotection step during manual synthesis. In case of automated synthesis, Kaiser test was just performed before manual coupling of Boc-Cys(Trt)-OH or after coupling of N^{10} -(Trifluoroacetyl)pteroic acid.

A small amount of beads were transferred to an Eppendorf tube. One drop of each solution [80% (w/v) phenol in EtOH, 5% (w/v) ninhydrin in EtOH, 0.02mM potassium cyanide in pyridine] was added to the resin, vortexed and heated to 99°C for 4min.

2.2.4. Synthesis of shielding polymers

2.2.4.1. Synthesis of monovalent AzMMMan-PEG(5000)-MeO

Monovalent AzMMMan-PEG(5000)-MeO was synthesized by a one-step modification of DBCO-PEG(5000)-MeO (10mg, 2 μ mol) with AzMMMan (1.34mg, 8 μ mol). Therefore, all reagents were dissolved in MeOH (500 μ L) and the reaction was performed for 3h. The excess of AzMMMan was removed by precipitation of AzMMMan-PEG(5000)-MeO in 50mL diethyl ether (yield 90-95%).

2.2.4.2. Synthesis of bifunctional FoIA-PEG(5000)-AzMMMan and bifunctional FoIA-PEG(5000)-NHS via FoIA-PEG₆-cysteamine

AzMMMan-modified bifunctional FoIA-PEG(5000) was synthesized by a three-step reaction. Firstly, OPSS-PEG(5000)-NHS (10mg, 2 μ mol) was modified with DBCO-PEG₄-NH₂ (4.2mg, 8 μ mol). Therefore, OPSS-PEG(5000)-NHS was dissolved in 450 μ L MeOH and DBCO-PEG₄-NH₂ in 50 μ L DMSO. Afterwards, reagents were mixed and reaction was performed for 3h at 25°C. The excess of DBCO-PEG₄-NH₂ was removed by size exclusion chromatography (SEC) using a PD Midi Trap self-packed with Sephadex LH 20 and MeOH as an eluent. The first fraction corresponding to the high-molecular weight OPSS-PEG(5000)-DBCO was collected and solvent was evaporated. Secondly, the targeting ligand FoIA was introduced by

Material and Methods

dissolving 1eq OPSS-PEG(5000)-DBCO (10mg, 2 μ mol) in 450 μ L MeOH and 4eq FoIA-PEG₆-cysteamine (6.6mg, 8 μ mol) in 50 μ L DMF. The reaction was performed for 2h and purified by SEC using a PD Midi Trap self-packed with Sephadex LH 20 and MeOH as an eluent. The first fractions were collected and solvent was evaporated. Lastly, 1eq FoIA-PEG(5000)-DBCO (10mg, 2 μ mol) was modified with 4q AzMMMan (1.34mg, 8 μ mol) accordingly the monovalent AzMMMan-PEG-MeO as stated above.

N-Hydroxysuccinimide (NHS)-modified bifunctional FoIA-PEG(5000) was synthesized by dissolving 1eq OPSS-PEG(5000)-NHS (10mg, 2 μ mol) in 450 μ L MeOH and 4eq FoIA-PEG₆-cysteamine (6.6mg, 8 μ mol) in 50 μ L DMF. The reaction was performed for 2h and purified by SEC using a PD Midi Trap self-packed with Sephadex LH 20 and MeOH as an eluent. The first fraction was collected and solvent was evaporated.

2.2.4.3. Synthesis of bifunctional FoIA-PEG(5000)-AzMMMan and bifunctional FoIA-PEG(5000)-NHS via NHS-FoIA

In a different approach FoIA-PEG(5000)-AzMMMan and FoIA-PEG(5000)-NHS was synthesized via NHS-FoIA. In the first step NHS-FoIA was synthesized according Liu et al. [110]. After removing the insoluble byproduct dicyclohexylurea by filtration, the FoIA-NHS solution was precipitated in ACN and solvent was removed by evaporation. In the next step, 4eq DBCO-PEG₄-Mal (5.4mg, 8 μ mol) was coupled to 1eq NH₂-PEG(5000)-SH (10mg, 2 μ mol). In this regard, NH₂-PEG(5000)-SH was dissolved in 450 μ L MeOH and DBCO-PEG₄-Mal in 50 μ L DMSO. Coupling was performed for 3h and the excess of DBCO-PEG₄-Mal was removed by SEC using a PD MidiTrap column self-packed with Sephadex LH20 and MeOH as an eluent. The first fraction was collected and the solvent was evaporated. Afterwards, the targeting ligand FoIA was introduced by dissolving NH₂-PEG(5000)-DBCO (10mg, 2 μ mol) in 450 μ L MeOH/DMF [1/1 (v/v)] and NHS-FoIA (4.2mg, 8 μ mol) in 50 μ L DMF. Reaction was performed for 4h under the atmosphere of an inert gas at RT. The product was purified by SEC using a PD MidiTrap column self-packed with Sephadex LH20 and DMF as an eluent. Again, the first fractions were collected and the solvent was evaporated. In the last step, 1eq FoIA-PEG(5000)-DBCO (10mg, 2 μ mol) was modified either with 4eq AzMMMan (1.34mg, 8 μ mol) or NHS-C₃-Azide (1.8mg, 8 μ mol). Therefore, FoIA-PEG(5000)-DBCO and AzMMMan or NHS-C₃-Azide were

Material and Methods

dissolved in 500 μ L MeOH and reaction was performed for 4h at RT. The product was purified by precipitation in 50mL diethyl ether.

Note: These syntheses were unsuccessful according biological characterization section 3.3.1.

2.2.4.4. Synthesis of monovalent pHPMA-AzMMMMan and monovalent pHPMA-TT

Monovalent poly*N*-(2-Hydroxypropyl)methacrylamide (pHPMA) polymers were synthesized, characterized and kindly provided by Dr. Libor Kostka.

2.2.4.5. Synthesis of multivalent pHPMA-AzMMMMan and multivalent pHPMA-TT

Multivalent pHPMA polymers were synthesized, characterized and kindly provided by Dr. Libor Kostka.

2.2.4.6. Polyplex formation

Unless stated otherwise, polyplexes were prepared in HEPES-buffered glucose (HBG) by adding pCMVL to the oligomer solution at indicated N/P ratios (protonable nitrogen/phosphate ratio), followed by rapid mixing and a 3h incubation at 25°C, 900rpm. In case of shielded polyplexes, indicated molar equivalents of shielding polymer (calculated as molar ratio over the oligomer applied in the polyplex formation) was dissolved in HBG and added 3h post polyplex formation, followed by further incubation for 24h or 48h at RT. For cell uptake studies, assessed by flow cytometry and laser scanning microscopy (LSM), 20% of pCMVL was labeled with Cy5 (Mirus Bio, Madison, USA). For *in vivo* experiments polyplexes were prepared in a total volume of 250 μ L HBG. In case of unshielded polyplexes, polyplexes were formed 45min prior *i.v.* injection.

Material and Methods

2.2.4.7. Measurement of particle size and zeta potential

Polyplex formation as well as shielding and deshielding of polyplexes was monitored via particle size and zeta potential measurements by dynamic and electrophoretic light scattering (DLS) using a Zetasizer Nano ZS (Malvern Instruments, Worcestershire, U.K.) with following parameters: equilibration time 0min, viscosity 0,8872cP, dielectric constant 78.5, temp 25°C, F(Ka) 1.5 (Smoluchowski), measurement point 2.00mm, attenuator 11.

2.2.4.8. Agarose gel shift assay

To study pCMVL condensation as a function of N/P ratio, an agarose gel shift assay was performed. To visualize pCMVL, 120µL GelRed was added to the 1% agarose gel. Polyplexes were formed as stated above and 4µL of DNA loading buffer was added prior to loading to the gel. Electrophoresis was performed at a constant current of 120V for 80min. Thereafter, fluorescence of incorporated GelRed was detected using a transilluminator (Biostep, Jahnsdorf, Germany).

2.2.4.9. Ethidium bromide exclusion assay (EtBr assay)

Ethidium bromide exclusion assay was performed to study pCMVL condensation ability using a Cary Eclipse spectrophotometer (Varian, Bergisch Gladbach, Germany), Exc: 510nm Em: 590nm. The effect of polyplex stability was assessed by stepwise addition of oligomer solution to 10µg pCMVL in 1mL HBG containing 0.4µg EtBr. Free pCMVL and EtBr solution were set as 100% and an EtBr solution was set as a background value. Fluorescence intensity was measured 30s after each addition of oligomer aliquot.

2.2.4.10. Oligomer buffering capacity

The buffering capacity of oligomers was determined via back titration with an automatic titration system Titrando 905 (Metrohm, Filderstadt, Germany). An oligomer sample, containing 15µmol protonatable amines, was diluted in a total volume of 3.5mL 50mM NaCl solution and pH was adjusted to 2.1 by addition of 0.1M HCl. Back titration was performed with 0.05M NaOH solution until a pH of 11 was

Material and Methods

reached. A control titration was performed with 3.5mL 50mM NaCl solution and 0.05M NaOH. The percentage of buffer capacity C in a certain pH range (x-y) was calculated according to equation (1). The volume consumption of NaOH in the considered pH range is represented by ΔV .

$$(1) C_{pH(x-y)} = \frac{\Delta V_{pH(x-y)} \times 0.05M}{0.015mmol} \times 100$$

2.2.4.11. Cell culture

Mouse neuroblastoma cells (Neuro-2a) were grown in Dulbecco's Modified Eagle's Medium- low glucose (DMEM) and hepatocarcinoma cells (HUH7) in a 50:50 mixture of Dulbecco's Modified Eagle's medium and Ham's F12 medium. All cell lines were cultured at 37°C in a humidified atmosphere of 5% CO₂ and 95% air. All media were supplemented with 10% fetal calf serum (FCS), 100U/mL penicillin and 100µg/mL streptomycin. Cells were harvested by treatment with trypsin/EDTA solution at 37°C for 5 min. Cells were mycoplasma free as tested by MycoAlert™ mycoplasma detection kit (Lonza, Köln, Germany).

2.2.4.12. Luciferase gene expression

In vitro experiments were performed in 96-well plates with 10⁴ seeded Neuro-2a cells per well or in collagen-coated 96-well plates with 8x10³ or 4x10³ seeded HUH7 cells per well, 24h prior to pCMVL delivery. Before transfection, cell medium was replaced with 80µL fresh medium. Polyplex solution (20µL) was added to each well and incubated at 37°C for an indicated period of time (24-48h). After transfection cells were treated with 100µL luciferase cell culture 5x lysis buffer. Luciferase gene expression was measured in a Centro LB 960 plate reader luminometer (Berthold Technologies, Bad Wildbad, Germany) by monitoring luciferase activity in cell lysates using LAR buffer supplemented with 10% 10mM luciferin solution (240mg luciferin, 2.35mL 1M glycyglycine, 80mL H₂O, pH 8). Linear polyethylenimine [LPEI; N/P 6] or unmodified 784 (N/P 12) was used as a positive control. HBG was used as a negative control.

Material and Methods

2.2.4.13. Cell viability assay (MTT)

Viability of HUH7 and Neuro-2a cells was evaluated subsequently to the transfection experiments. Transfections were performed similar to luciferase gene expression studies. At indicated post-transfection time, 10 μ L 3-(4,5-dimethyl-2-thiazolyl)-2,5-diphenyl-2H-tetrazolium bromide (MTT) was added to each well reaching a final concentration of 0.5mg MTT/mL. After 2h of incubation, unreacted dye and medium were removed and the 96-well plates were stored at -80°C for one hour. The purple formazan product was dissolved in 100 μ L/well DMSO and quantified by a microplate reader (Tecan, Männedorf, Switzerland) at 530nm with background correction at 630nm. The relative cell viability (%) related to control wells containing cell culture medium with 20 μ L HBG was calculated by $[A]_{\text{test}}/[A]_{\text{control}} \times 100$.

2.2.4.14. Cellular uptake: flow cytometry studies

Cellular internalization of the polyplexes was assessed by flow cytometry of Cy5-labeled polyplexes (Exc:636nm, Em:665nm) in a Cyan™ ADP flow Cytometer (Dako, Hamburg, Germany) equipped with Summit™ acquisition software (Summit, Jamesville, USA). Data were analyzed by FlowJo® 7.6.5 flow cytometric analysis software. Cells were appropriately gated by forward/sideward scatter and pulse width for exclusion of doublets. All experiments were performed in triplicates.

HUH7 cells were seeded 24h prior to transfection into collagen-coated 24-well plates at a density of 4x10⁴ cells per well. Before transfection medium was replaced with 400 μ L fresh medium. Polyplex solution (100 μ L) was added and incubated for 2h at 37°C. Thereafter, cells were washed twice with 500 μ L phosphate-buffered saline (PBS), incubated on ice for 15min with 100I.U. heparin and again washed twice with 500 μ L PBS. Thereafter, cells were collected and after centrifugation (5min, 1000g) re-suspended in FACS solution (10% FCS in PBS). DAPI staining was applied to discriminate between viable and non-viable cells.

Material and Methods

2.2.4.15. Intracellular localization: laser scanning microscopy (LSM)

Neuro-2a cells (3×10^4 per well) were seeded 24h prior to transfection in Nunc™ Labtek™ chamber slides (Sigma-Aldrich). Before transfection cell medium was replaced with 80µL fresh medium. Polyplexes solution (20µL per well) was added and incubated for 24h at 37°C. Cells were washed three times with PBS and fixed with 4% paraformaldehyde for 30min. Staining was performed using DAPI and rhodamine phalloidin. Results were analyzed in a Zeiss Laser Scanning Microscope LSM 510 Meta and Axiovert 200 software (Zeiss).

2.2.4.16. *In vivo* delivery and expression

All animal experiments were performed according to the guidelines of the German law for the protection of animal life and were approved by the local animal ethics committee. Six weeks old female Rj:NMRI nu (nu/nu) (Janvier, Le-Genest-St-Isle, France) mice were housed in isolated ventilated cages with a 12h day/night interval and food and water ad libitum.

Neuro-2a cells (5×10^6) suspended in 150µL PBS were injected subcutaneously into the left flank. On day 12 and 13 after tumor cell inoculation, 250µL polyplex solution containing 60µg pCMVL was administered via tail vein injection. Mice were euthanized on day 15 and tumor/organs were collected to assess luciferase activity via *ex vivo* luciferase assay. Tumor and organs were homogenized in 500µL cell lysis buffer using a tissue and cell homogenizer (FastPrep®-24). To separate insoluble cell components, the samples were centrifuged at 3000g at 4°C for 10min. Luciferase activity was measured in the supernatant using a Centro LB 960 luminometer.

2.2.4.17. Statistical analysis

Results are presented as mean \pm SEM. Statistical significance was determined in two-tailed t-tests. Significance levels are indicated as follows: *: $P \leq 0.05$; **: $P \leq 0.01$; ***: $P \leq 0.001$.

Results

3. Results

3.1. Designing new sequence-defined oligomers: evaluation of stabilizing effects of lysine residues on DNA polyplexes

Minimal polymer cytotoxicity is one key aim for developing polyplexes toward therapeutic use. Polyethylenimine (PEI) has been developed as pDNA carrier with encouraging transfection properties [46, 111, 112]. It combines the ability to form stable pDNA polyplexes with a superior pH-reversible protonation and buffer capacity within the pH range of pH 6.0 to 7.4. Nevertheless, cytotoxicity limits its application as gene therapy carrier. Different approaches have been reported for reducing the toxicity by dissecting PEI into smaller segments of repeating diaminoethane units connected in a more biocompatible, biodegradable manner [113-119]. To combine low cytotoxicity with high precision polymer synthesis [120], we developed artificial oligo(ethanamino) amino acids such as succinoyl pentaethylene hexamine (Sph) in properly protected form for use in standard solid-phase supported peptide synthesis (SPPS) [55, 58]. This chemical peptide synthesis uses linkers attached to small porous beads, resins, for building up peptide chains. Repeated deprotection-washing-coupling-washing cycles are characterizing this method. The advantage of SPPS lies in the opportunity to remove excess of reagents by filtration as well as to perform washing steps after each reaction due to the immobilization of the peptide on the resin. This enables effective and fast coupling of amino acids to the growing peptide chain. Figure 3.1. illustrates the principles of SPPS. Figure 3.2. is showing the structures of used protected artificial amino acid Sph as well as natural amino acids for SPPS.

Results

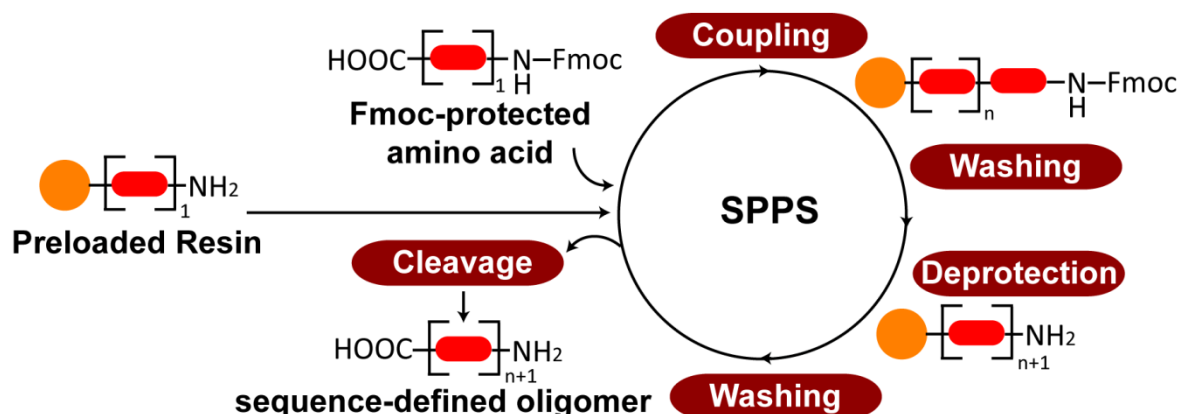


Figure 3.1. Illustration of repeating cycles of deprotection-washing-coupling-washing steps characterizing SPPS. Firstly, the C-terminal amino acid is coupled to the linker, which is attached to the resin. By repeating a cycle of deprotection, washing, coupling and washing steps the peptide chain is elongated. At the end of the synthesis, the final peptide is obtained after the cleavage from the resin and removal of permanent protecting groups.

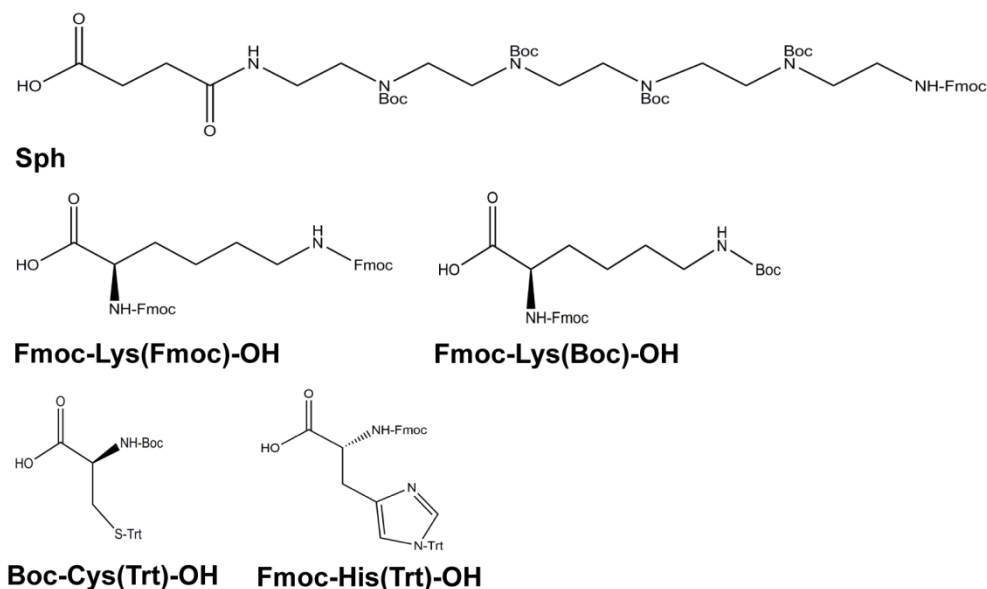


Figure 3.2. Structures of used protected artificial amino acid Sph containing a diaminoethane building block and protected natural amino acids histidine, lysine and cysteine.

Results

Based on this strategy, new sequence-defined DNA carriers were designed and synthesized. These carriers represent the third generation of previously reported oligomers with four-arm topology. In the first generation, the methods of four-arm oligomer syntheses [58], the discovery of Sph as particularly effective building block, and the polyplex-stabilizing properties of terminal cysteines [55] was established. In the previous second generation, incorporation of histidine residues for fine-tuning the proton sponge activity resulted in oligomers such as AK[HK[(H-Sph)₃C]₂]₂ (compound ID: 606) which already showed high endosomal escape and DNA transfer efficacy both *in vitro* and *in vivo* [56]. The current third-generation oligomers contain additional lysine residues to provide primary amino groups facilitating conjugation of amine-reactive shielding agents to the surface of polyplexes. Furthermore, an increased binding ability toward the negatively charged phosphates of DNA was hypothesized. Oligolysines have been extensively studied before, and are today well known for their ability to form stable particles [121-123]. Figure 3.3. and Table 3.1. give an overview over the synthesized oligomers.

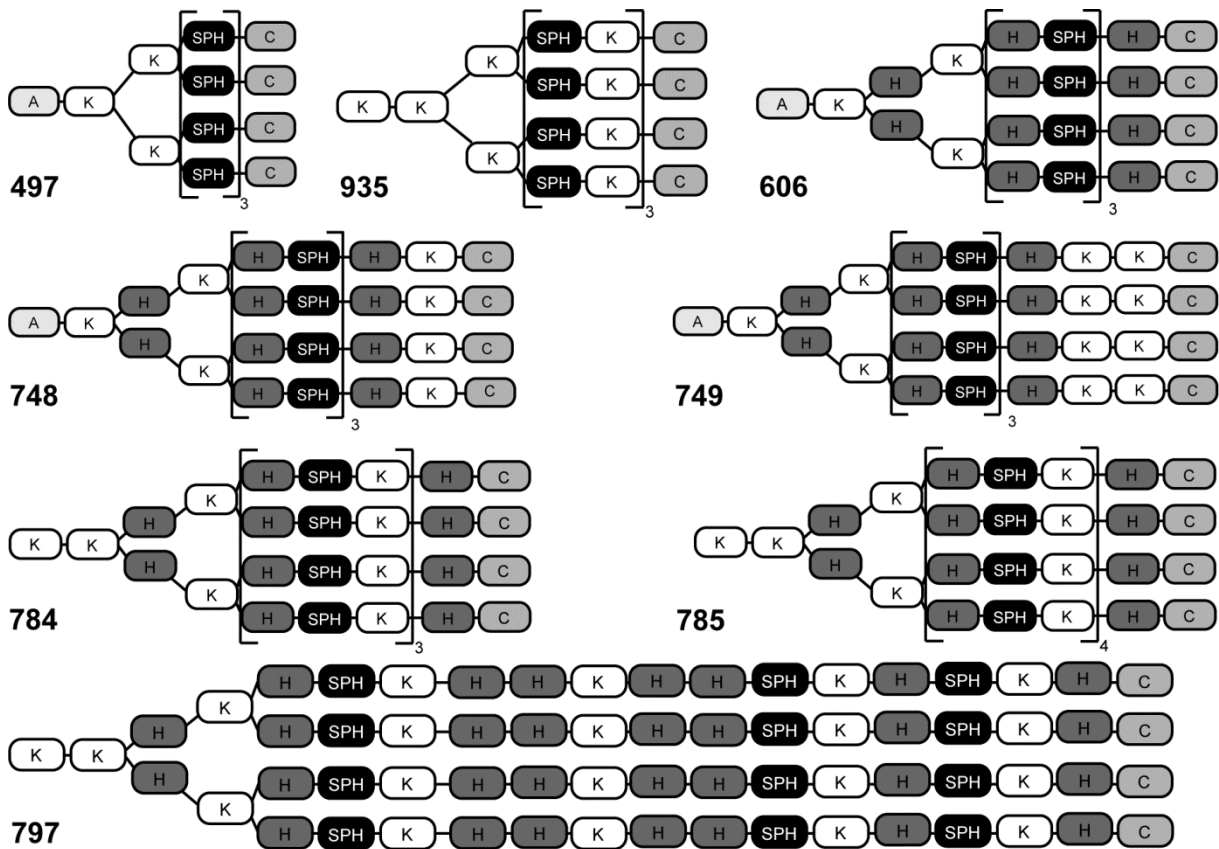


Figure 3.3. Illustration of the synthesized four-arm structured oligomers comprising of different natural and artificial amino acid residues.

Results

Table 3.1. Compound ID, abbreviation, molecular weight and amount of protonatable amines of all investigated oligomers. Oligomer 497 was synthesized by Dr. Edith Salcher (Pharmaceutical Biotechnology, LMU).

Compound ID	Abbreviation	Molecular weight [Da]	Protonatable amines
497	A(SpH) ₃	6557.31	52
606	A/0K	9647.67	70
748	A/1K	10304.43	74
749	A/2K	10961.19	78
784	K(H-Sph-K) ₃	11711	83
785	K(H-Sph-K) ₄	14902	107
797	K(H-Sph-K) ₃ + extra His	13908.67	95
935	K(Sph-K) ₃	8619.58	65

Initially, one (compound ID 748) or two (compound ID 749) lysine residue(s) were introduced in the four-arm pattern just before the terminal cysteines. However, oligomer 748 and 749 showed only a slight increased DNA binding efficiency respectively polyplex stability compared to the counterpart structure 606. Therefore, additional lysine residues were incorporated within the H-Sph repeating pattern of the four-arm sequence (oligomer ID 784). This repeating H-Sph-K pattern was further elongated from 3 to 4 moieties forming oligomer 785. To increase endosomal release a histidine-rich area was introduced within the sequence of oligomer 784 resulting in oligomer 797. Additionally, control oligomer 935 containing a four-arm Sph-K repeating pattern and oligomer 497 (synthesis by Dr. Edith Salcher, Pharmaceutical Biotechnology, LMU) comprising only Sph within the four-arm sequence were synthesized. Polyplexes were formed and evaluated in concern of nucleic acid binding efficiency, size and zeta potential, buffer capacity as well as *in vitro* and *in vivo* transfection efficiency.

Results

3.1.1. Biophysical characterization of oligomers concerning DNA binding ability, particle size, zeta potential and buffering capacity

The binding ability of the various synthesized oligomers is expected to increase by the introduction of lysine residues and was therefore evaluated by agarose gel shift assays (Fig. 3.4.). In this assay, free pCMVL is migration without hindrance in the gel, whereas sufficient polyplex formation is resulting in a complete loss of electrophoretic mobility indicated by a sharp band at the position of the samples' well. In case of lysine-rich oligomers complete pCMVL binding, even at low nitrogen/phosphate ratio (N/P ratio) of 3, was observed with the exception of oligomer 748 and 749. Those oligomers displayed similar to the control oligomer 497 and 606, which are comprised of no additional stabilizing lysine residues, no sufficient pCMVL binding at N/P 3, suggesting a lower pCMVL binding affinity.

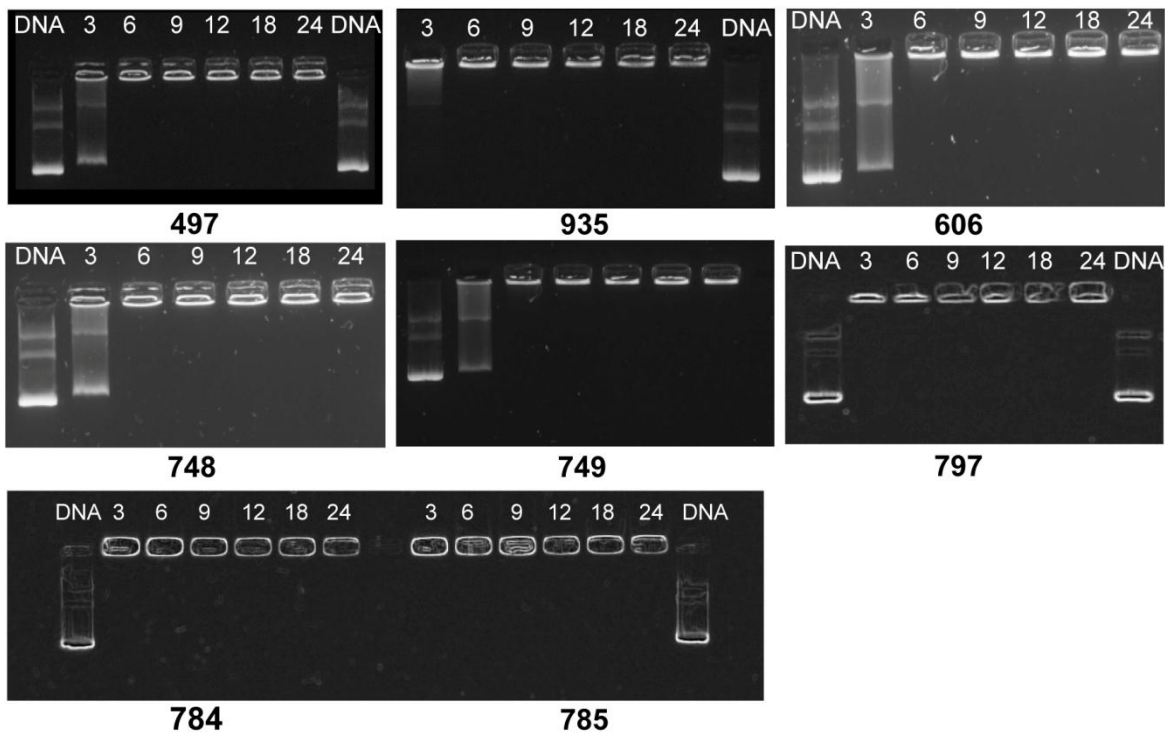


Figure 3.4. Agarose gel shift assays evaluating pCMVL binding ability of oligomers at different N/P ratios. To visualize pCMVL, 120 μ L GelRed was added to the 1% agarose gel. Polyplexes containing 200ng pCMVL and oligomer at indicated N/P ratio were prepared for 3h, 900rpm at 25°C. DNA loading buffer was added prior placing the polyplexes into the sample pockets. Electrophoresis was performed at 120V for 80min.

Results

To confirm these findings, ethidium bromide (EtBr) assays were performed. In this assay, the pDNA binding ability of the oligomer correlates with a decreasing in fluorescence activity of ethidium bromide, which was monitored after stepwise addition of an oligomer solution to a solution containing free pCMVL. In accordance to the gel shift assays, results revealed that in presence of lysine-rich oligomers 784, 785, 797 and 935, less pCMVL is available to bind EtBr as compared to the lysine-free counterpart structures 497 and 606. Figure 3.5. suggests that the pCMVL binding affinity of the lysine-rich oligomers at N/P 12 correlates to the amount of lysine residues present in the oligomeric structure. Oligomer 785 with the highest amount of lysine residues present in the oligomeric structure showed least pCMVL availability to bind EtBr compared to all other oligomers. In comparison oligomer 748 and 749 comprising of one or two terminal lysine residue(s) mediated only a slight increased pCMVL binding affinity compared to the lysine-free counterparts. These findings confirm the well-know ability of lysines to form stable particle and further support the inclusion within the oligomeric structure to improve polyplex stability.

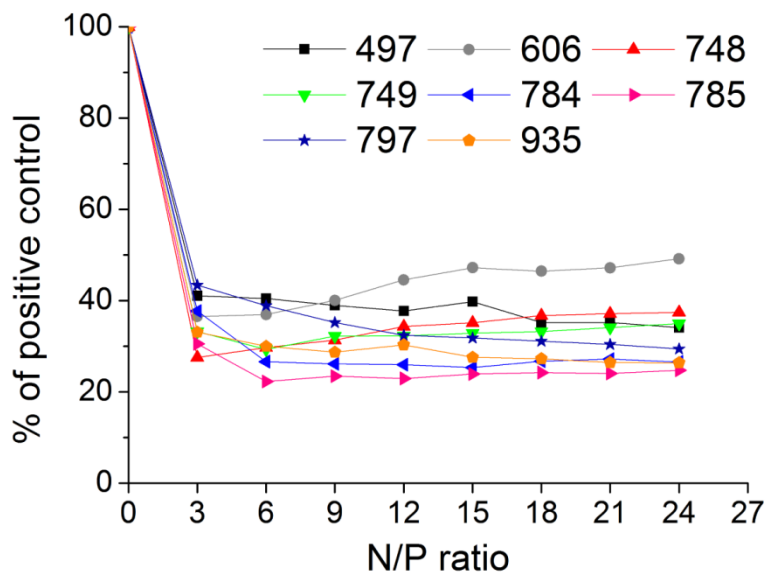


Figure 3.5. Ethidium bromide exclusion assay comparing pCMVL binding ability of the oligomers. EtBr fluorescence without pCMVL was used as a blank, and EtBr in the presence of pCMVL and absence of oligomer was set to 100%. Oligomer solution was added at increasing protonable nitrogen/phosphate ratio (N/P ratio) to the pCMVL solution and EtBr fluorescence intensity was determined.

Results

For a better understanding of these pCMVL particles, size (Z-average) and zeta potential of the polyplexes formed at N/P 12 was assessed (Table 3.2.). No significant differences were observed between the zeta potential of pCMVL polyplexes formed by lysine-rich and lysine-free oligomers. The observed zeta potentials were in the range between 22.9-32.4mV. However, polyplex sizes received by DLS measurements were in the range between 86.73 nm and 370nm. Polyplexes formed by lysine-rich oligomers 784, 785, 797 and 935 were of significantly smaller size (below 100nm) compared to those formed by lysine-free oligomers 606 and 497 (191-370nm) at the same N/P ratio. The incorporation of one (oligomer ID 748) or two terminal lysine residue(s) (oligomer ID 749) within the oligomer structure showed only a slight reduction of particle size compared to the 606 counterpart structure. Due to the fact that polyplex size is a critical parameter for successful gene delivery and bigger particle sizes are often connected to lower stability, those oligomers were not further evaluated.

Table 3.2 Particle size (Z-average), polydispersity index (PDI) and zeta potential of four-arm structured polyplexes formed at N/P 12 (n=3).

Oligomer ID	Z-average [d.nm]	PDI	Zeta potential [mV]
606	191 ± 8.64	0.176	23,5 ± 1.7
748	168.6 ± 6.8	0.285	22.9 ± 1.4
749	135.8 ± 3.9	0.234	25.0 ± 0.4
784	86.73 ± 2.14	0.22	32.4 ± 0.49
785	94.56 ± 3.2	0.114	32.3 ± 1.39
797	94.4 ± 0.89	0.245	28.23 ± 0.95
935	96.31 ± 0.86	0.056	27.97 ± 0.64
497	370 ± 65	0.314	28.3 ± 1.0

Results

In order to determine the most suitable excess of oligomer over pCMVL indicated by N/P ratio DLS was re-measured for polyplexes formed at N/P ratio 9, 12 and 18. Again, lysine-rich oligomers formed polyplexes of significant smaller sizes and slightly higher zeta potential compared to the lysine-free benchmark oligomer 606 (Fig. 3.6.). The formation of particles in case of lysine-rich oligomers seemed to be N/P-independent. Small and stable polyplexes were observed even at low N/P ratio of 9 and not further improved due to a higher N/P ratio. Within the lysine-rich oligomers, no differences in size or zeta potential were observed.

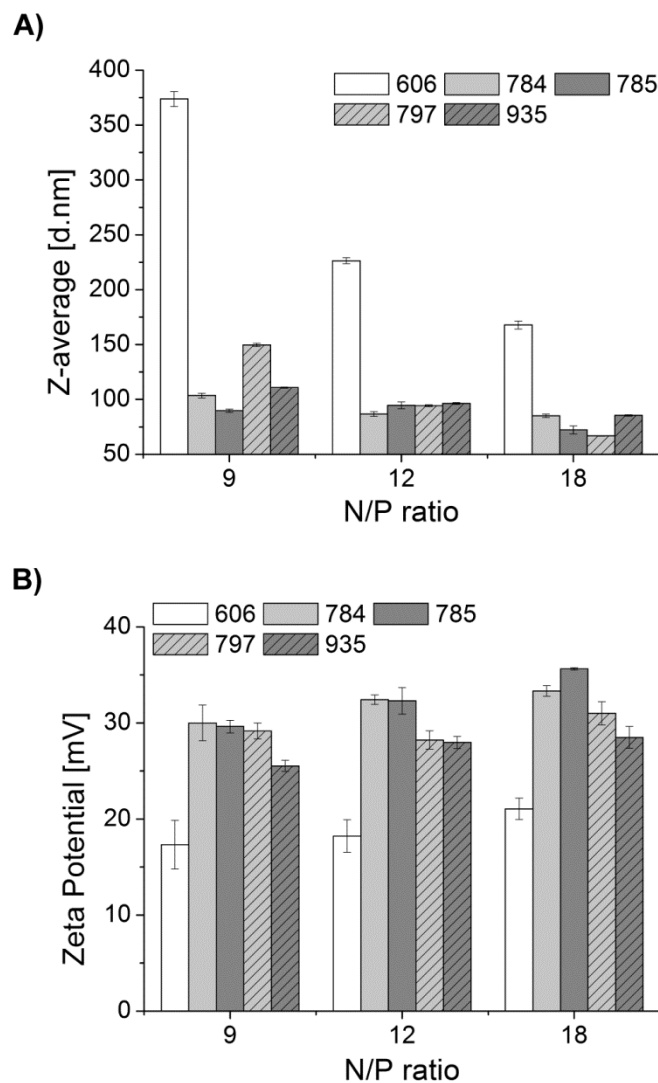


Figure 3.6. Dynamic laser light scattering measurements comparing A) particle size (z-Average, diameter in nm) and B) zeta potential of pCMVL polyplexes formed at different N/P ratios (n=3) at 25°C.

Results

Since the endolysosomal pathway presents a threat to the nucleic acids' integrity, escaping from the endosome and buffering its pH has proven essential requirements for pCMVL polyplexes [124, 125]. For this reason the buffer capacity of the oligomers was assessed via acidimetric back titration in order to evaluate the effect of lysine residues present in the oligomeric structure on buffer capacity respectively endosomal escape. Figure 3.7. shows the titration curves between the endosomal pH of 5.0 and the physiological pH of 7.4, which has to be covered by the oligomer in order to mediate sufficient endosomal release. The results indicate a decreased buffer capacity for lysine-containing oligomers in comparison to the counterpart structure 606. However, due to the introduction of a histidine-rich moiety within the H-Sph-K repeating pattern of oligomer 797 buffer capacity is increased by 24% compared to oligomer 606. Within the whole set, the flattest slope was found for oligomer 797 identifying the highest endosomal buffer capacity of all evaluated oligomers. In contrast, oligomer 935 comprising of a Sph-K repeating sequence pattern, exhibit the lowest buffering within the endosomal pH range, supporting the incorporation of histidine residues within the oligomer structure.

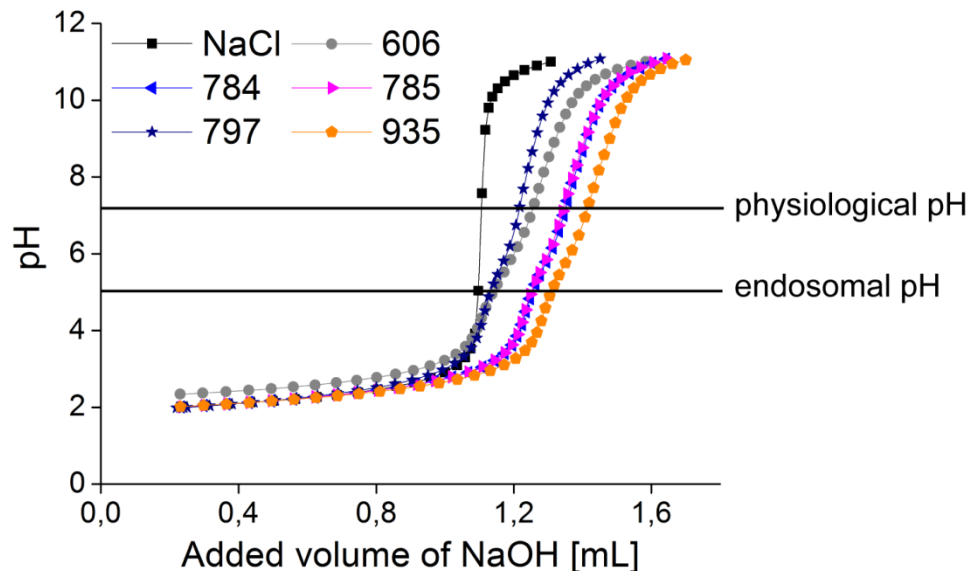


Figure 3.7. Buffer capacity of oligomers determined between pH 2.0 and 11.0 by acidimetric back titration. The highlighted range between pH 5.0 and 7.4 identifies the endosomal respectively physiological pH.

Results

3.1.2. *In vitro* characterization of DNA polyplexes

The effect of the incorporation of lysine residues within the oligomer structure on pCMVL transfection activity was evaluated using Neuro-2a cells. A bioluminescence assay was applied to quantify transgene expression after the transfection of pCMVL polyplexes. All oligomers showed up to 9-fold higher pCMVL transfection activity compared to standard carrier LPEI (Fig. 3.8.). Transgene expression mediated by the lysine-rich oligomers was up to 1800-fold improved compared to the expression level of oligomer 606 at N/P 9. Interestingly, despite the lower buffering capacity, the pCMVL polyplexes formed by oligomer 784, 785 and 935 still resulted in higher gene expression levels to those mediated by oligomer 606. Lysine-containing oligomers showed no N/P dependence in transfection efficiency, whereas for oligomers without lysine residues (497, 606) transgene expression was highly N/P-dependent. This suggests that polyplex size and zeta potential, which are closely connected to polyplex stability, are crucial parameters for successful transgene expression. For oligomer 935 containing a histidine-free Sph-K repeating pattern transgene expression was highly affected by the presence of chloroquine. In absence of chloroquine transfection efficiency was reduced by up to 200-fold, highlighting the importance of histidines within the sequence for mediating sufficient endosomal escape. Those results obtained from pCMVL transfection were in accordance to biophysical characterization and confirmed the favorable effects of lysine residue integration.

Importantly, within the investigated concentrations, the high transfection levels were not accompanied by increased cell toxicity as shown by cell metabolic activity assays. However, the addition of chloroquine showed a slightly reduction of cell viability (Fig. 3.9.).

Results

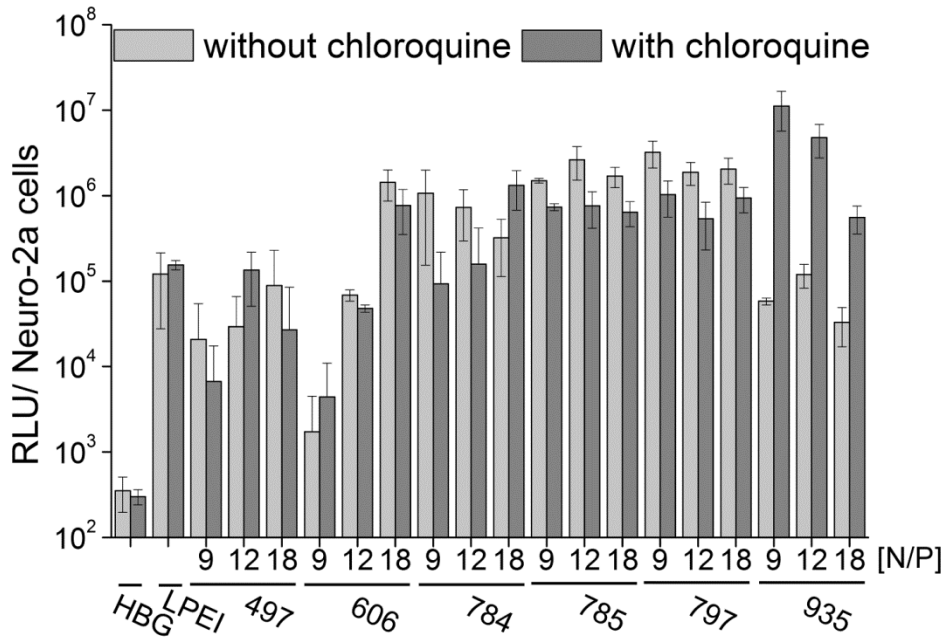


Figure 3.8. Luciferase pCMVL transfection of Neuro-2a cells with four-arm structured oligomers at indicated N/P ratio. HBG is serving as a negative control, LPEI was used as a positive control (n=5). Transfection was performed with (dark grey bars) or without (light grey bars) endosomolytic chloroquine. Data are presented as mean value (\pm SEM) of relative light units (RLU) per 10^4 cells.

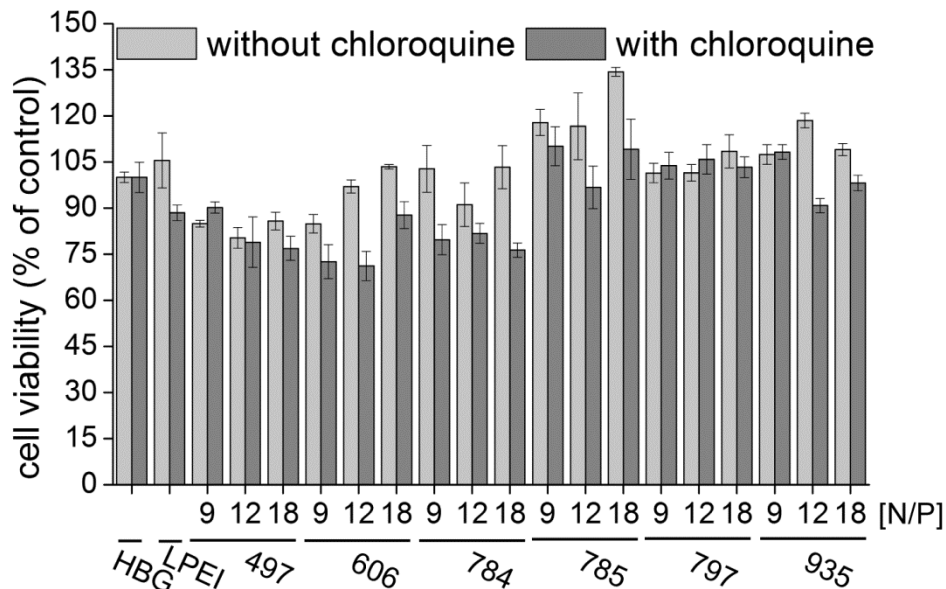


Figure 3.9. Cell viability assay on Neuro-2a cells after 24h transfection with pCMVL polyplexes determined via MTT assay at different N/P ratios. Cells were treated during transfection with (dark grey bars) or without (light grey bars) chloroquine supplemented medium. Data are presented as mean value (\pm SEM) of relative light units (RLU) per 10^4 cells.

Results

In sum, the incorporation of multiple lysine residues within the oligomer structure led to stabilized polyplexes, a prerequisite for the successful implementation of a pH-sensitive shielding concept. Based on the results obtained in the biophysical and transfection studies oligomer 784 was chosen as benchmark oligomer for the formation of shielded polyplexes.

3.2. Design and biophysical characterization of shielded polyplexes

This chapter has been adopted from:

Linda Beckert, Libor Kostka, Eva Kessel, Ana Krhac Levacic, Hana Kostkova, Tomas Etrych, Ulrich Lächelt, Ernst Wagner: "Acid-labile pHPMA modification of four-arm oligoaminoamide pDNA polyplexes balances shielding and gene transfer activity *in vitro* and *in vivo*." Eur. J. Pharm. Biopharm., doi:10.1016/j.ejpb.2016.05.019 (2016).

Polyplexes devoid of surface shielding tend to form large aggregates under physiological conditions. Therefore, shielding molecules are often attached to the surface of the polyplexes to increase their physiological stability and to avoid unwanted interactions, in particular with blood components (RES cells, opsonins), as a result of the reduction in the positive surface charge [85, 126]. Aiming at a system capable of *in vivo* delivery, we studied and compared side by side two of the most commonly used shielding polymers: PEG and pHPMA (mono- and multivalent) concerning their impact on physiological stability of pCMVL/784 polyplexes. We applied the "post-coating" approach, a well-established strategy [75, 78, 101], where the shielding polymer is subsequently attached to the particle surface via reactive groups after pCMVL complex formation [101, 104]. However, although the introduction of shielding material may increase circulation time and avoid unwanted interactions, it also reduces the interaction of polyplexes with the target cells and prevents endosomal escape, hereby decreasing transfection efficiency [126]. Therefore, we used the pH-sensitive linker AzMMMan to connect the shielding components to the polyplexes via the primary lysine amines present in the cationic oligomer structure. Under mild acidic conditions, such as those found in tumor tissue or in the endosome, the AzMMMan linker will be hydrolyzed and the shielding polymer be released from the polyplex surface (deshielding effect), re-exposing the

Results

charged pCMVL polyplex to the surrounding environment. To test the utility of such polyplex vectors with acid-labile bond-containing coating, we have compared the delivery efficiencies to those of stably shielded polyplexes, prepared by coating with polymers containing NHS groups in case of PEG or TT groups in case of pHPMA (10kDa, 20kDa, 30kDa). Figure 3.10. illustrates this concept of a pH-sensitive shielding/deshielding of polyplexes.

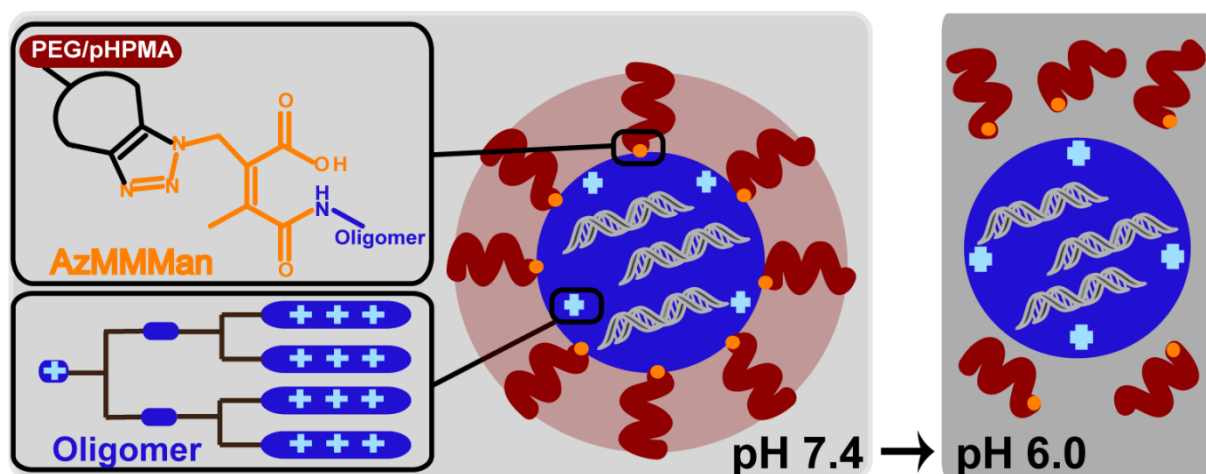


Figure 3.10. Schematic illustration of pH-reversibly surface-shielded (light grey) and deshielded (dark grey) pCMVL/784 polyplexes. Light grey: Formation of pCMVL/784 polyplex through charge-charge interactions. Complexes were pH-sensitively shielded with AzMMMan-PEG/-pHPMA at physiological pH of 7.4. Dark grey: Deshielding of the polyplexes as a result of AzMMMan-PEG/-pHPMA cleavage at mild acidic conditions of pH 6.0.

3.2.1. Biophysical characterization of shielded polyplexes

Firstly, stability studies were carried out to evaluate the influence of molecular weight and amount of reactive groups in the different shielding polymers. 5eq or 20eq of shielding material (calculated as molar excess over the oligomer) was conjugated with the pCMVL/784 polyplex, and the shielding efficiency was determined by DLS. Evaluation of particles size and zeta potential suggested that a molar excess of 20 equivalents of monovalent pHPMA and PEG resulted in an efficient decrease in zeta potential (Fig. 3.11.). The obtained zeta potential was within the range of 1mV in the case of the monovalent form of TT-pHPMA (30kDa) to 8mV in the case of AzMMMan-PEG. AzMMMan-modified polyplexes had a slightly higher zeta potential

Results

between 0.4mV for PEG and 5.3mV for monovalent pHPMA (10kDa) compared to NHS- or TT-modified polyplexes. Shielding was more efficient for pHPMA with higher molecular weight compared to pHPMA with lower molecular weight.

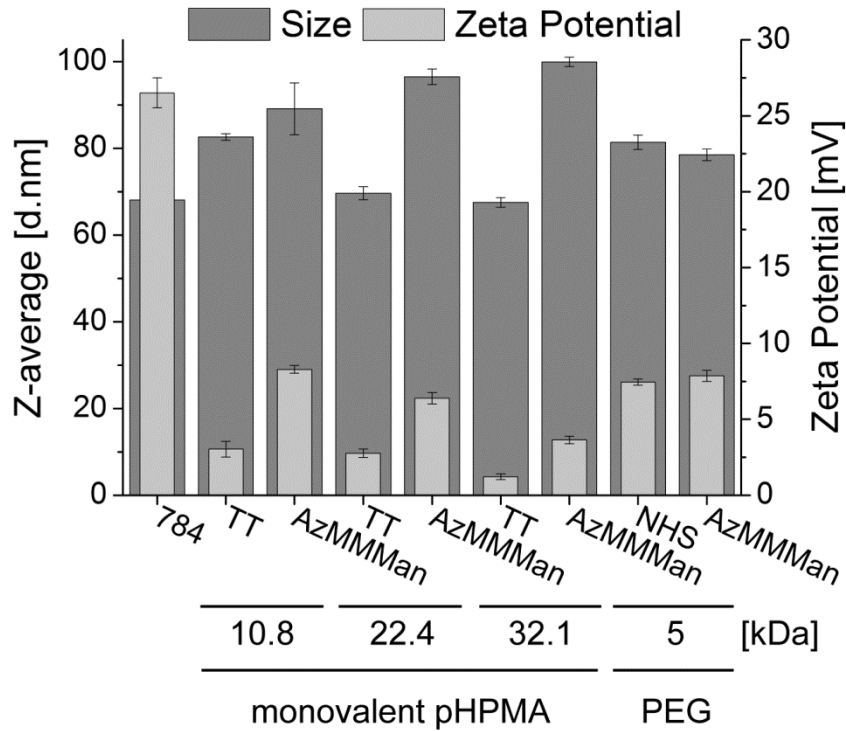


Figure 3.11. Size (diameter in nm; dark grey bars) and zeta potential [mV] (light grey bars) analysis of pCMVL polyplexes (784; N/P 12). Polyplexes were shielded with 20eq monovalent AzMMMan-pHPMA or 20eq AzMMMan-PEG. As a stable control polyplexes were shielded with 20eq TT-HPMA or 20eq NHS-PEG. All samples were measured 24h after coating at 25°C via DLS. Variations refer to the mean (\pm SEM) of three measurements of the same sample.

However, results obtained from multivalent pHPMA-shielded polyplexes shown in Fig. 3.12. identify that already 5eq is sufficient for efficient polyplex shielding. Especially, 20kDa and 30kDa multivalent pHPMA display a superior shielding efficiency. A comparison of Fig. 3.11. and Fig. 3.12. reveals that modification with 5eq excess of AzMMMan-modified pHPMA (20 and 30kDa) results in a zeta potential below -10mV, whereas 20eq of the same molecular weight monovalent pHPMA was needed to decrease zeta potential below +6mV. Particles shielded with monovalent

Results

pHPMA or PEG were stable without an increase in size or zeta potential for at least 24h, whereas shielding with multivalent pHPMA prolonged polyplex stability up to 48h. Particle size analysis showed that all coated polyplexes had an average diameter between 72nm and 100nm, suggesting no significant effect of the shielding material and used linker on particle size.

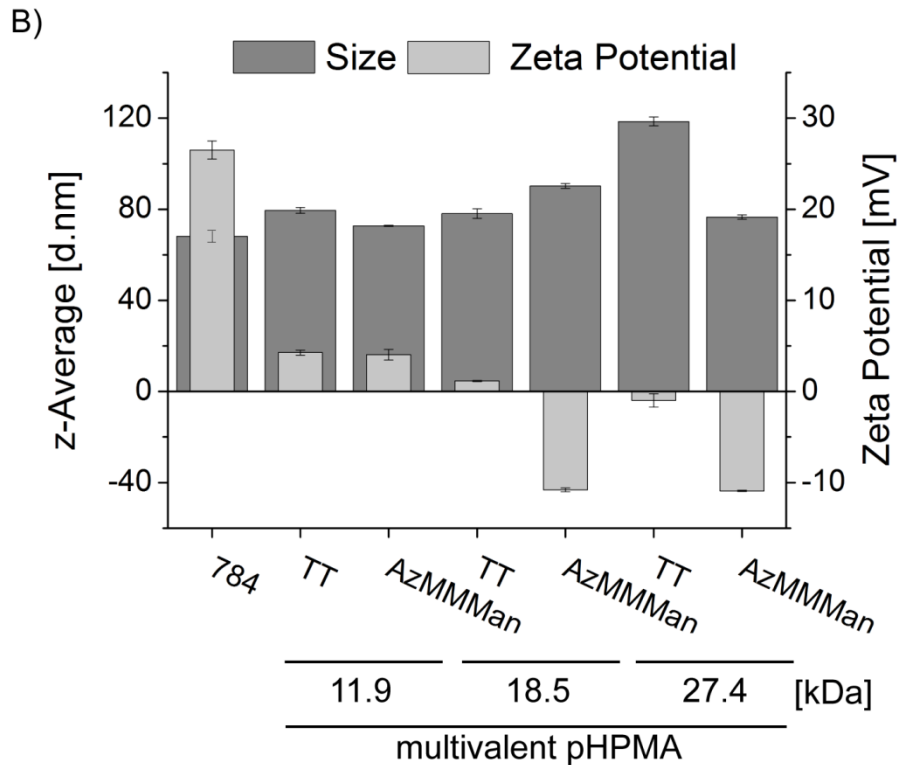


Figure 3.12. Size (diameter in nm; dark grey bars) and zeta potential [mV] (light grey bars) analysis of pCMVL polyplexes (784; N/P 12). Polyplexes were shielded with 5eq multivalent AzMMMMan-pHPMA or as a stable control with 20eq TT-pHPMA. All samples were measured 24h after coating at 25°C via DLS. Variations refer to the mean (\pm SEM) of three measurements of the same sample.

Results

Previous studies have demonstrated a stabilizing effect of various shielding materials by measuring size of polyplexes after the addition of salt, plasma or isolated blood proteins such as albumin into incubation solution [74, 127]. In an analogous fashion we studied the stability of unshielded and shielded pCMVL/784 polyplexes in highly concentrated phosphate-buffered saline, plasma and albumin solution. For this purpose, pCMVL and 784 were mixed to form the polyplex under salt-free conditions and kept for 3h before the addition of 20eq shielding material. After 24h PBS, plasma or albumin was added. In case of surface unmodified polyplexes, those solutions were added directly 3h after polyplex formation and size of the particles was measured. As expected, unmodified polyplexes rapidly aggregated after the addition of PBS, whereas shielded polyplexes remained stable, with no increase in average size within the measured time (Fig. 3.13.A). Because upon *i.v.* injection of polyplexes, interaction with blood components will likely occur, which may lead to a reduction in transgene expression activity and alteration of tissue distribution [128], and we have also studied the particle stability in plasma. Shielded polyplexes showed moderate size increase after 5min of incubation, in contrast to a rapid aggregation of unmodified pCMVL/784 complexes (Fig. 3.13.B). However, the heterogenic nature of plasma complicates the interpretation of data obtained from DLS measurements. For this purpose, the stability of particles was also evaluated in the presence of only albumin, the main protein of human blood plasma. Consistent with the stability results obtained in PBS and plasma, the incubation of pCMVL/784 polyplexes with albumin resulted in the aggregation of unshielded pCMVL/784 particles already after 5min (Fig. 3.13.C), while the incorporation of a shielding polymer had a stabilizing effect. Only after 180min of incubation the surface-modified polyplexes showed minor signs of interaction with albumin (Fig. 3.13.D).

Results

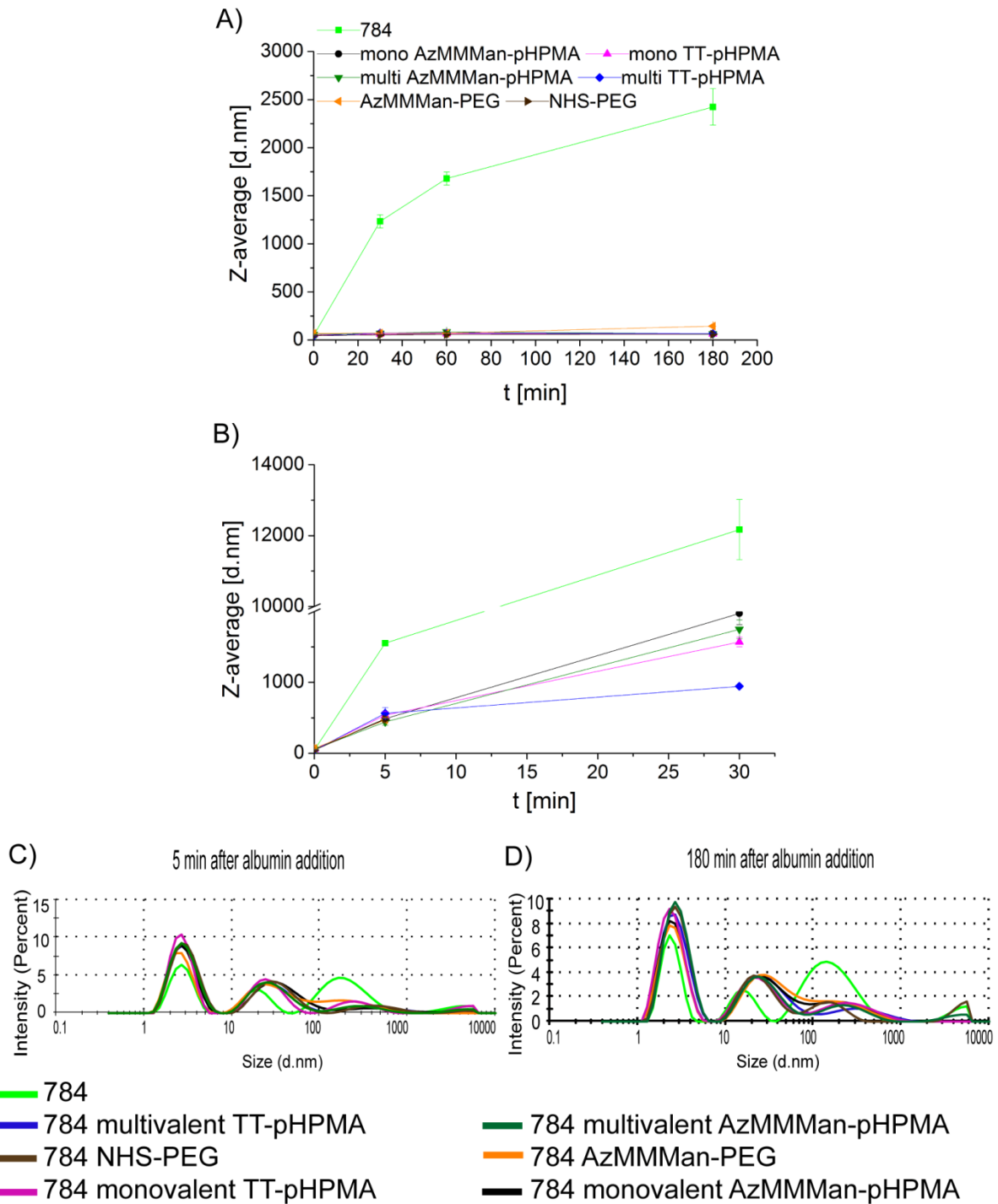


Figure 3.13. Stability testing of pCMVL/784 polyplexes (N/P 12) against A) PBS, B) plasma and C-D) albumin. Polyplexes were prepared in A) water or B-D) HEPES. Size was measured after the addition of A) 500 μ L PBS, B) 500 μ L plasma solution (8.6 μ L human plasma in 500 μ L HEPES) or C-D) 500 μ L albumin solution (50mg/mL) in HEPES and incubation at 37°C. Size (diameter in nm) was measured after different time intervals of A) 0min, 5min, 30min, 60min and 180min, B) 0min, 5min and 30min, C) 5min and D) 180min via DLS. A) Variations refer to the mean (\pm SEM) of three measurements of the same sample.

Results

The acid-triggered cleavage of the AzMMMan-polymer shielding was investigated by comparing PEG and multivalent pHPMA at endosomal pH 6.0 via size and zeta potential measurements (Fig. 3.14.). At physiological pH 7.4, NHS-PEGylated and AzMMMan-PEGylated polyplexes as well as multivalent TT- and AzMMMan-modified pHPMA polyplexes are stable in size and zeta potential for many hours up to days (compare Fig. 3.14. and 3.15.). However, 30min after acidification to pH 6.0 AzMMMan-polymer modified polyplexes started to increase in zeta potential due to the cleavage of the acid-labile linker AzMMMan. At 180min after adjustment to pH 6.0, AzMMMan-PEG or AzMMMan-pHPMA was cleaved what was detectable also by particle aggregation. These characteristics are similar to those of the unshielded pCMVL/784 polyplexes, which were also found to aggregate after acidification. As opposed to the acid-labile linker, and as expected, the polyplexes shielded with polymers, containing TT-or NHS-groups, remained stably shielded over the measurement interval.

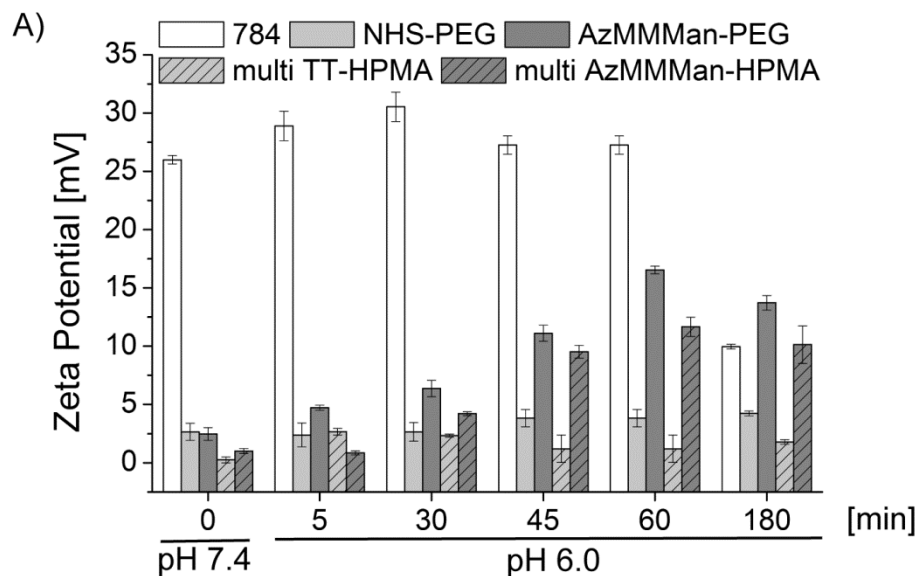


Figure 3.14.A Zeta potential analysis of pCMVL/784 polyplexes (N/P 12) shielded with 20eq AzMMMan-PEG (dark grey bars), NHS-PEG (light grey bars), multivalent AzMMMan-pHPMA (striped dark grey bars) and multivalent TT-pHPMA (striped light grey bars). Deshielding efficiency of polyplexes was evaluated at various time points at 25°C. At time point 0min, polyplexes were measured at pH 7.4. Afterwards, the pH was adjusted to 6.0 by addition of small amounts of 1N HCl. Polyplexes were measured 5-180min after incubations at pH 6.0. Variations refer to the mean (\pm SEM) of three measurements of the same sample.

Results

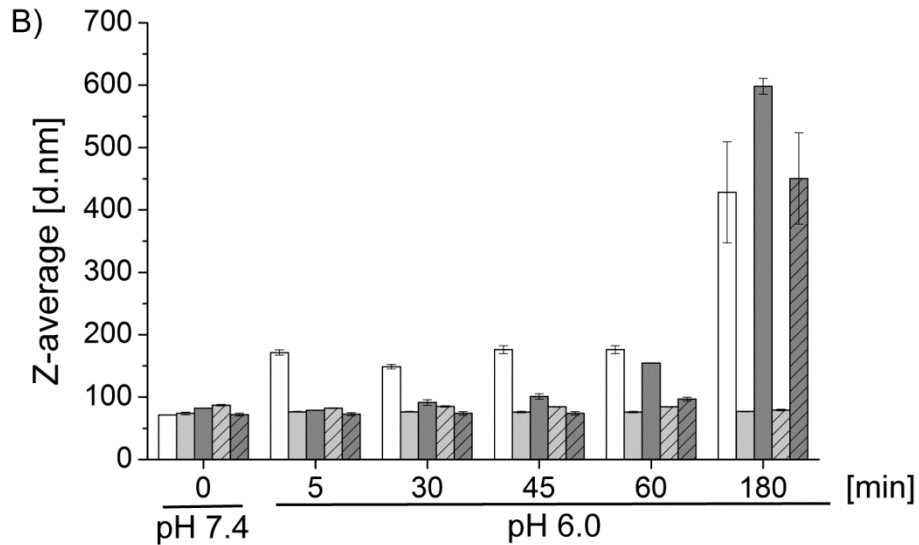


Figure 3.14.B Size analysis of pCMVL/784 polyplexes (N/P 12) shielded with 20eq AzMMMan-PEG (dark grey bars), NHS-PEG (light grey bars), multivalent AzMMMan-pHPMA (striped dark grey bars) and multivalent TT-pHPMA (striped light grey bars). Deshielding efficiency of polyplexes was evaluated at various time points at 25°C. At time point 0min, polyplexes were measured at pH 7.4. Afterwards, the pH was adjusted to 6.0 by addition of small amounts of 1N HCl. Polyplexes were measured 5-180min after incubations at pH 6.0. Variations refer to the mean (\pm SEM) of three measurements of the same sample.

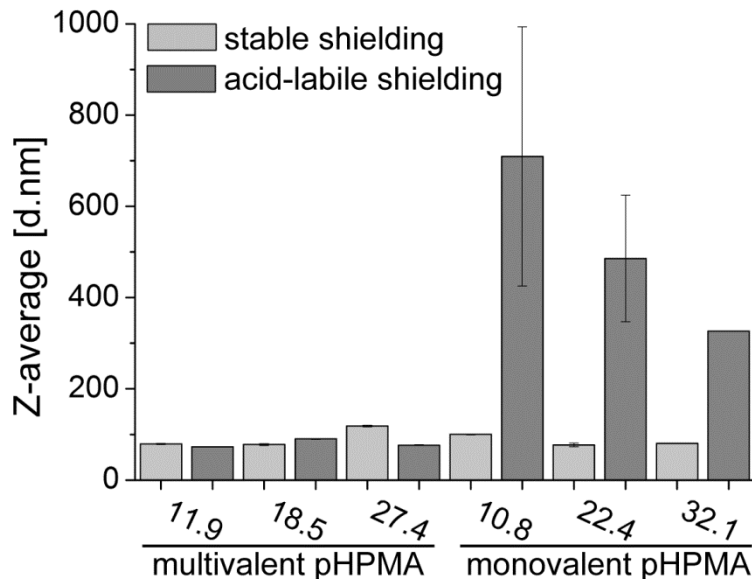


Figure 3.15. Size analysis of pCMVL/784 polyplexes (N/P 12) shielded with 5eq multivalent or 20eq monovalent pHPMA. Sizes of TT-modified (light grey bars) or AzMMMan-modified (dark grey bars) polyplexes were measured at 25°C after 48h. Variations refer to the mean (\pm SEM) of three measurements of the same sample.

Results

3.2.2. *In vitro* characterization of shielded polyplexes

The influence of polyplex shielding on luciferase gene transfer efficacy was evaluated using HUH7 hepatocellular carcinoma cells. Generally, modification of the polyplex surface with acid-labile shielding materials led to a higher luciferase transgene expression as compared to the analogous stably shielded polyplexes (Fig. 3.16.). Shielding of polyplexes with 20eq multivalent pHPMA (20kDa and 30kDa) significantly decreased transgene expression in comparison with polyplexes shielded either with 20eq monovalent pHPMA or with 20eq PEG. Fig. 3.16.A reveals a reduction in transgene expression by 13-fold for TT-pHPMA (20kDa) modified polyplex, 40-fold for AzMMMan-pHPMA (20kDa) coated, 24-fold for TT-pHPMA (30kDa) coated and 7-fold in case of AzMMMan-pHPMA (30kDa) modified polyplex compared to the monovalent shielded counterpart. By the prolongation of the transfection time from 24h to 48h (Fig. 3.16.B) the transgene expression was increased both for TT- and AzMMMan-modified multivalent pHPMA-shielded polyplexes with the highest effect of about 50-fold found for AzMMMan-pHPMA (20kDa). Nevertheless, at both transfection times pH-sensitively shielded polyplexes showed significantly higher transgene expression. Based on these data 20kDa multivalent pHPMA was considered as an optimal compromise between efficient shielding and dynamic deshielding and selected for further evaluation *in vivo*.

Results

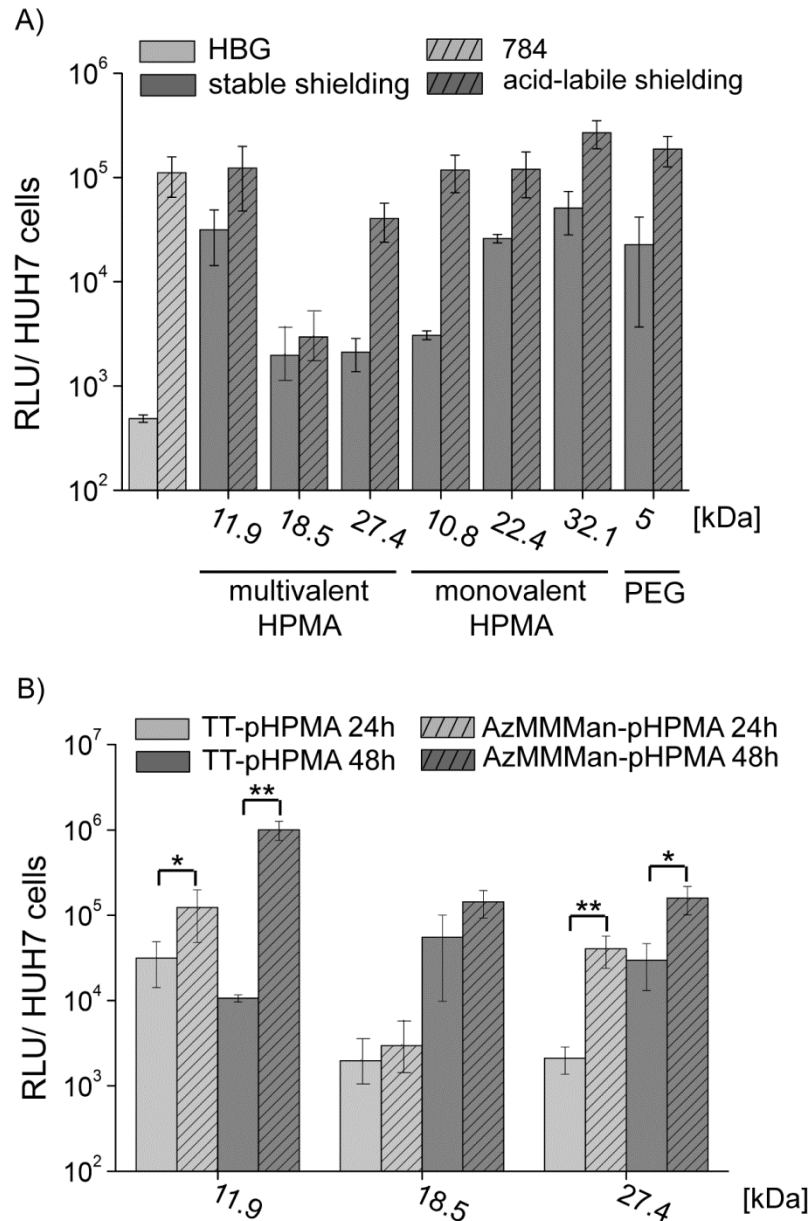


Figure 3.16. Luciferase gene transfer in HUH7 cells presented as relative light units (RLU) per well by polyplexes (pCMVL/784 at N/P 12) coated with A) 20eq multi-/monovalent AzMMMan-pHPMA or AzMMMan-PEG (striped dark grey bars) or 20eq multi-/monovalent TT-pHPMA or NHS-PEG (dark grey bars). B) Polyplexes were coated with 20eq multivalent AzMMMan-pHPMA (striped bars) or multivalent TT-pHPMA (solid bars). A) 8000 or B) 4000 HUH7 cells per well were seeded 24h prior transfection. Samples were measured A) 24h or B) 24h and 48h after transfection. Data are presented as mean value (\pm SEM) out of quintuplicates. (* P <0.05; ** P <0.01)

Results

Since often higher delivery efficiency is accompanied by undesired cell toxicity, we have assessed the effect of our polyplexes of interest on cell viability. In this regard, MTT assay revealed no significant cytotoxicity accompanying the cell transfection (Fig. 3.17.).

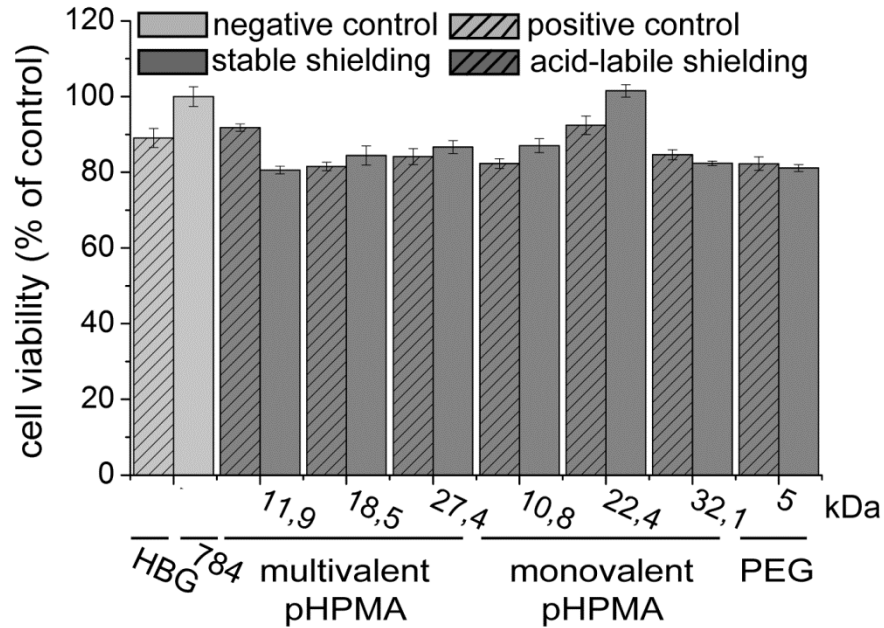


Figure 3.17. Cell viability assay (MTT assay) in HUH7 cells 24h after transfection with surface-shielded pCMVL/784 polyplexes (N/P 12). Polyplexes were shielded with 20eq AzMMMan-modified multi-/monovalent pHPMA or AzMMMan-PEG (striped bars) or TT-modified multi-/monovalent pHPMA or NHS-PEG (solid bars). Data are presented as mean value (\pm SEM) out of quintuplicates.

Furthermore, we assessed the cellular uptake, to get an indication for the underlying mechanism causing the differences in transgene expression between pH-sensitively and stably shielded polyplexes. Therefore, we generated pCMVL-labeled polyplexes shielded with 20eq NHS- and AzMMMan-PEG. After 24h transfection laser scanning microscopy (LSM) was performed to examine the cellular distribution of fluorescently labeled pCMVL. A higher amount of pCMVL was found inside the cells in case of AzMMMan-PEG-shielded compared to NHS-PEG-shielded polyplexes (Fig. 3.18.).

Results

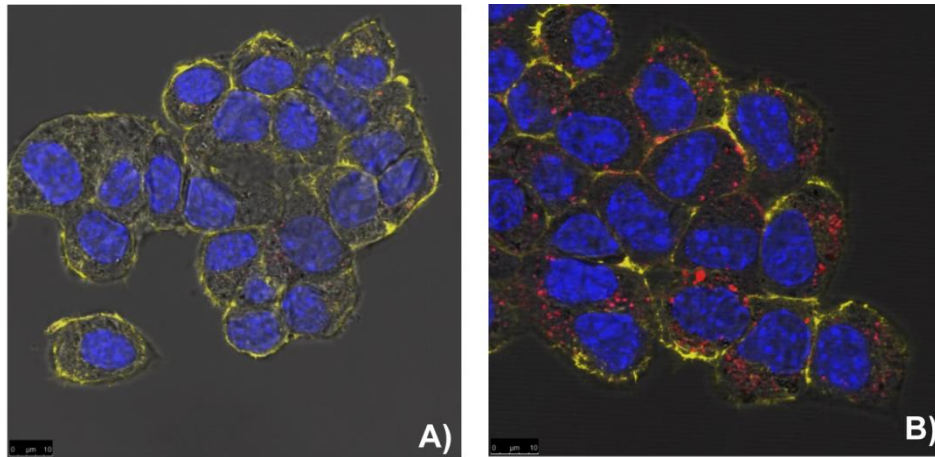


Figure 3.18. Laser scanning microscopy of Neuro-2a cells transfected with pCMVL/784 polyplexes (N/P 12) coated with A) 20eq NHS-PEG or B) 20eq AzMMMan-PEG. Pictures were obtained after 24h. DAPI was used for nuclear staining (blue), polyplexes were labeled using Cy5-labeled pCMVL (red) and rhodamine phalloidin was used to visualize cell membranes (yellow). LSM was performed by Miriam Höhn (Pharmaceutical Biotechnology, LMU).

To support these findings also with pHPMA flow cytometry analysis was performed for 20kDa mono- and multivalent pHPMA-shielded polyplexes (Fig. 3.19.). Likewise, pH-sensitively shielded polyplexes showed higher uptake efficiency after short time incubation for 2h compared to stably shielded polyplexes. In addition, the valency of pHPMA had a great influence on uptake efficacy, which corresponds to results obtained in transfection experiments. AzMMMan modification led to a 4-fold higher uptake efficacy for polyplexes shielded with multivalent pHPMA compared to 2-fold uptake in case of polyplexes shielded with monovalent pHPMA. Furthermore, this experiment revealed a 9-fold higher uptake of polyplexes with stable monovalent polymer shield compared to polyplexes with stable multivalent polymer shield. In case of AzMMMan-polymer modified polyplexes this difference was decreased to 2-fold. These results seem to be consistent with those obtained by LSM. Again, we found a superior shielding efficiency of multivalent pHPMA compared to monovalent pHPMA and an increased uptake efficiency of polyplexes due to AzMMMan modification in accordance with our DLS as well as transfection studies.

Results

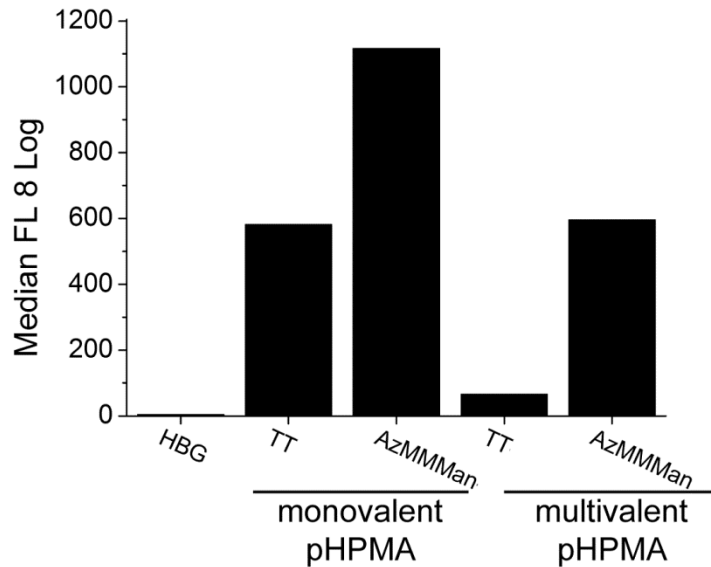


Figure 3.19. Cellular internalization of Cy5-labeled pCMVL/784 polyplexes (N/P 12) shielded with 20eq mono- or multivalent AzMMMan-/TT-modified pHPMA (20kDa) determined by flow cytometry. Assay was carried out after 2h transfection of HUH7 cells at 37°C. (n=3)

3.2.3. *In vivo* evaluation of shielded polyplexes

The *in vitro* studies encouraged us to evaluate our new DNA carrier 784 in comparison with oligomer 606 *in vivo*. Additionally, we included pCMVL/784 polyplexes that are surface-modified with multivalent AzMMMan-pHPMA (20kDa) in the *in vivo* study. Administration of the polyplexes was well tolerated by the mice and no sign of acute toxicity was obtained. Importantly, Fig. 3.20.A shows predominant gene expression of both shielded and unshielded polyplexes in the Neuro-2a tumor to a comparable level. The pH-sensitively shielded polyplexes displayed the highest gene expression followed by unshielded 784 and 606 polyplexes. Additionally, the incorporation of lysine moieties in the oligomeric structure did not have a negative influence on transgene expression in the tumor tissue, which was at least comparable to the lysine-free structure of oligomer 606. Comparing the tumor/liver ratio of luciferase expression level, AzMMMan-pHPMA shielded polyplexes displayed a high tumor/liver expression ratio of 6, whereas a ratio below 2 was observed in case of unshielded 784 and 606 polyplexes. To draw comparisons to our pH-sensitively shielded polyplexes we included multivalent TT-pHPMA-modified pCMVL/784 polyplexes in the *in vivo* study (Fig. 3.20.B). The substitution of AzMMMan for TT results in a decreased gene expression in tumor and liver.

Results

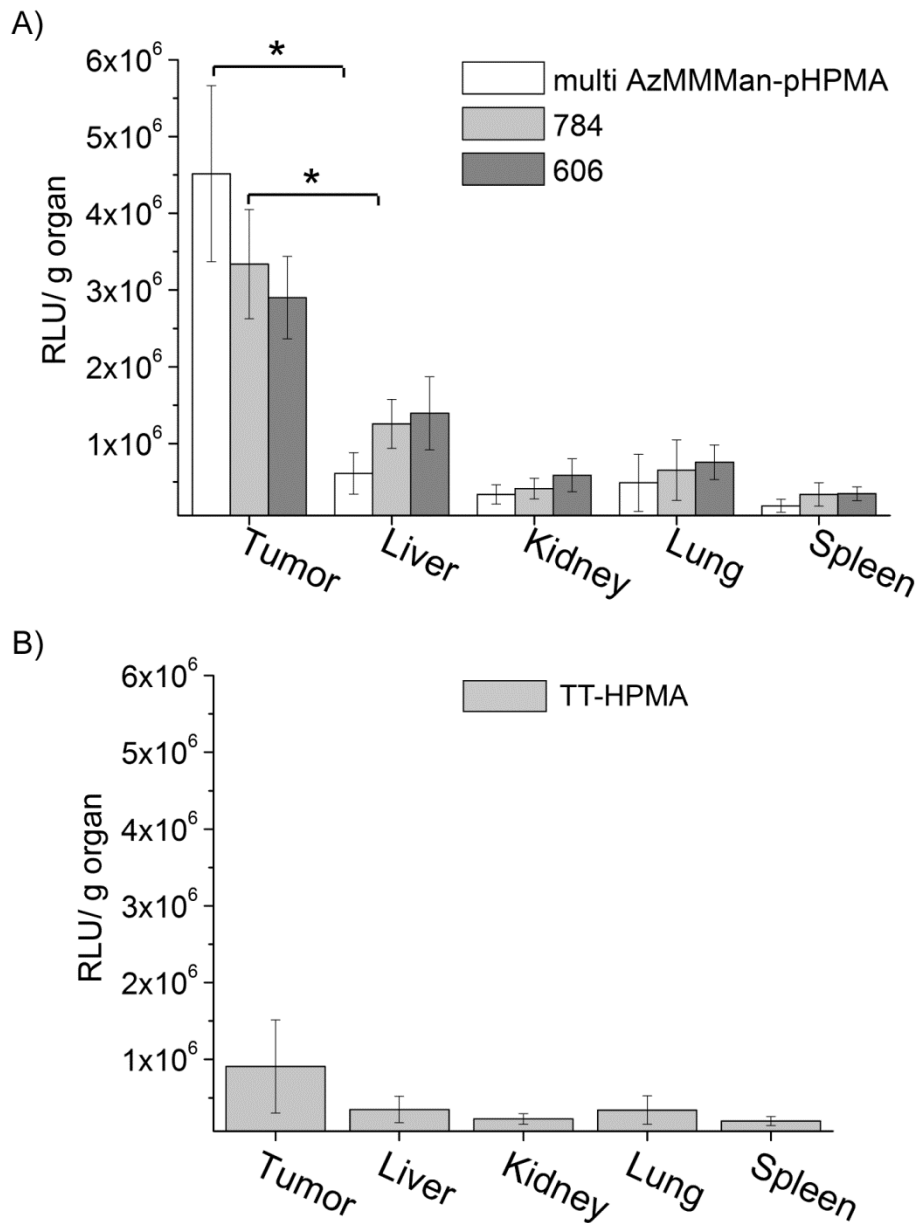


Figure 3.20. A) Luciferase gene expression *in vivo* after systemic *i.v.* administration of pCMVL polyplexes in Neuro-2a tumor bearing NMRI mice. Comparison of non-shielding pCMVL polyplexes formulated with polymer 606 (N/P 12; dark bars), 784 (N/P 12; grey bars), and AzMMMan-pHPMA-shielded pCMVL/784 polyplexes (N/P 12), shielded with 5eq AzMMMan-modified multivalent 20kDa pHPMA (white bars). B) *In vivo* luciferase gene expression after systemic *i.v.* administration of multivalent TT-pHPMA (20kDa) shielded pCMVL/784 polyplexes in Neuro-2a tumor bearing NMRI mice.

Luciferase gene expression is presented as relative light units per organ weight (RLU/g of organ; n=5). *In vivo* experiments were performed by Eva Kessel (Pharmaceutical Biotechnology, LMU). (*P<0.05)

Results

3.3. Folate receptor-directed pCMVL/784 polyplexes for gene transfer *in vitro*

Folic acid is involved in several biochemical reactions as one of the basic building blocks and catalyst. It is essential for DNA synthesis (and in cell division processes), thus affecting rapidly dividing cells such as hematopoietic cells or blood forming cells as well as cancer cells. Consequently, the folate receptor protein (FR) has emerged as a therapeutic target for the treatment of various cancers, such as ovarian, lung or breast cancer, as well as chronic inflammatory diseases. The over-expression of FR on the surface of malignant cells and the high natural affinity of folic acid for the FR enables selective delivery of folate-conjugated drugs with minimal collateral damage of mammalian cells. Additionally, folate acid as a targeting ligand has numerous advantages over macromolecular ligands (e.g. antibodies) such as: (1) the small size which reduces the probability of activating the immune system thus enabling repeating administration, (2) easy chemical conjugation, (3) low cost, (4) ease of synthesis or commercial availability and (5) internalization via endocytosis without alteration of covalently conjugation of small molecules [73, 129, 130]. To date, protein toxins, chemotherapeutic agents, immunotherapeutic agents, liposomes, oligonucleotides, radioimaging agents and radiotherapeutic agents have been linked to folic acid for tumor specific drug delivery demonstrating the considerable promises of FR as therapeutic target [131]. In addition, several groups have successfully applied Folate as a targeting ligand for nucleic acid delivery. For example, He et al. demonstrated targeted gene transfer *in vitro* using sequence-defined cationic polymer-DNA as well as siRNA complexes linked with folic acid [132]. Furthermore, Dohmen et al. showed that an endosomolytic influenza peptide-siRNA conjugate encapsulated within folate-targeted sequence-defined carrier mediated receptor-specific cell-targeting *in vitro* and *in vivo* in absence of unspecific accumulation in non-targeted tissue such as lung, spleen and liver [133]. Within twenty-five years after the first identification of the upregulation of FR in cancer the development of folate-linked drugs has moved from bench to bedside with current four ongoing clinical trials evaluating the potency in concern of cancer treatment [131, 134].

Results

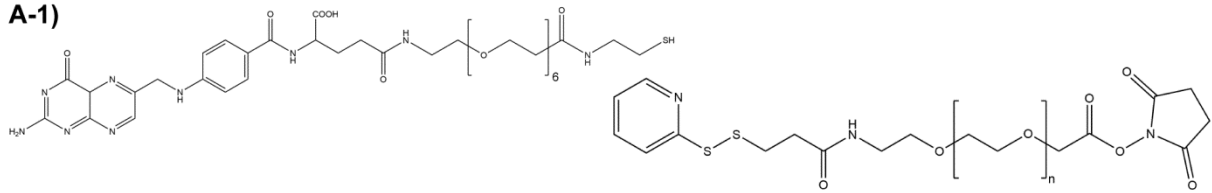
3.3.1. Synthesis of the post-PEGylation reagents FoIA-PEG(5000)-AzMMMan and FoIA-PEG(5000)-NHS

In order to achieve highly efficient gene transfer to FR over-expressing tumor cells the targeting ligand folic acid was integrated within the shielding moiety of the polyplexes. Therefore, two chemical synthesis approaches were evaluated suitable for the attachment of the targeting ligand folic acid to a bifunctional PEG reagent. The synthesis of FoIA-PEG₆-cysteamine via solid-phase assisted synthesis is one route for the ligand preparation (Fig. 3.21.A-1/A-2). As solid support a 1-amino-ethane-2-thiol(cysteamine)-2-chlorotrityl resin was used. First, Fmoc-N-amido-dPEG₆-acid was coupled to the resin. The reactor was agitated until Kaiser test indicated complete conversion. After Fmoc cleavage, Fmoc-Glu(OH)-tBu and N¹⁰-(Trifluoroacetyl)pteroic acid were attached in additional separate steps followed by the removal of the TFA group and the cleavage of the targeting ligand off the resin. A short PEG spacer consisting of 6 ethylene oxides monomers was inserted to increase solubility of the targeting ligand. A bifunctional PEG reagent was used subsequent functionalized with a pyridyldisulfide at the ω-end of the PEG chain and an activated ester (NHS-group) for amide bond formation (OPSS-PEG(5000)-NHS). For the synthesis of a FoIA-modified pH-sensitive shielding moiety the activated ester was firstly modified with DBCO-PEG₄-NH₂ and afterwards the pH-sensitive linker AzMMMan was attached.

Additionally, an alternative synthesis route via the preparation of FoIA-NHS according to Liu et al. [110] was evaluated. In this regard, folic acid, 1.1eq NHS and 1.1eq *N,N*-dicyclohexylcarbodiimid (DCC) were dissolved in DMSO and the reaction mixture was stirred for 2h in the dark. Filtration was applied to remove the insoluble byproduct dicyclohexylurea. The product was precipitated in ACN, washed with diethyl ether and dried to a powder. For this alternative synthesis route SH-PEG(5000)-NH₂ was used and modified with DBCO-PEG₄-Mal. Thereafter, the targeting ligand FoIA-NHS was attached. Furthermore, the pH-sensitive linker AzMMMan or, as a stable control, NHS-C₃-Azide was introduced (Fig. 3.21.B).

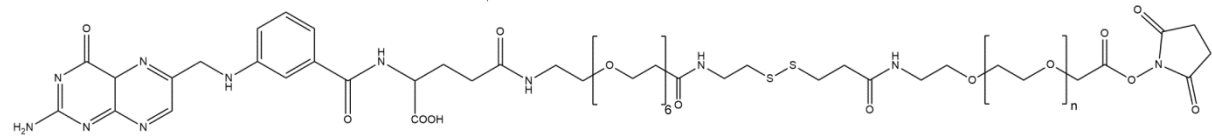
Results

A-1)



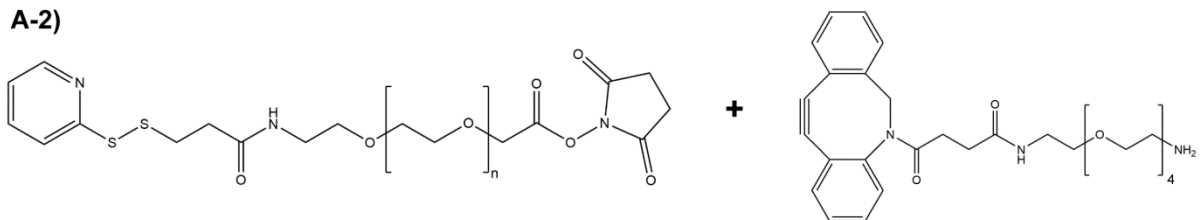
FoIA-PEG(5000)-NHS

OPSS-PEG(5000)-NHS



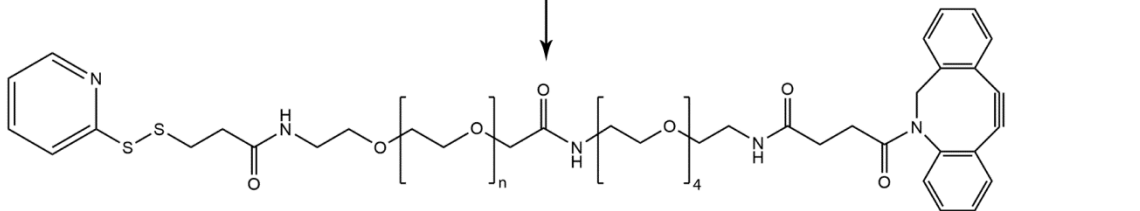
FoIA-PEG(5000)-NHS

A-2)



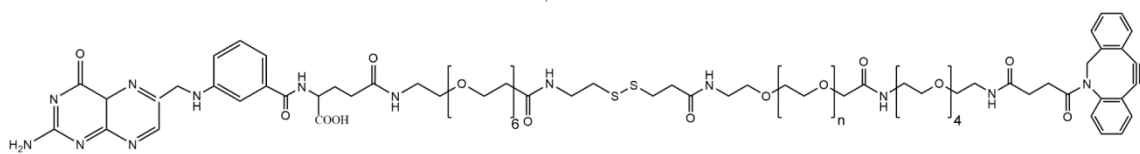
OPSS-PEG(5000)-NHS

DBCO-PEG₄-NH₂



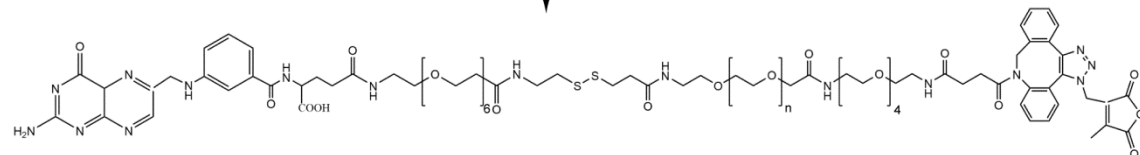
OPSS-PEG(5000)-DBCO

+ FoIA-PEG₆-Cysteamine*



FoIA-PEG(5000)-DBCO

+ AzMMMan



FoIA-PEG(5000)-AzMMMan

* synthesized by solid-phase assisted peptide synthesis

Results

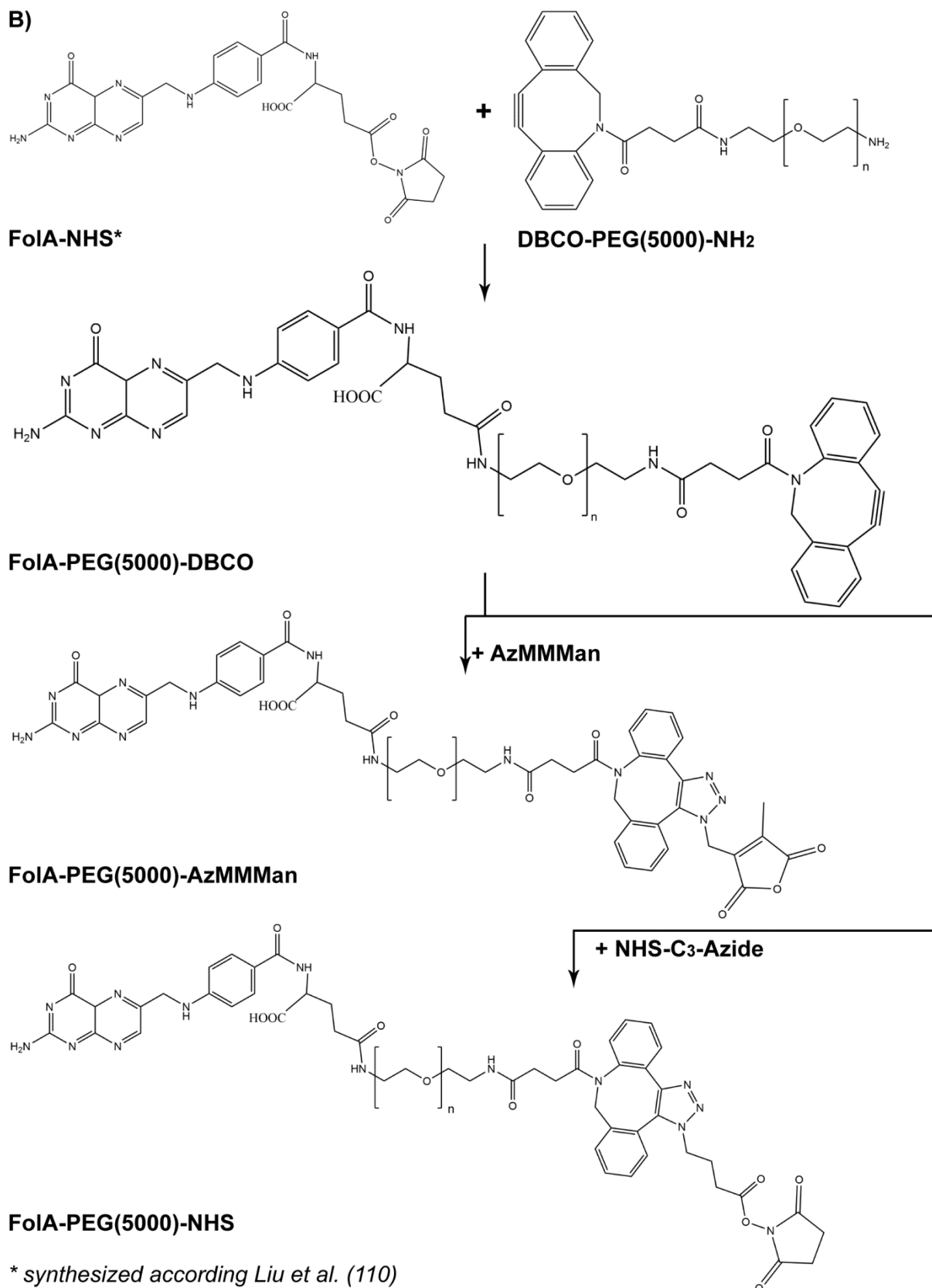


Figure 3.21. Synthesis of AzMMMan- or NHS-modified FoIA-targeted bifunctional post-PEGylation reagent via A-1/A-2) FoIA-PEG₆-cysteamine, synthesized via solid-phase approach, or B) FoIA-NHS, synthesized according Liu et al. [110].

Results

Initial attempts to characterize the newly synthesized targeting-shielding reagent and to evaluate the two synthesis approaches for ligand preparation concerning feasibility and compatibility via NMR failed due to several reasons. Firstly, NMR analysis was limited due to the lack of a clear reference peak of the PEG(5000) moiety. Additionally, the overlap of Folate peaks and the large PEG backbone peak complicated the interpretation of NMR data. Furthermore, the quantitative estimation of linked Folate to the PEG(5000) moiety via NMR analysis was difficult due to the much larger and undefined MW of the PEG(5000) moiety compared to the rather small MW of the targeting ligand Folate. For this purpose, laser scanning microscopy was performed using KB cells to evaluate indirectly the two synthesis approaches for ligand preparation. In this regard, receptor binding efficiency of labeled Folate-modified PEG toward the FR was examined (Fig. 3.22.A-C). Therefore, an azide-modified TAMRA dye was attached to the Folate-PEG(5000)-DBCO reagent prepared either by synthesis via Folate-NHS or Folate-PEG₆-cysteamine. KB cells were incubated for 45min with A) 50nmol unmodified TAMRA-azide dye, B) 50nmol Folate-PEG(5000)-TAMRA synthesized via Folate-NHS or C) 50nmol Folate-PEG(5000)-TAMRA prepared from Folate-PEG₆-cysteamine. Afterwards, cells were washed and stained with DAPI. In a control experiment cells were preincubated with folic acid saturated RPMI medium to compete receptor binding between an excess of Folate and the targeting-shielding reagent to examine the receptor specific attachment (Fig. 3.22.D-F).

Figure 3.22.A displays high fluorescence intensity of TAMRA-azide dye in the endosomes without intensity changes after the preincubation of KB cells in folic acid saturated RPMI medium (Fig. 3.22.D) suggesting an unspecific uptake of the dye by the cells. The same findings were made for Folate-PEG(5000)-TAMRA prepared from Folate-NHS (Fig. 3.22.B, 3.22.E). Those results show that the attempt to synthesize a Folate-modified shielding reagent via Folate-NHS was unsuccessful. However, in case of the targeting-shielding reagent synthesized via Folate-PEG₆-cysteamine a bright fluorescent ring around the cell membrane was visible (Fig. 3.22.C). This fluorescent ring on the cell surface was only observed in absence of a folic acid excess suggesting receptor specificity of the targeting-shielding reagent prepared from Folate-PEG₆-cysteamine via SPPS (Fig. 3.22.E). Consequently, the synthesis approach of the targeting-shielding reagent via Folate-PEG₆-cysteamine was used for the preparation of Folate-targeted PEG-shielded polyplexes, characterized in the following experiments.

Results

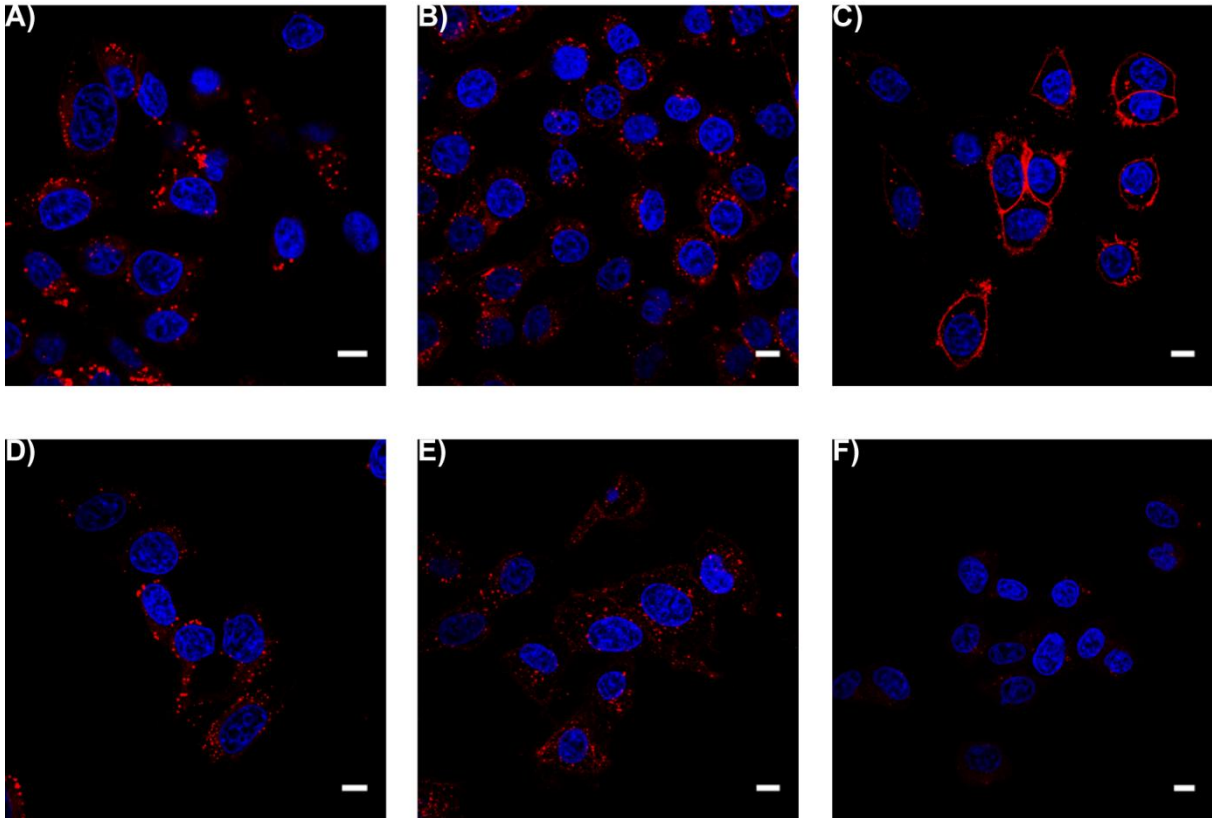


Figure 3.22. Laser scanning microscopy evaluating receptor-specific binding of A) 50nmol TAMRA-azide dye, B) 50nmol FoIA-PEG(5000)-TAMRA prepared from FoIA-NHS and C) 50nmol FoIA-PEG(5000)-TAMRA synthesized via FoIA-PEG₆-cysteamine using solid-phase assisted peptide synthesis. FR-positive KB cells were incubated in FoIA-free RPMI medium. In a control experiment receptor-specific binding was evaluated for D) 50nmol TAMRA-azide dye, E) 50nmol FoIA-PEG(5000)-TAMRA synthesized via FoIA-NHS and F) 50nmol FoIA-PEG(5000)-TAMRA prepared from FoIA-PEG₆-cysteamine. For this experiment FR-positive KB cells were preincubated in FoIA-saturated RPMI medium to compete receptor binding. DAPI was used for nuclear staining. Microscopy was carried out by Kenneth Börner (Molecular Biology, LMU).

Results

3.3.2. Biophysical characterization of F_oIA-targeted, stably or pH-sensitively shielded pCMVL/784 polyplexes

Targeting strategies aim at the improvement of the specificity of pharmaceutical formulations e.g. gene delivery systems to certain cell types or tumors. Previous experiments in this thesis have shown a beneficial effect of introducing the pH-sensitive linker AzMMMan between the shielding material and the polyplexes by evading the "PEG dilemma". Additionally, "passive targeting" was shown for polyplexes surface-modified with 20eq multivalent AzMMMan-modified pHPMA (20kDa) in a xenograft mouse model *in vivo* due to the enhanced permeability and retention effect. However, to enable cell type specific uptake beyond the tissue accumulation the introduction of a targeting ligand is indispensable. In this regard, the effect of introducing a F_oIA-targeted NHS- or AzMMMan-modified PEG moiety within pCMVL/784 polyplexes on size and zeta potential was firstly evaluated via DLS measurements.

According to previous *in vitro* studies the post-PEGylation approach was once again chosen for the surface modification of pCMVL polyplexes. However, due to the structural complexity of the stable- or pH-sensitive-modified F_oIA-targeted PEG moiety, various approaches to attach this moiety to the polyplex surface were evaluated concerning the effect on polyplex size and zeta potential as well as on *in vitro* transfection efficiency. Additionally, the effect of varying amounts of the targeting ligand F_oIA was determined. In this respect, pCMVL/784 polyplexes were formed for 45min and post-PEGylation reagent was added and incubated for 3h prior DLS measurements (Fig. 3.24.A-B). In case of polyplexes numbered No.2 and No.3 20eq AzMMMan (No.2) respectively 20eq NHS-C₃-Azide (No.3) were added 2h prior the addition of 20eq F_oIA-PEG(5000)-DBCO. Shielding reaction was performed for 1h. Similar to polyplexes No.2 and No.3, 20eq of AzMMMan (No.4) or 20eq NHS-C₃-Azide (No.5) were added in case of polyplexes numbered 4 and 5. Thereafter, 5eq F_oIA-PEG(5000)-DBCO was added 15min prior the addition of 15eq DBCO-PEG(5000). DLS was measured 45min after the addition of DBCO-PEG(5000). Polyplexes No.6 and No.7 were shielded in one step with 20eq F_oIA-PEG(5000)-AzMMMan (No.6) or F_oIA-PEG(5000)-NHS (No.7) for 3h followed by DLS measurements. Figure 3.23. outlines the different post-coating strategies applied for the formation of F_oIA-targeted PEG-shielded pCMVL/784 polyplexes.

Results

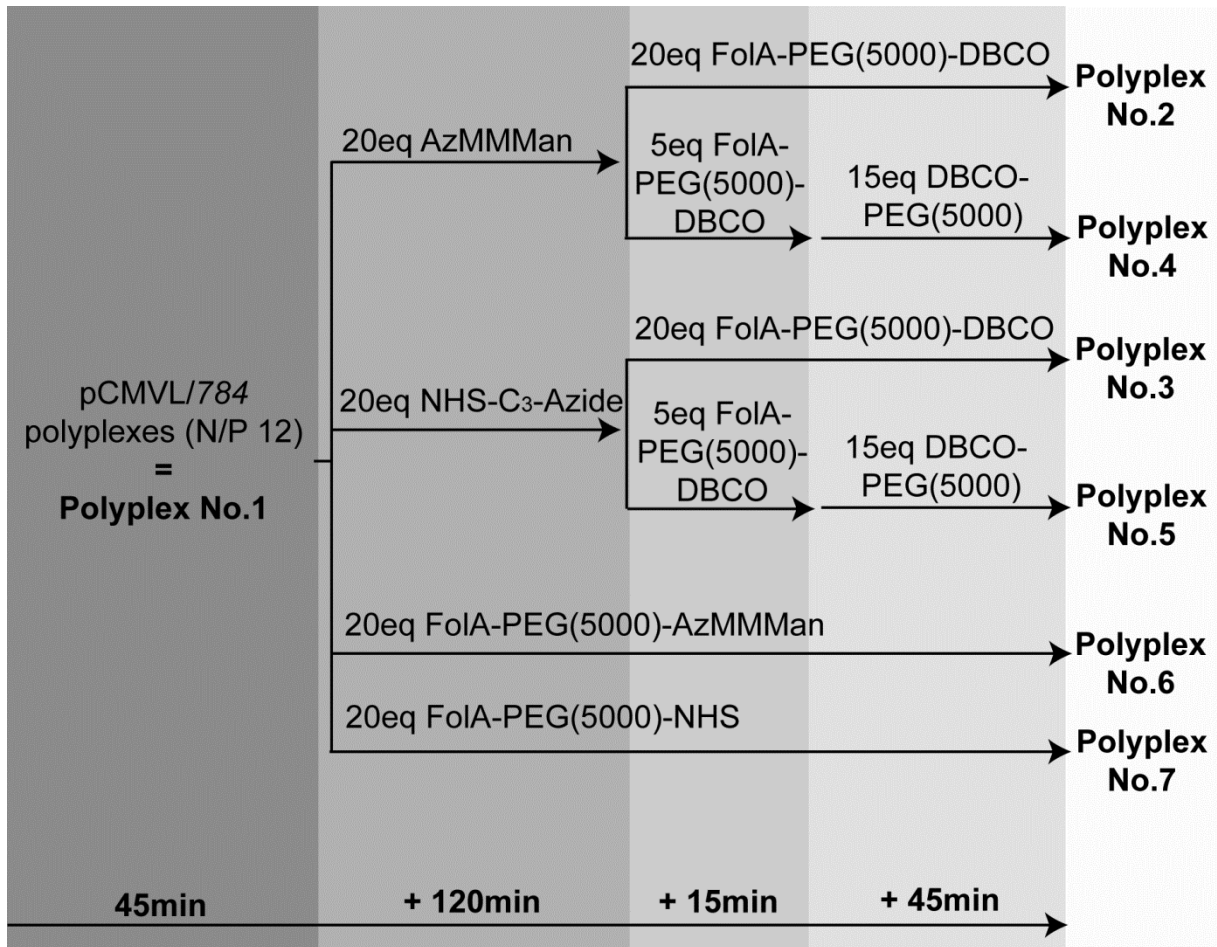
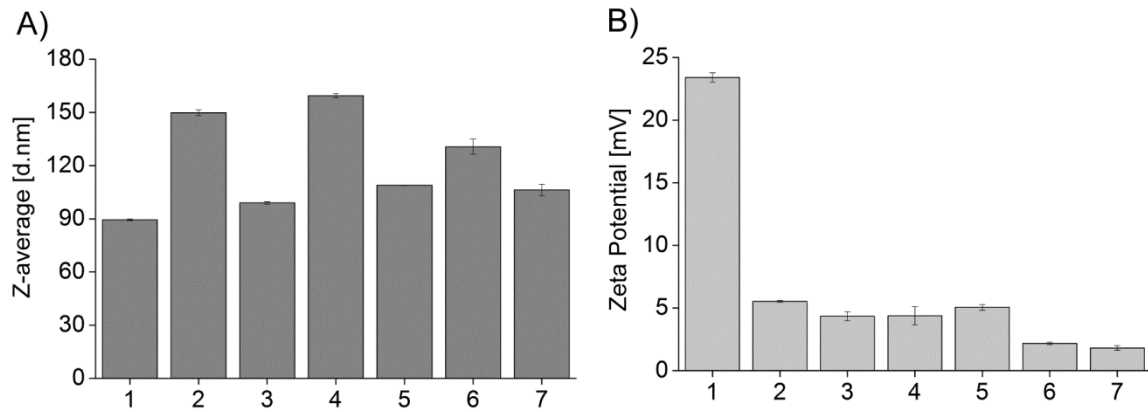


Figure 3.23. Brief outline of the different strategies applied for the formation of targeted post-PEGylated polyplexes (pCMVL/784; N/P 12). The effect of the applied strategy on size and zeta potential was evaluated using DLS analysis (Fig. 3.24.). Polyplex No.1 was prepared as a control polyplex without surface modification. Polyplex No.2 was shielded with 20eq AzMMMan incubated for 120min followed by the addition of 20eq FoIA-PEG(5000)-DBCO for 60min. Polyplex No.3 was prepared as a stable control to polyplex No. 2. Therefore, the acid-stable linker NHS-C₃-Azide was used instead of AzMMMan. Polyplex No.4 was surface modified with 20eq AzMMMan, which was, incubated for 120min prior the addition of 5eq FoIA-PEG(5000)-DBCO for 15min followed by the addition of 15eq DBCO-PEG(5000). Polyplex No. 5 was prepared as a stable control to polyplex No.4. Again, the acid-stable linker NHS-C₃-Azide was used instead of AzMMMan. In case of polyplex No.6, 20eq of the targeting-shielding reagent FoIA-PEG-AzMMMan was added in one step and incubated for 180min. Polyplex No. 7 was prepared as control polyplex using 20eq FoIA-PEG(5000)-NHS. FoIA-PEG(5000)-DBCO, FoIA-PEG(5000)-AzMMMan or FoIA-PEG(5000)-NHS was prepared from FoIA-PEG₆-cysteamine which was synthesized via SPPS according Fig. 3.21.A-1/A-2.

Results

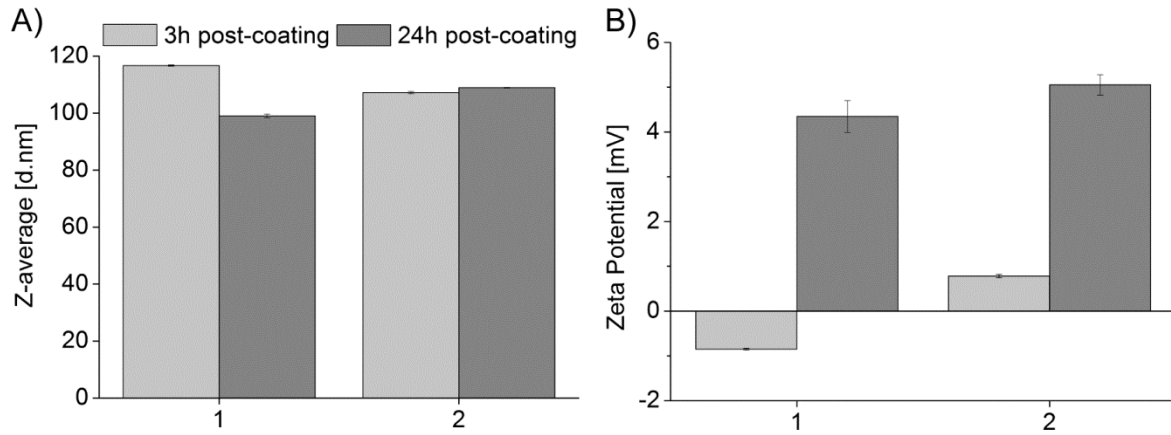


- 1) without targeting/shielding
- 2) 20eq AzMMMan (2h) + 20eq FoIA-PEG(5000)-DBCO (1h)
- 3) 20eq NHS-C3-Azide (2h) + 20eq FoIA-PEG(5000)-DBCO (1h)
- 4) 20eq AzMMMan (2h) + 20eq FoIA-PEG(5000)-DBCO (15min) + 20eq DBCO-PEG(5000)
- 5) 20eq NHS-C3-Azide (2h) + 20eq FoIA-PEG(5000)-DBCO (15min) + 20eq DBCO-PEG(5000)
- 6) 20eq FoIA-PEG(5000)-AzMMMan (3h)
- 7) 20eq FoIA-PEG(5000)-NHS (3h)

Figure 3.24. Size (A) and zeta potential (B) analysis of pCMVL/784 polyplexes (N/P 12) evaluating different "post-coating" strategies. Polyplexes were formed for 45min prior 3h post-PEGylation with a FoIA-targeted stably or pH-reversibly modified PEG reagent. Unmodified pCMVL/784 polyplexes were used as control. Data are presented as mean value (\pm SEM) out of triplicates.

Figure 3.24.A reveals that polyplexes shielded with 20eq FoIA-PEG(5000)-NHS were of smaller sizes, below 110nm, when compared to AzMMMan-modified polyplexes that showed sizes between 130nm-159nm. However, unshielded pCMVL/784 polyplexes were of smallest size of 89nm. Zeta potential measurements displayed a significant decrease in zeta potential, of values below 5mV, for all shielded complexes compared to 23.4mV measured in case of unmodified pCMVL/784 polyplexes (Fig. 3.24.B). The shielding method, whether polyplexes were shielded directly with 20eq AzMMMan- or NHS-modified FoIA-PEG(5000) or if the linker was coupled prior the coupling of the FoIA-modified PEGylation reagent, as well as the excess of FoIA within the polyplexes, had no significant effect on size or zeta potential. However, polyplex stability was significant decrease in case of polyplexes shielded with FoIA-PEG(5000)-AzMMMan. AzMMMan-modified polyplexes did not remain stable over a period of 24h, therefore no DLS data were obtained, compared to FoIA-PEG(5000)-NHS-shielded polyplexes (Fig. 3.25.A-B).

Results



- 1) 20eq NHS-C3-Azide (2h) + 20eq FoIA-PEG(5000)-DBCO
- 2) 20eq NHS-C3-Azide (2h) + 5eq FoIA-PEG(5000)-DBCO + 15eq DBCO-PEG(5000)

Figure 3.25. Size (A) and zeta potential (B) analysis of pCMVL/784 polyplexes (N/P 12) at 25°C. Polyplexes were prepared 45min prior 3h (light grey bars) or 24h (dark grey bars) post-PEGylation. Data are presented as mean value (\pm SEM) out of triplicates.

3.3.3. *In vitro* characterization of FoIA-targeted, stably or pH-sensitively shielded pCMVL/784 polyplexes

The ability of FoIA-targeted pH-sensitively or stably shielded pCMVL/784 polyplexes to mediate efficient cell-uptake via the FR was evaluated by pCMVL transfection of KB cells and subsequent bioluminescence quantification (Fig. 3.26.A-B). Polyplexes were formed according the DLS protocol for 45min. Post-PEGylation was performed either in one step in case of polyplexes numbered 6 and 7 by direct addition of 20eq FoIA-PEG(5000)-AzMMMan or FoIA-PEG(5000)-NHS and subsequent shielding for 3h. In case of polyplexes numbered 8 and 9 shielding was performed in two steps by adding 5eq FoIA-PEG(5000)-AzMMMan or FoIA-PEG(5000)-NHS 15min prior the addition of 15eq AzMMMan-PEG(5000) or NHS-PEG(5000). Untargeted NHS- or AzMMMan-shielded pCMVL/784 polyplexes and untargeted unshielded pCMVL/784 polyplexes were used as positive control. HBG was used as a negative control. In an control experiment examining the receptor specific uptake of FoIA-targeted pCMVL/784 polyplexes KB cells were preincubated with folic acid saturated RPMI medium to compete receptor binding between an excess of folic acid and the FoIA-targeted PEG-shielded polyplexes (Fig. 3.26.B).

Figure 3.26.A shows a significant increase in luciferase activity of FoIA-targeted PEG-shielded polyplexes compared to untargeted PEG-shielded polyplexes or even

Results

unmodified pCMVL/784 polyplexes. Consistent with *in vitro* results obtained from untargeted PEG- or pHPMA-shielded pCMVL/784 polyplexes, transgene expression was in all cases higher for pH-sensitively shielded FoliA-targeted polyplexes compared to stably modified polyplexes. Interestingly, transfection efficiency of targeted polyplexes was dependent on the shielding process in case of NHS-modified polyplexes. The direct addition of 20eq FoliA-PEG(5000)-NHS and incubation for 3h led to polyplexes, which mediated higher luciferase activity compared to polyplexes shielded by adding the targeting-shielding reagent in two steps. However, in case of AzMMMan-modified polyplexes the shielding-targeting method as well as the different concentration of folic acid within the polyplex had no effect on gene transfer efficiency. Nevertheless, transgene expression due to receptor specific uptake of FoliA-targeted PEG-shielded polyplexes was significantly decreased near background signal by competitive incubation of cells in folic acid saturated RPMI medium (Fig. 3.26.B).

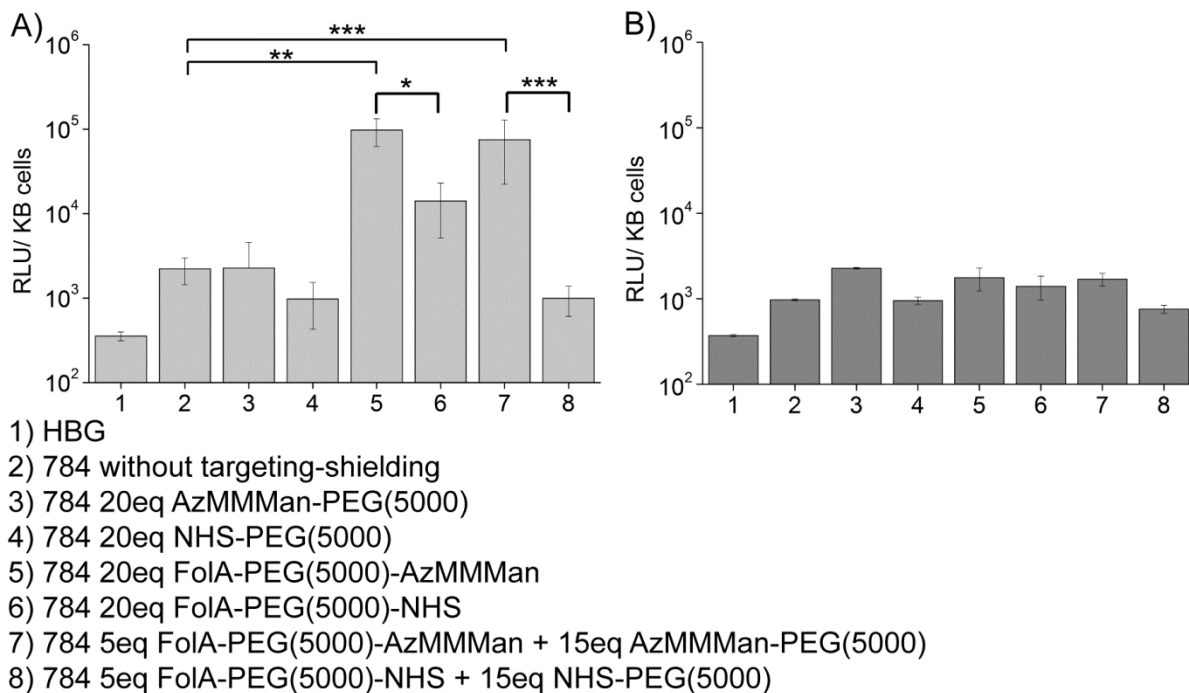


Figure 3.26. Luciferase activity presented as relative light units (RLU) per well after transfection of KB cells (8000 cells/well) with pCMVL/784 polyplexes (N/P 12). Cells were preincubated in A) FoliA-free RPMI medium or B) in FoliA-saturated RPMI medium (n=5).

Results

Taken together, these encouraging preliminary results suggest that the incorporation of the targeting ligand Folate within the delivery system is a convenient approach to enhance cellular internalization via FR-specific cell-uptake. Folate was synthesized using standard SPPS. Efficient surface shielding was accomplished by the attachment of the Folate-PEG moiety in a post-coating manner. *In vitro* transfection studies using FR-positive KB cells revealed higher gene expression by Folate-targeted pH-sensitively shielded polyplexes as compared to their irreversibly shielded counterparts. Overall, the incorporation of Folate within the shielding moiety increased transfection efficiency over untargeted PEG-shielded polyplexes. However, surface modification of polyplexes with Folate-PEG-AzMMMan or Folate-PEG-NHS was shown to increase particle size and reduce particle stability compared to untargeted polyplexes surface-modified with AzMMMan- or NHS-PEG. Additionally, the delivery efficiency was found to be below of that observed by using polyplexes, which were surface-modified with a Folate-PEG moiety in a pre-coating manner.

Discussion

4. Discussion

4.1. Evaluation of new sequence-defined oligomers concerning stabilizing effects of lysine residues on DNA polyplexes

Gene therapy based on non-viral carriers is one powerful method for the therapy of various diseases. Unfortunately, several barriers faced by the carrier during the delivery process significantly affect gene delivery efficiency. Additionally, therapeutic effective application is still hindered by problems of the carriers such as stability or off-target effects. In this regard, our research is directed toward sequence-defined carriers with tailored properties. Moreover, the concept of SPPS offers the possibility to incorporate versatile building blocks within the carrier sequence as well as a high flexibility in carrier design.

Hence, four-arm structured sequence-defined oligocations were designed, containing artificial oligo(ethanamino) amino acids as effective building blocks, terminal cysteines for polyplex stabilization and histidine residues to mediate endosomal release. Additional lysine residues were incorporated to ensure increased polyplex stability, thus making the polyplexes more serum resistant and enhancing gene delivery efficiency. Subsequently, an increased polyplex stability is required for the successful implementation of a pH-sensitive shielding approach. First, the effect of lysine residues integrated at different positions within the oligomer structure on polyplex stability was evaluated by agarose gel shift assays. Oligomers based on a H-Sph-K or Sph-K repeating sequence pattern showed a favorable DNA binding compared to lysine-free oligomers. Additionally performed EtBr assays confirmed these findings. Comparing agarose gel shift and EtBr assay data generated a sequence of DNA binding ability of the differently modified oligomers as follows: 606≤497<748=749<797<935<784=785. Therefore, the amount of lysine residues correlated with an increased DNA binding affinity of the oligomers. Consistent with former studies these findings confirm the today well-known ability of lysine-containing carriers to bind DNA very efficiently and to form compact and stable particles, respectively [121, 123], supporting the introduction of lysine residues with the repeating sequence pattern of well-defined oligocations.

On account of the beneficial stability of polyplex formed by lysine-rich oligomers, DLS measurements were performed to evaluate the effect of lysine residues within the oligomeric structure on polyplex size. Lysine-rich oligomers with a repeating

Discussion

sequence pattern of H-Sph-K or Sph-K formed polyplexes with sizes below 100nm compared to polyplexes with sizes above 190nm formed by lysine-free oligomers. Particle size is one critical parameter affecting the pharmacokinetic and biodistribution profile of the polyplexes. It has been shown that very small particles (below 5.5nm) are rapidly cleared by the kidney [135], whereas particles up to 400nm are capable of accumulation within highly vascularized solid tumors. As a result of the EPR effect particles can pass through the leaky vessels of those solid tumors enabling passive tumor-targeted drug delivery [136]. However, various studies have identified different size limits and extents of accumulation depending on the certain type of tumor [137, 138]. Additionally, the cellular uptake pathway is influenced by particle size. Particles with a size below 200nm are preferable taken up by clathrin-mediated pathway, whereas caveolin-mediated uptake is suggested to be the predominant route for particles of larger size [139]. Due to its degree and rate of acidification, the clathrin-mediated pathway may be the preferred uptake route for the polyplexes described in this thesis.

After the polyplex was taken up by the cell, the endosomal entrapment has to be overcome to ensure sufficient release of the carrier and its cargo into the cytosol. Currently, two mechanism have been suggested to explain the escape of polyplexes from the endosome, one of the most critical step in the delivery process. One involves the direct interaction of the positively charged polyplex with the negatively charged endosomal membrane causing membrane disruption. The positive zeta potential of all prepared polyplexes in the range between 23-32mV favors this interaction and membrane burst, respectively. The other mechanism, referred to as "proton sponge" effect, suggests that carrier protonation triggers an influx of chloride counter-ions followed by water. This increases the osmotic pressure within the endosomal vesicle resulting in a rupture of the endosomal membrane and carrier release. However, lysine-based carriers e.g. PLL are known to cover only a narrow buffering range as a consequence of their distinct pKa. Thus, efficient gene transfer fails in case of PLL due to its lack of endosomolytic potency despite the positive surface charge [140, 141]. It has been shown that histidine residues as well as artificial amino acids, containing the diaminoethane motif, are important within the oligomer structure for tuned protonation of the cationic oligomer in different relevant pH ranges especially the endosomal pH [56, 112]. To this regard, the buffer capacity of the newly synthesized oligomers was assessed identifying a decreased buffering

Discussion

in case of lysine-rich oligomers 784, 785 and 935 compared to lysine-free oligomers 606. Interestingly, the introduction of a histidine-rich area within a lysine-rich structure (oligomer ID 797) restored, moreover increased buffer capacity by 24% compared to the counterpart oligomer 606. The outstanding importance of integrating histidine residues within the oligomer structure is shown in case of oligomer 935. This oligomer comprising of a histidine-free K-Sph repeating sequence exhibit the lowest buffering in the relevant pH range.

Despite that some oligomers showed a decreased buffer capacity, *in vitro* transfection efficiency of DNA polyplexes was evaluated. In all cases DNA polyplexes formed by lysine-rich oligomers showed an enhanced gene transfer efficiency in Neuro-2a cells compared to lysine-free structures 606 and 497. This suggests that the lower buffering capacity of oligomer 784 and 785 and therefore expected lower transfection efficiency can be compensated by a higher polyplex compaction and beneficial bio-characteristics. However, in case of oligomer 935 chloroquine was needed to enforce the endosomal escape to receive transfection levels similar to oligomer 784, 785 and 797 indicating the need of histidine residues within the oligomer structure. Based on these data, we hypothesis that the improved transfection efficiency is a result of the endosomal membrane disruption mediated by direct charge interaction and "proton sponge" effect. Interestingly, the increase in transfection efficiency was not connected to an increased cytotoxicity. This is very promising since some of the non-viral carriers mediated only good transfection efficiency after the toxicological profile increased [142].

Overall, these results indicate that the incorporation of lysine residues within the oligomeric sequence led to smaller and better compacted polyplexes. In combination with histidine residues the polyplexes showed favorable biocharacteristics with superior *in vitro* distribution.

Discussion

4.2. Evaluation of pH-sensitively or stably modified PEG or pHPMA-shielded DNA polyplexes

Mimicking the dynamic pH-dependent cell-entry process of viruses may prove a successful approach to improve non-viral gene delivery. Therefore, we designed a carrier with incorporated pH-sensitive structures that undergo programmed structural changes triggered by environmental changes. In particular, a four-arm-structured sequence-defined cationic oligomer $\text{KK}[\text{HK}[(\text{H-Sph-K})_3\text{C}]_2]_2$ (compound ID: 784) was synthesized and functionalized with amine-reactive shielding polymers, monovalent PEG or monovalent and multivalent pHPMA. Despite the several advantages of shielded polyplexes over the unmodified form, the incorporation of a shielding polymer within the carrier appears to reduce the interaction of polyplexes with the target cells and prevents endosomal escape, hereby decreasing transfection efficiency. Therefore, we used the pH-sensitive linker AzMMMan to attach the hydrophilic shielding polymers to the polyplex via the primary lysine amines present in the cationic oligomer structure.

Overall, surface modification with PEG or pHPMA resulted in a decrease in the zeta potential of polyplexes, consistent with degree of surface shielding. Shielding was more efficient for multivalent pHPMA (20kDa, 30kDa) as compared to monovalent pHPMA (10kDa, 20kDa, 30kDa) or PEG (5kDa). Additionally, a lower molar excess of only 5eq was necessary for efficient surface shielding of pCMVL/784 polyplexes with multivalent pHPMA compared to 20eq needed by applying monovalent pHPMA or PEG as shielding agents. These findings can be explained by the differences in valency of pHPMA polymers and the "zip" mechanism of multivalent reactive polymers. In this respect partial hydrolysis of unreacted groups (TT and AzMMMan) of the multivalent pHPMA yields to negatively charged carboxyl groups, which may further improve particle stability and circulation due to a decrease in zeta potential. Additionally, it has been shown that a higher shielding polymer density on a particle surface results in increased particle stability due to cross-linking of the polycation chains with the multivalent pHPMA [74, 143]. Particles shielded with multivalent pHPMA prolonged polyplex stability up to 48h compared to polyplexes shielded with monovalent pHPMA or PEG, which were stable for 24h. These findings are consistent with former studies focusing on DNA/poly-L-lysine (PLL) complexes stably shielded either with multivalent pHPMA [143] or with multiblock PEG copolymer [144]. Comparing shielded and unshielded polyplexes, the attachment of a shielding

Discussion

moiety had no effect on particle sizes. Still, size measurements revealed polyplexes with an average size below 100nm. Additionally, the size was not affected by the used pH-sensitive or pH-stable linker molecule. These are very promising findings, since particle size affects the cell uptake and endosomal escape mechanism. This suggests that shielded as well as unshielded polyplexes are taken up by clathrin-mediated pathway (the preferred uptake route for particles smaller than 200nm [139] where they are exposed to mildly acidic pH.

Additionally, the interaction of polyplexes with blood components was studied which may lead to a reduction of transgene expression activity and alteration of tissue distribution [145]. Therefore, the polyplex stability of surface-modified polyplexes compared to unmodified polyplexes was monitored by DLS measurements after the addition of salt, plasma and isolated blood proteins such as albumin into incubation solution. The size of pCMVL/784 polyplexes modified with monovalent and multivalent pHPMA or PEG remained stable over 180min after the addition of PBS, slightly increased after 180min in albumin and increased significantly after 30min in plasma. However, unshielded polyplexes increased in size immediately after the addition of the various solutions probably due to their association. This is in good correlation with previous studies focusing on polyplex stability of pHPMA- or PEG-modified DNA/PLL or DNA/PEI polyplexes within artificial biological fluids such as salt or plasma [128, 143]. Considering that, in ideal scenario, after such circulation time most of the DNA particles should have already accumulated in the tissue of interest, these particles revealed high stability.

The acid-triggered deshielding of AzMMMan-modified pCMVL/784 polyplexes was monitored at endosomal pH of 6.0 by size and zeta potential measurements. As predicted, at pH 6.0, only polyplexes modified via the acid-labile linkage showed an increase in zeta potential after 45min, consistent with "deshielding". This release of the shielding polymer coat permits the interaction of polyplex with the endosomal membrane and its consequent endosomal escape. At the same time, the high stability of polyplexes at pH 7.4 suggests to be sufficient for tumor targeting and reducing unspecific interactions.

In vitro transfection studies revealed higher gene expression by the AzMMMan-pHPMA- or PEG-modified polyplexes as compared to their irreversibly shielded counterparts. However, luciferase gene expression levels were reduced in case of

Discussion

AzMMMan-modified multivalent pHPMA-shielded polyplexes in comparison to polyplexes shielded with monovalent pHPMA or PEG. One likely cause for the decreased transgene expression, which is closely connected to the excellent shielding ability of the multivalent pHPMA shielding polymer, is the reduction in unspecific cellular uptake [145]. The expression level was increased for both TT- and AzMMMan-modified multivalent pHPMA shielded polyplexes after the prolongation of transfection time from 24h to 48h. This finding suggests a time-dependent transfection efficiency also for stably shielded polyplexes. However, at both transfection time points AzMMMan modification led to a higher transgene expression.

Additionally, LSM and flow cytometry analysis were performed to assess the cellular uptake, in order to determine the underlying mechanism which causes the differences in gene expression levels between pH-sensitively shielded and stably shielded polyplexes. Various studies on pH-sensitive shielding have identified variations in cell trafficking efficiency such as endosomal release as determining factor for the enhanced transfection efficiency [85]. However, the gradual hydrolysis of the linker might be another factor explaining higher transfection efficacy of pH-sensitively shielded polyplexes. In case of pCMVL, sufficient transgene expression after extra- [146] as well as intracellular [53, 78, 82] cleavage of the shielding material has been reported. A higher intracellular distribution of pCMVL was found in LSM as well as flow cytometry analysis in case of AzMMMan-modified polyplexes compared to their stably shielded counterparts. Again, we found a superior shielding efficiency of multivalent pHPMA compared to monovalent pHPMA and an increased uptake efficiency of polyplexes due to AzMMMan modification in accordance to our DLS as well as transfection studies.

Most importantly, AzMMMan-pHPMA-modified polyplexes mediated, after intravenous administration in an *in vivo* tumor mouse model, enhanced gene expression levels in the subcutaneous tumor and reduced undesirable gene expression levels in the liver compared to their stably shielded counterparts. This data clearly demonstrate that pH-sensitive and stable pHPMA shielding upon systemic delivery provides protection within the blood stream sufficient to target transgene expression toward the tumor and to reduce expression in other organs such as the liver. A similar benefit of pH-shielding was observed previously in related settings [78, 85], demonstrating a favorable predominant tumor gene transfer of pH-

Discussion

labile PEG-hydrazone-shielded pCMVL/PEI polyplexes, as compared to stably shielded particles. Remarkably, pH-sensitively shielded polyplexes showed transgene expression levels similar to those of unshielded polyplexes. In conclusion, we hypothesize that the efficiency of our best performing polyplex formulation with highest gene transfer in the tumor is a result of the combination of all three novel components of the system; the new oligocation *784* provides improved polyplex stability and gene transfer efficiency, the multivalent pHPMA (20kDa) provides improved shielding against biological fluids, and the AzMMMan linkage allows dynamic deshielding to restore the initial polyplex activity within the target tissue. These results emphasize that polyplexes with deshielding ability may circumvent the "PEG dilemma" and restore their *in vivo* transfection efficiency at least to the extent of surface-unmodified polyplexes.

4.3. Evaluation of FoIA-targeted pH-sensitively or stably PEGylated DNA polyplexes

The novel designed four-arm structured sequence-defined cationic oligomer *784* has shown to efficiently bind DNA, form stable nanoparticles and transfect cells. The functionalization of polyplexes with hydrophilic shielding polymers resulted in reduced surface charge and provided steric protection of the carrier. In combination with the pH-sensitive linker AzMMMan, incorporated between the polyplex surface and the shielding polymer, the release of the shielding polymer was promoted and thereby membrane interactions as well as endosomal release enhanced. However, to overcome the major limitation of the current carrier of poor systemic cell-specific targeting efficiency, a FoIA-targeted bifunctional shielding polymer was synthesized and attached to the polyplex surface. FoIA was chosen as targeting ligand due to the fact it has been frequently exploited to target gene carriers to cells, especially cancer cells, which over-express the FR [73, 132, 147-149]. Additionally, the structure of FoIA is not comprised of primary amino groups, which would prevent surface shielding of polyplexes due to the competition with primary amino groups of the polymer for binding to AzMMMan- or NHS-groups of the bifunctional shielding polymer.

The synthesis of bifunctional FoIA-PEG(5000)-AzMMMan or FoIA-PEG(5000)-NHS was accomplished first by the synthesis of FoIA-PEG₆-cysteamine via SPPS, second

Discussion

by the reaction of FoliA-PEG₆-cysteamine with OPSS-PEG(5000)-NHS or OPSS-PEG(5000)-DBCO and last by the attachment of the pH-sensitive linker AzMMMan to the DBCO-groups to form a pH-sensitive PEG derivative. The incorporation of a short PEG spacer within the FoliA-PEG₆-cysteamine structure was beneficial in terms of an increased solubility of the targeting ligand. Additionally, it was shown that the addition of a spacer reduces the tendency of the folate moiety to self-aggregate which results in a reduced coupling as well as targeting efficiency [110]. The missing PEG spacer might be one explanation why the synthesis of FoliA-PEG(5000)-AzMMMan or FoliA-PEG(5000)-NHS via FoliA-NHS was not successful.

The FoliA-targeted PEG reagent was further modified with a TAMRA-azide dye (attached instead of the AzMMMan) to qualify this reagent via LSM. Specific FR targeting of the TAMRA-labeled FoliA-targeted PEG reagent was observed after short time incubation using KB cells. Most interestingly, cellular binding was not observed after preincubation of cells with FoliA saturated medium, suggesting specific FR targeting and functionality of the FoliA-targeted PEG derivative synthesized via SPPS.

Polyplex size and zeta potential of PEG-shielded FoliA-targeted pCMVL/784 polyplexes was determined by DLS. Similar to untargeted stably or pH-sensitively shielded polyplexes, surface modification with FoliA-PEG(5000)-NHS or FoliA-PEG(5000)-AzMMMan resulted in a decrease in zeta potential below 5mV. However, in comparison to untargeted PEG-shielded polyplexes, particle size increased from 79nm (untargeted) to 130nm-159nm (FoliA-targeted). Nevertheless, particles of such size (below 200nm) are still taken up by the preferred clathrin-mediated endocytosis pathway [139]. This size increase was accompanied by a decreased polyplex stability in case of AzMMMan-modified polyplexes. Polyplexes surface-modified with FoliA-PEG(5000)-AzMMMan were not stable over a period of 24h compared to untargeted AzMMMan-modified polyplexes. Interestingly, FoliA-targeted NHS-modified polyplexes remained stable in size over 24h suggesting that the linker molecule has an effect on polyplex stability. However, this was not observed in case of untargeted stably or pH-sensitively shielded polyplexes. One likely cause of the observed instability of targeted polyplexes is the hydrophobicity of the FoliA ligand causing polyplex aggregation [132, 149]. Recently, similar findings were made by Müller et al. after post-PEGylation of sequence-defined siRNA polyplexes with a FoliA-targeted PEG reagent. However, polyplex aggregation was not observed after substituting the

Discussion

targeting ligand Folate with an alternative tetra- γ -glutamyl folic acid (gE4-Folate) ligand. One possible explanation was given by the author referring to an increased negative zeta potential of gE4-Folate-targeted PEG-shielded siRNA polyplexes which is suggested to prevent polyplex aggregation due to an increased electrostatic repulsion [147].

In transfection experiments using the FR-expressing KB cells, post-PEGylated Folate-targeted pCMV/784 polyplexes strongly increased luciferase expression level both for stably as well as pH-sensitively shielded polyplexes in comparison to untargeted polyplexes. This suggests that the introduction of a targeting ligand positively affects cellular binding and internalization as previously reported [73, 78, 103]. Overall, consistent with transfection experiments performed with untargeted shielded polyplexes, a pH-sensitively surface shielding with Folate-PEG-AzMMMan resulted in an improved transfection activity over targeted stably shielded polyplexes. These results are consistent with other reports, which found an increased gene transfer efficiency in case of EGF- or Tf-targeted pDNA/PEI polyplexes shielded with a pH-sensitive PEG-acetal [82] or EGF-targeted pDNA/PEI polyplexes surface-modified with a pH-sensitive pyridylhydrazone-based PEG (HZN-PEG) reagent [78]. Pyridylhydrazone-based reversibly shielded polyplexes were further tested in an *in vivo* setting, demonstrating an enhanced tumor specific transgene expression after intravenous administration in a murine model of subcutaneous tumor. Taken together, these results provide further support for the hypothesis that polyplexes capable of cleaving off their PEG shield may overcome intracellular barriers such as endosomal membranes to promote significantly higher gene expression levels.

Although these preliminary results are promising toward the design of polyplexes, which mimic the dynamic pH-dependent cell-entry process of viruses, transfection efficiency is still below that observed in case of pre-PEGylated Folate-targeted sequence-defined pDNA polyplexes [56, 132]. A possible explanation may be the complexity of the post-PEGylation process using a bifunctional Folate-targeted pH-sensitively or stably modified PEG reagent. Additionally, the accessibility of the targeting ligand toward the FR might be reduced due to the rather high MW of the PEG(5000) moiety. In case of the above mentioned Folate-targeted sequence-defined siRNA polyplexes [147] or the pre-PEGylated pDNA polyplexes [132] a PEG(1200) moiety was used. Together with the hydrophobicity of Folate, DNA complexity and

Discussion

stability might be decreased to an extent that after the addition of salt-containing cell medium, polyplexes tend to aggregate resulting in a ligand-independent gene transfer. Therefore, future research needs to examine more closely the post-PEGylation process. In this regard, an optimized PEG length is required for maximizing polyplex stability as well as shielding efficiency. Another reasonable approach to tackle this issue could be the substitution of the targeting ligand F_oLA with a tetra- γ -glutamyl folic acid ligand, which provides four additional negative charges contributing to an increased polyplex stability due to an increased electrostatic repulsion.

Summary

5. Summary

Enhancing gene transfection efficiency of non-viral carriers still remains as challenge for researchers beyond discipline boundaries. The future of non-viral gene therapy depends on an improved understanding of the barriers imposed to non-viral gene transfer, and on the development of realistic delivery strategies that can circumvent these obstacles. In this regard, researchers can learn from the attributes of natural viruses, which have evolved to invade cells and to deliver their genetic payload. For instance, viruses use the endosomal acidification process after endocytosis to trigger conformational changes of key viral proteins in order to facilitate membrane fusion or disruption. This strategy of structural transformation upon acidification was adopted in the design of pH-sensitively shielded non-viral gene carriers to overcome the "PEG dilemma". PEGylation of polyplexes provides excellent particle stability and prolongation of blood circulation time but affords only suboptimal membrane fusion and endosomal release. Polyplexes surface-modified with a pH-sensitive shielding polymer are intended to remain shielded at physiological pH. However, after entering a slight acidic environment, the pH-sensitive linkage is hydrolyzed and the delivery system with its original endosomolytic capacity is restored enabling endosomal release.

One aim of this thesis was a tailor-design of precise multifunctional four-arm oligocations as basis for the preparation of well-compacted, stable pDNA polyplexes highly effective in gene transfer, both *in vitro* and *in vivo*. Therefore, lysine residues were incorporated into the sequence of a previously synthesized four-arm oligomer 606. Those new oligomers, comprising H-Sph-K or Sph-K repeating sequence pattern, form polyplexes of higher stability and smaller sizes. Additionally, luciferase marker gene expression levels *in vitro* and *in vivo* are increased compared to the lysine-free benchmark oligomer 606.

The additional lysine residues not only improved DNA polyplex stability, but also provided attachment points for subsequent polyplex functionalization with amine-reactive pH-sensitively or stably modified shielding polymers PEG or pHPMA, the second aim of this thesis. Surface-shielding of pDNA polyplexes with PEG or pHPMA resulted in a very efficient decrease in the zeta potential of the polyplexes, consistent with the degree of shielding. Additionally, modification of the surface of polyplexes with shielding polymers strongly reduced the interaction with PBS, albumin and

Summary

human plasma. Comparisons of the different shielding polymers revealed a better shielding ability of the multivalent pHPMA (20kDa, 30kDa) over monovalent PEG (5kDa) or monovalent pHPMA (10kDa, 20kDa, 30kDa).

At pH 6.0, only AzMMMan-modified pDNA polyplexes underwent a deshielding process, which is expected to be beneficial for endosomal escape. As a result, pH-sensitively shielded polyplexes achieved higher luciferase gene expression levels compared to their stably shielded counterparts. Moreover, pH-sensitively multivalent pHPMA-shielded polyplexes mediated an enhanced *in vivo* transgene expression toward the tumor and a reduced expression in other organs such as the liver.

The third aim of this thesis was the incorporation of the targeting ligand F_oIA within this delivery system to promote receptor-mediated cellular uptake. Preliminary DNA transfection studies *in vitro* identified binding of the F_oIA-targeted PEGylated polyplexes to the FR and an increased transfection efficiency over the untargeted counterparts. In combination with a pH-sensitive shielding *in vitro* transgene expression levels were increased compared to the stably shielded polyplexes.

Hence, results presented in this thesis demonstrate that by using AzMMMan as a pH-sensitive linker, primary amino group containing pDNA polyplexes can be shielded in a dynamic, bioreversible way. This provides an excellent starting point for further advances in existing carriers toward new bioresponsive polyplexes.

References

6. References

- [1] M.H. Amer, Gene therapy for cancer: present status and future perspective, *Mol. Cell. Ther.* 2 (2014) 27.
- [2] M. Cavazzana-Calvo, S. Hacein-Bey, B.G. de Saint, F. Gross, E. Yvon, P. Nusbaum, F. Selz, C. Hue, S. Certain, J.L. Casanova, P. Bousso, F.L. Deist, A. Fischer, Gene therapy of human severe combined immunodeficiency (SCID)-X1 disease, *Science* 288 (2000) 669-672.
- [3] C.G. Fathman, C.M. Seroogy, Application of Gene Therapy in Autoimmune Disease, *Gene Ther.* 7 (2000) 9-13.
- [4] J.L. Badano, N. Katsanis, Beyond Mendel: an evolving view of human genetic disease transmission, *Nat. Rev. Genet.* 3 (2002) 779-789.
- [5] O.T. Avery, C.M. MacLeod, M. McCarty, Studies on the chemical nature of the substance inducing transformation of pneumococcal types induction of transformation by a desoxyribonucleic acid fraction isolated from pneumococcus type III, *J. Exp. Med.* 79 (1944) 137-158.
- [6] J.D. Watson, F.H. Crick, Molecular structure of nucleic acids, *Nature* 171 (1953) 737-738.
- [7] T. Friedmann, R. Roblin, Gene therapy for human genetic disease?, *Science* 175 (1972) 949-955.
- [8] J. Schmutz, J. Wheeler, J. Grimwood, M. Dickson, J. Yang, C. Caoile, E. Bajorek, S. Black, Y.M. Chan, M. Denys, J. Escobar, D. Flowers, D. Fotopulos, C. Garcia, M. Gomez, E. Gonzales, L. Haydu, F. Lopez, L. Ramirez, J. Retterer, A. Rodriguez, S. Rogers, A. Salazar, M. Tsai, R.M. Myers, Quality assessment of the human genome sequence, *Nature* 429 (2004) 365-368.
- [9] J.M. Kidd, G.M. Cooper, W.F. Donahue, H.S. Hayden, N. Sampas, T. Graves, N. Hansen, B. Teague, C. Alkan, F. Antonacci, E. Haugen, T. Zerr, N.A. Yamada, P. Tsang, T.L. Newman, E. Tuzun, Z. Cheng, H.M. Ebling, N. Tusneem, R. David, W. Gillett, K.A. Phelps, M. Weaver, D. Saranga, A. Brand, W. Tao, E. Gustafson, K. McKernan, L. Chen, M. Malig, J.D. Smith, J.M. Korn, S.A. McCarroll, D.A. Altshuler, D.A. Peiffer, M. Dorschner, J. Stamatoyannopoulos, D. Schwartz, D.A. Nickerson, J.C. Mullikin, R.K. Wilson, L. Bruhn, M.V. Olson, R. Kaul, D.R. Smith, E.E. Eichler, Mapping and sequencing of structural variation from eight human genomes, *Nature* 453 (2008) 56-64.
- [10] J.C. Venter, M.D. Adams, E.W. Myers, P.W. Li, R.J. Mural, G.G. Sutton, H.O. Smith, M. Yandell, C.A. Evans, R.A. Holt, J.D. Gocayne, P. Amanatides, R.M. Ballew, D.H. Huson, J.R. Wortman, Q. Zhang, C.D. Kodira, X.H. Zheng, L. Chen, M. Skupski, G. Subramanian, P.D. Thomas, J. Zhang, G.L. Gabor Miklos, C. Nelson, S. Broder, A.G. Clark, J. Nadeau, V.A. McKusick, N. Zinder, A.J. Levine, R.J. Roberts, M. Simon, C. Slayman, M. Hunkapiller, R. Bolanos, A. Delcher, I. Dew, D. Fasulo, M. Flanigan, L. Florea, A. Halpern, S. Hannenhalli, S. Kravitz, S. Levy, C. Mobarry, K. Reinert, K. Remington, J. Abu-Threideh, E. Beasley, K. Biddick, V. Bonazzi, R.

References

Brandon, M. Cargill, I. Chandramouliswaran, R. Charlab, K. Chaturvedi, Z. Deng, V. Di Francesco, P. Dunn, K. Eilbeck, C. Evangelista, A.E. Gabrielian, W. Gan, W. Ge, F. Gong, Z. Gu, P. Guan, T.J. Heiman, M.E. Higgins, R.R. Ji, Z. Ke, K.A. Ketchum, Z. Lai, Y. Lei, Z. Li, J. Li, Y. Liang, X. Lin, F. Lu, G.V. Merkulov, N. Milshina, H.M. Moore, A.K. Naik, V.A. Narayan, B. Neelam, D. Nusskern, D.B. Rusch, S. Salzberg, W. Shao, B. Shue, J. Sun, Z. Wang, A. Wang, X. Wang, J. Wang, M. Wei, R. Wides, C. Xiao, C. Yan, A. Yao, J. Ye, M. Zhan, W. Zhang, H. Zhang, Q. Zhao, L. Zheng, F. Zhong, W. Zhong, S. Zhu, S. Zhao, D. Gilbert, S. Baumhueter, G. Spier, C. Carter, A. Cravchik, T. Woodage, F. Ali, H. An, A. Awe, D. Baldwin, H. Baden, M. Barnstead, I. Barrow, K. Beeson, D. Busam, A. Carver, A. Center, M.L. Cheng, L. Curry, S. Danaher, L. Davenport, R. Desilets, S. Dietz, K. Dodson, L. Doup, S. Ferriera, N. Garg, A. Gluecksmann, B. Hart, J. Haynes, C. Haynes, C. Heiner, S. Hladun, D. Hostin, J. Houck, T. Howland, C. Ibegwam, J. Johnson, F. Kalush, L. Kline, S. Koduru, A. Love, F. Mann, D. May, S. McCawley, T. McIntosh, I. McMullen, M. Moy, L. Moy, B. Murphy, K. Nelson, C. Pfannkoch, E. Pratts, V. Puri, H. Qureshi, M. Reardon, R. Rodriguez, Y.H. Rogers, D. Romblad, B. Ruhfel, R. Scott, C. Sitter, M. Smallwood, E. Stewart, R. Strong, E. Suh, R. Thomas, N.N. Tint, S. Tse, C. Vech, G. Wang, J. Wetter, S. Williams, M. Williams, S. Windsor, E. Winn-Deen, K. Wolfe, J. Zaveri, K. Zaveri, J.F. Abril, R. Guigo, M.J. Campbell, K.V. Sjolander, B. Karlak, A. Kejariwal, H. Mi, B. Lazareva, T. Hatton, A. Narechania, K. Diemer, A. Muruganujan, N. Guo, S. Sato, V. Bafna, S. Istrail, R. Lippert, R. Schwartz, B. Walenz, S. Yooseph, D. Allen, A. Basu, J. Baxendale, L. Blick, M. Caminha, J. Carnes-Stine, P. Caulk, Y.H. Chiang, M. Coyne, C. Dahlke, A. Mays, M. Dombroski, M. Donnelly, D. Ely, S. Esparham, C. Fosler, H. Gire, S. Glanowski, K. Glasser, A. Glodek, M. Gorokhov, K. Graham, B. Gropman, M. Harris, J. Heil, S. Henderson, J. Hoover, D. Jennings, C. Jordan, J. Jordan, J. Kasha, L. Kagan, C. Kraft, A. Levitsky, M. Lewis, X. Liu, J. Lopez, D. Ma, W. Majoros, J. McDaniel, S. Murphy, M. Newman, T. Nguyen, N. Nguyen, M. Nodell, S. Pan, J. Peck, M. Peterson, W. Rowe, R. Sanders, J. Scott, M. Simpson, T. Smith, A. Sprague, T. Stockwell, R. Turner, E. Venter, M. Wang, M. Wen, D. Wu, M. Wu, A. Xia, A. Zandieh, X. Zhu, The sequence of the human genome, *Science* 291 (2001) 1304-1351.

[11] E. Duncan, M. Brown, E.M. Shore, The revolution in human monogenic disease mapping, *Genes (Basel)* 5 (2014) 792-803.

[12] F.S. Collins, V.A. McKusick, Implications of the Human Genome Project for medical science, *JAMA* 285 (2001) 540-544.

[13] C.S. Pareek, R. Smoczynski, A. Tretyn, Sequencing technologies and genome sequencing, *J. Appl. Genet.* 52 (2011) 413-435.

[14] S.A. Rosenberg, P. Aebersold, K. Cornetta, A. Kasid, R.A. Morgan, R. Moen, E.M. Karson, M.T. Lotze, J.C. Yang, S.L. Topalian, Gene transfer into humans--immunotherapy of patients with advanced melanoma, using tumor-infiltrating lymphocytes modified by retroviral gene transduction, *New Engl. J. Med.* 323 (1990) 570-578.

[15] T. Wirth, N. Parker, S. Yla-Herttuala, History of gene therapy, *Gene* 525 (2013) 162-169.

References

- [16] R.M. Blaese, K.W. Culver, A.D. Miller, C.S. Carter, T. Fleisher, M. Clerici, G. Shearer, L. Chang, Y. Chiang, P. Tolstoshev, T lymphocyte-directed gene therapy for ADA- SCID: initial trial results after 4 years, *Science* 270 (1995) 475-480.
- [17] K.W. Culver, Clinical applications of gene therapy for cancer, *Clin. Chem.* 40 (1994) 510-512.
- [18] D.B. Kohn, M. Sadelain, J.C. Glorioso, Occurrence of leukaemia following gene therapy of X-linked SCID, *Nat. Rev. Cancer* 3 (2003) 477-488.
- [19] S. Ylä-Herttuala, Endgame: glybera finally recommended for approval as the first gene therapy drug in the European union, *Mol. Ther.* 20 (2012) 1831.
- [20] S. Chira, C.S. Jackson, I. Oprea, F. Ozturk, M.S. Pepper, I. Diaconu, C. Braicu, L.-Z. Raduly, G.A. Calin, I. Berindan-Neagoe, Progresses towards safe and efficient gene therapy vectors, *Oncotarget* 6 (2015) 30675-30703.
- [21] A.D. Miller, Human gene therapy comes of age, *Nature* 357 (1992) 455-460.
- [22] S.L. Ginn, I.E. Alexander, M.L. Edelstein, M.R. Abedi, J. Wixon, Gene therapy clinical trials worldwide to 2012—an update, *J. Gene Med.* 15 (2013) 65-77.
- [23] T. Wirth, N. Parker, S. Ylä-Herttuala, History of gene therapy, *Gene* 525 (2013) 162-169.
- [24] Gene therapy clinical trials worldwide,
<http://www.wiley.com/legacy/wileychi/genmed/clinical/>.
- [25] U. Lächelt, E. Wagner, Nucleic Acid Therapeutics Using Polyplexes: A Journey of 50 Years (and Beyond), *Chem. Rev.* 115 (2015) 11043-11078.
- [26] M.R. Capecchi, High efficiency transformation by direct microinjection of DNA into cultured mammalian cells, *Cell* 22 (1980) 479-488.
- [27] E. Neumann, M. Schaefer-Ridder, Y. Wang, P.H. Hofschneider, Gene transfer into mouse lymphoma cells by electroporation in high electric fields, *EMBO J.* 1 (1982) 841-845.
- [28] R. Heller, M. Jaroszeski, A. Atkin, D. Moradpour, R. Gilbert, J. Wands, C. Nicolau, In vivo gene electroinjection and expression in rat liver, *FEBS Lett.* 389 (1996) 225-228.
- [29] N.S. Yang, J. Burkholder, B. Roberts, B. Martinell, D. McCabe, In vivo and in vitro gene transfer to mammalian somatic cells by particle bombardment, *Proc. Natl. Acad. Sci. U.S.A.* 87 (1990) 9568-9572.
- [30] F. Scherer, M. Anton, U. Schillinger, J. Henke, C. Bergemann, A. Kruger, B. Gansbacher, C. Plank, Magnetofection: enhancing and targeting gene delivery by magnetic force in vitro and in vivo, *Gene Ther.* 9 (2002) 102-109.
- [31] C. Tros de Ilarduya, Y. Sun, N. Duzgunes, Gene delivery by lipoplexes and polyplexes, *Eur. J. Pharm. Sci.* 40 (2010) 159-170.

References

- [32] C. Li, Y. Feng, G. Coukos, L. Zhang, Therapeutic microRNA strategies in human cancer, *AAPS J.* 11 (2009) 747-757.
- [33] G. Zhang, V. Budker, J.A. Wolff, High levels of foreign gene expression in hepatocytes after tail vein injections of naked plasmid DNA, *Hum. Gene Ther.* 10 (1999) 1735-1737.
- [34] G. Prasad, H. Wang, D.L. Hill, R. Zhang, Recent advances in experimental molecular therapeutics for malignant gliomas, *Curr. Med. Chem. Anticancer Agents* 4 (2004) 347-361.
- [35] J. Prieto, C. Qian, R. Hernandez-Alcoceba, G. Gonzalez-Aseguinolaza, G. Mazzolini, B. Sangro, M.G. Kramer, Gene therapy of liver diseases, *Expert Opin. Biol. Ther.* 4 (2004) 1073-1091.
- [36] S.-X. Liu, Z.-S. Xia, Y.-Q. Zhong, Gene therapy in pancreatic cancer, *World J. Gastroentero.* 20 (2014) 13343-13368.
- [37] M.E. Davis, Z.G. Chen, D.M. Shin, Nanoparticle therapeutics: an emerging treatment modality for cancer, *Nat. Rev. Drug Discov.* 7 (2008) 771-782.
- [38] C. Plank, K. Mechtler, F.C. Szoka, Jr., E. Wagner, Activation of the complement system by synthetic DNA complexes: a potential barrier for intravenous gene delivery, *Hum. Gene Ther* 7 (1996) 1437-1446.
- [39] E. Wagner, D. Curiel, M. Cotten, Delivery of drugs, proteins and genes into cells using transferrin as a ligand for receptor-mediated endocytosis, *Adv. Drug Deliv. Rev.* 14 (1994) 113-136.
- [40] G.J. Wolbink, M.C. Brouwer, S. Buysmann, I.J. ten Berge, C.E. Hack, CRP-mediated activation of complement in vivo: assessment by measuring circulating complement-C-reactive protein complexes, *J. Immunol.* 157 (1996) 473-479.
- [41] M. Ogris, P. Steinlein, S. Carotta, S. Brunner, E. Wagner, DNA/polyethylenimine transfection particles: Influence of ligands, polymer size, and PEGylation on internalization and gene expression, *AAPS PharmSci.* 3 (2001).
- [42] K. de Bruin, N. Ruthardt, K. von Gersdorff, R. Bausinger, E. Wagner, M. Ogris, C. Brauchle, Cellular dynamics of EGF receptor-targeted synthetic viruses, *Mol. Ther.* 15 (2007) 1297-1305.
- [43] S. Mukherjee, R.N. Ghosh, F.R. Maxfield, Endocytosis, *Physiol. Rev.* 77 (1997) 759-803.
- [44] R. Duncan, S.C. Richardson, Endocytosis and intracellular trafficking as gateways for nanomedicine delivery: opportunities and challenges, *Mol. Pharm.* 9 (2012) 2380-2402.
- [45] J. Mercer, M. Schelhaas, A. Helenius, Virus entry by endocytosis, *Annu. Rev. Biochem.* 79 (2010) 803-833.

References

- [46] O. Boussif, F. Lezoualc'h, M.A. Zanta, M.D. Mergny, D. Scherman, B. Demeneix, J.P. Behr, A versatile vector for gene and oligonucleotide transfer into cells in culture and in vivo: polyethylenimine, *Proc. Natl. Acad. Sci. U.S.A.* 92 (1995) 7297-7301.
- [47] E.E. Vaughan, J.V. DeGiulio, D.A. Dean, Intracellular trafficking of plasmids for gene therapy: mechanisms of cytoplasmic movement and nuclear import, *Curr. Gene Ther.* 6 (2006) 671-681.
- [48] D.V. Schaffer, N.A. Fidelman, N. Dan, D.A. Lauffenburger, Vector unpacking as a potential barrier for receptor-mediated polyplex gene delivery, *Biotechnol. Bioeng.* 67 (2000) 598-606.
- [49] V.A. Sethuraman, K. Na, Y.H. Bae, pH-responsive sulfonamide/PEI system for tumor specific gene delivery: an in vitro study, *Biomacromolecules* 7 (2006) 64-70.
- [50] D.B. Rozema, D.L. Lewis, D.H. Wakefield, S.C. Wong, J.J. Klein, P.L. Roesch, S.L. Bertin, T.W. Reppen, Q. Chu, A.V. Blokhin, J.E. Hagstrom, J.A. Wolff, Dynamic PolyConjugates for targeted in vivo delivery of siRNA to hepatocytes, *Proc. Natl. Acad. Sci. U.S.A.* 104 (2007) 12982-12987.
- [51] H. Hatakeyama, H. Akita, K. Kogure, M. Oishi, Y. Nagasaki, Y. Kihira, M. Ueno, H. Kobayashi, H. Kikuchi, H. Harashima, Development of a novel systemic gene delivery system for cancer therapy with a tumor-specific cleavable PEG-lipid, *Gene Ther.* 14 (2007) 68-77.
- [52] B. Romberg, F.M. Flesch, W.E. Hennink, G. Storm, Enzyme-induced shedding of a poly (amino acid)-coating triggers contents release from dioleoyl phosphatidylethanolamine liposomes, *Int. J. Pharm.* 355 (2008) 108-113.
- [53] R.C. Carlisle, T. Etrych, S.S. Briggs, J.A. Preece, K. Ulbrich, L.W. Seymour, Polymer-coated polyethylenimine/DNA complexes designed for triggered activation by intracellular reduction, *J. Gene Med.* 6 (2004) 337-344.
- [54] T. Wang, J.R. Upponi, V.P. Torchilin, Design of multifunctional non-viral gene vectors to overcome physiological barriers: dilemmas and strategies, *Int. J. Pharm.* 427 (2012) 3-20.
- [55] E.E. Salcher, P. Kos, T. Fröhlich, N. Badgujar, M. Scheible, E. Wagner, Sequence-defined four-arm oligo(ethan amino)amides for pDNA and siRNA delivery: Impact of building blocks on efficacy, *J. Control. Release* 164 (2012) 380-386.
- [56] U. Lächelt, P. Kos, F.M. Mickler, A. Herrmann, E.E. Salcher, W. Rödl, N. Badgujar, C. Brauchle, E. Wagner, Fine-tuning of proton sponges by precise diaminoethanes and histidines in pDNA polyplexes, *Nanomedicine* 10 (2014) 35-44.
- [57] T. Fröhlich, D. Edinger, R. Klager, C. Troiber, E. Salcher, N. Badgujar, I. Martin, D. Schaffert, A. Cengizeroglu, P. Hadwiger, H.P. Vornlocher, E. Wagner, Structure-activity relationships of siRNA carriers based on sequence-defined oligo (ethane amino) amides, *J. Control. Release* 160 (2012) 532-541.

References

- [58] D. Schaffert, C. Troiber, E.E. Salcher, T. Fröhlich, I. Martin, N. Badgujar, C. Dohmen, D. Edinger, R. Klager, G. Maiwald, K. Farkasova, S. Seeber, K. Jahn-Hofmann, P. Hadwiger, E. Wagner, Solid-phase synthesis of sequence-defined T-, i-, and U-shape polymers for pDNA and siRNA delivery, *Angew. Chem. Int. Ed. Engl.* 50 (2011) 8986-8989.
- [59] C. Troiber, D. Edinger, P. Kos, L. Schreiner, R. Klager, A. Herrmann, E. Wagner, Stabilizing effect of tyrosine trimers on pDNA and siRNA polyplexes, *Biomaterials* 34 (2013) 1624-1633.
- [60] M.L. Read, K.H. Bremner, D. Oupicky, N.K. Green, P.F. Searle, L.W. Seymour, Vectors based on reducible polycations facilitate intracellular release of nucleic acids, *J. Gene Med.* 5 (2003) 232-245.
- [61] S. Huth, F. Hoffmann, K. von Gersdorff, A. Laner, D. Reinhardt, J. Rosenecker, C. Rudolph, Interaction of polyamine gene vectors with RNA leads to the dissociation of plasmid DNA-carrier complexes, *J. Gene Med.* 8 (2006) 1416-1424.
- [62] V. Bulmus, M. Woodward, L. Lin, N. Murthy, P. Stayton, A. Hoffman, A new pH-responsive and glutathione-reactive, endosomal membrane-disruptive polymeric carrier for intracellular delivery of biomolecular drugs, *J. Control. Release* 93 (2003) 105-120.
- [63] D. Schaffert, C. Troiber, E. Wagner, New Sequence-Defined Polyaminoamides with Tailored Endosomolytic Properties for Plasmid DNA Delivery, *Bioconjug. Chem.* 23 (2012) 1157-1165.
- [64] P.M. Klein, K. Muller, C. Gutmann, P. Kos, A. Krhac Levacic, D. Edinger, M. Hohn, J.C. Leroux, M.A. Gauthier, E. Wagner, Twin disulfides as opportunity for improving stability and transfection efficiency of oligoaminoethane polyplexes, *J. Control. Release* 205 (2015) 109-119.
- [65] M. Nishikawa, T. Nakano, T. Okabe, N. Hamaguchi, Y. Yamasaki, Y. Takakura, F. Yamashita, M. Hashida, Residualizing indium-111-radiolabel for plasmid DNA and its application to tissue distribution study, *Bioconjug. Chem.* 14 (2003) 955-961.
- [66] D. Oupicky, C. Konak, P.R. Dash, L.W. Seymour, K. Ulbrich, Effect of albumin and polyanion on the structure of DNA complexes with polycation containing hydrophilic nonionic block, *Bioconjug. Chem.* 10 (1999) 764-772.
- [67] K. Kunath, A. von Harpe, H. Petersen, D. Fischer, K. Voigt, T. Kissel, U. Bickel, The structure of PEG-modified poly(ethylene imines) influences biodistribution and pharmacokinetics of their complexes with NF-kappaB decoy in mice, *Pharm. Res.* 19 (2002) 810-817.
- [68] V. Subr, L. Kostka, T. Selby-Milic, K. Fisher, K. Ulbrich, L.W. Seymour, R.C. Carlisle, Coating of adenovirus type 5 with polymers containing quaternary amines prevents binding to blood components, *J. Control. Release* 135 (2009) 152-158.

References

- [69] H. Maeda, The enhanced permeability and retention (EPR) effect in tumor vasculature: the key role of tumor-selective macromolecular drug targeting, *Adv. Enzyme Regul.* 41 (2001) 189-207.
- [70] L. Kostka, C. Konak, V. Subr, M. Spirkova, Y. Addadi, M. Neeman, T. Lammers, K. Ulbrich, Removable nanocoatings for siRNA polyplexes, *Bioconjug. Chem.* 22 (2011) 169-179.
- [71] S.N. Alconcel, A.S. Baas, H.D. Maynard, FDA-approved poly (ethylene glycol)-protein conjugate drugs, *Polym. Chem.* 2 (2011) 1442-1448.
- [72] I. Martin, C. Dohmen, C. Mas-Moruno, C. Troiber, P. Kos, D. Schaffert, U. Lächelt, M. Teixido, M. Günther, H. Kessler, E. Giralt, E. Wagner, Solid-phase-assisted synthesis of targeting peptide-PEG-oligo(ethane amino)amides for receptor-mediated gene delivery, *Org. Biomol. Chem.* 10 (2012) 3258-3268.
- [73] C. Dohmen, T. Fröhlich, U. Lächelt, I. Rohl, H.-P. Vornlocher, P. Hadwiger, E. Wagner, Defined Folate-PEG-siRNA Conjugates for Receptor-specific Gene Silencing, *Mol. Ther. Nucleic Acids* 1 (2012) e7.
- [74] D. Oupicky, M. Ogris, K.A. Howard, P.R. Dash, K. Ulbrich, L.W. Seymour, Importance of lateral and steric stabilization of polyelectrolyte gene delivery vectors for extended systemic circulation, *Mol. Ther.* 5 (2002) 463-472.
- [75] P.R. Dash, M.L. Read, K.D. Fisher, K.A. Howard, M. Wolfert, D. Oupicky, V. Subr, J. Strohal, K. Ulbrich, L.W. Seymour, Decreased binding to proteins and cells of polymeric gene delivery vectors surface modified with a multivalent hydrophilic polymer and retargeting through attachment of transferrin, *J. Biol. Chem.* 275 (2000) 3793-3802.
- [76] J. Kopeček, P. Kopečková, HPMA copolymers: origins, early developments, present, and future, *Adv. Drug Deliv. Rev.* 62 (2010) 122-149.
- [77] M. Kurša, G.F. Walker, V. Roessler, M. Ogris, W. Roedl, R. Kircheis, E. Wagner, Novel Shielded Transferrin-Polyethylene Glycol-Polyethylenimine/DNA Complexes for Systemic Tumor-Targeted Gene Transfer, *Bioconjug. Chem.* 14 (2003) 222-231.
- [78] C. Fella, G.F. Walker, M. Ogris, E. Wagner, Amine-reactive pyridylhydrazone-based PEG reagents for pH-reversible PEI polyplex shielding, *Eur. J. Pharm. Sci.* 34 (2008) 309-320.
- [79] H. Hatakeyama, H. Akita, H. Harashima, A multifunctional envelope type nano device (MEND) for gene delivery to tumours based on the EPR effect: A strategy for overcoming the PEG dilemma, *Adv. Drug Deliv. Rev.* 63 (2010) 152-160.
- [80] M. Meyer, E. Wagner, pH-responsive shielding of non-viral gene vectors, *Expert. Opin. Drug Deliv.* 3 (2006) 563-571.
- [81] E. Wagner, Programmed drug delivery: nanosystems for tumor targeting, *Expert. Opin. Biol Ther.* 7 (2007) 587-593.

References

- [82] V. Knorr, L. Allmendinger, G.F. Walker, F.F. Paintner, E. Wagner, An acetal-based PEGylation reagent for pH-sensitive shielding of DNA polyplexes, *Bioconjug. Chem.* 18 (2007) 1218-1225.
- [83] V. Knorr, M. Ogris, E. Wagner, An acid sensitive ketal-based polyethylene glycol-oligoethylenimine copolymer mediates improved transfection efficiency at reduced toxicity, *Pharm. Res.* 25 (2008) 2937-2945.
- [84] N. Murthy, J. Campbell, N. Fausto, A.S. Hoffman, P.S. Stayton, Design and synthesis of pH-responsive polymeric carriers that target uptake and enhance the intracellular delivery of oligonucleotides, *J. Control. Release.* 89 (2003) 365-374.
- [85] G.F. Walker, C. Fella, J. Pelisek, J. Fahrmeir, S. Boeckle, M. Ogris, E. Wagner, Toward synthetic viruses: endosomal pH-triggered deshielding of targeted polyplexes greatly enhances gene transfer in vitro and in vivo, *Mol. Ther.* 11 (2005) 418-425.
- [86] L.M. Coussens, B. Fingleton, L.M. Matrisian, Matrix metalloproteinase inhibitors and cancer—trials and tribulations, *Science* 295 (2002) 2387-2392.
- [87] J. Li, Z. Ge, S. Liu, PEG-sheddable polyplex micelles as smart gene carriers based on MMP-cleavable peptide-linked block copolymers, *Chem. Commun.* 49 (2013) 6974-6976.
- [88] G.Y. Wu, C.H. Wu, Receptor-mediated in vitro gene transformation by a soluble DNA carrier system, *J. Biol. Chem.* 262 (1987) 4429-4432.
- [89] G.Y. Wu, C.H. Wu, Receptor-mediated gene delivery and expression in vivo, *J. Biol. Chem.* 262 (1988) 14621-14624.
- [90] M. Ogris, E. Wagner, Targeting tumors with non-viral gene delivery systems, *Drug Discov. Today* 7 (2002) 479-485.
- [91] J.M. Lajoie, E.V. Shusta, Targeting Receptor-Mediated Transport for Delivery of Biologics Across the Blood-Brain Barrier, *Annu. Rev. Pharmacol. Toxicol.* 55 (2015) 613-631.
- [92] J. Park, K. Singha, S. Son, J. Kim, R. Namgung, C. Yun, W. Kim, A review of RGD-functionalized nonviral gene delivery vectors for cancer therapy, *Cancer Gene Ther.* 19 (2012) 741-748.
- [93] R. Pasqualini, E. Koivunen, R. Kain, J. Lahdenranta, M. Sakamoto, A. Stryhn, R.A. Ashmun, L.H. Shapiro, W. Arap, E. Ruoslahti, Aminopeptidase N is a receptor for tumor-homing peptides and a target for inhibiting angiogenesis, *Cancer Res.* 60 (2000) 722-727.
- [94] M. Buschle, M. Cotten, H. Kirlappos, K. Mechtler, G. Schaffner, W. Zauner, M.L. Birnstiel, E. Wagner, Receptor-mediated gene transfer into human T lymphocytes via binding of DNA/CD3 antibody particles to the CD3 T cell receptor complex, *Hum. Gene Ther.* 6 (1995) 753-761.

References

- [95] R.W. Paul, K.E. Weisser, A. Loomis, D.L. Sloane, D. LaFoe, E.M. Atkinson, R.W. Overell, Gene transfer using a novel fusion protein, GAL4/invasin, *Hum. Gene Ther.* 8 (1997) 1253-1262.
- [96] R. Kircheis, A. Kichler, G. Wallner, M. Kursa, M. Ogris, T. Felzmann, M. Buchberger, E. Wagner, Coupling of cell-binding ligands to polyethylenimine for targeted gene delivery, *Gene Ther.* 4 (1997) 409-418.
- [97] S. Koppu, Y.J. Oh, R. Edrada-Ebel, D.R. Blatchford, L. Tetley, R.J. Tate, C. Dufes, Tumor regression after systemic administration of a novel tumor-targeted gene delivery system carrying a therapeutic plasmid DNA, *J. Control. Release* 143 (2010) 215-221.
- [98] R.Q. Huang, Y.H. Qu, W.L. Ke, J.H. Zhu, Y.Y. Pei, C. Jiang, Efficient gene delivery targeted to the brain using a transferrin-conjugated polyethyleneglycol-modified polyamidoamine dendrimer, *FASEB J.* 21 (2007) 1117-1125.
- [99] E. Wagner, M. Zenke, M. Cotten, H. Beug, M.L. Birnstiel, Transferrin-polycation conjugates as carriers for DNA uptake into cells, *Proc. Natl. Acad. Sci. U.S.A.* 87 (1990) 3410-3414.
- [100] M. Zenke, P. Steinlein, E. Wagner, M. Cotten, H. Beug, M.L. Birnstiel, Receptor-mediated endocytosis of transferrin-polycation conjugates: an efficient way to introduce DNA into hematopoietic cells, *Proc. Natl. Acad. Sci. U.S.A.* 87 (1990) 3655-3659.
- [101] T. Blessing, M. Kursa, R. Holzhauser, R. Kircheis, E. Wagner, Different strategies for formation of pegylated EGF-conjugated PEI/DNA complexes for targeted gene delivery, *Bioconjug. Chem.* 12 (2001) 529-537.
- [102] T.K. Lee, J.S. Han, S.T. Fan, Z.D. Liang, P.K. Tian, J.R. Gu, I.O. Ng, Gene delivery using a receptor-mediated gene transfer system targeted to hepatocellular carcinoma cells, *Int. J. Cancer* 93 (2001) 393-400.
- [103] P. Kos, U. Lächelt, A. Herrmann, F.M. Mickler, M. Döblinger, D. He, A.K. Levačić, S. Morys, C. Bräuchle, E. Wagner, Histidine-rich stabilized polyplexes for cMet-directed tumor-targeted gene transfer, *Nanoscale* 7 (2015) 5350-5362.
- [104] M. Ogris, G. Walker, T. Blessing, R. Kircheis, M. Wolschek, E. Wagner, Tumor-targeted gene therapy: strategies for the preparation of ligand-polyethylene glycol-polyethylenimine/DNA complexes, *J. Control. Release* 91 (2003) 173-181.
- [105] A.M. Deshpande, A.A. Natu, N.P. Argade, Chemoselective Carbon–Carbon Coupling of Organocuprates with (Bromomethyl)methylmaleic Anhydride: Synthesis of Chaetomelic Acid A, *J. Org. Chem.* 63 (1998) 9557- 9558.
- [106] K. Maier, E. Wagner, Acid-labile traceless click linker for protein transduction, *J. Am. Chem. Soc.* 134 (2012) 10169-10173.
- [107] D. Schaffert, N. Badgujar, E. Wagner, Novel Fmoc-polyamino acids for solid-phase synthesis of defined polyamidoamines, *Org. Lett.* 13 (2011) 1586-1589.

References

- [108] H.B. Jonassen, L. Westerman, Inorganic Complex Compounds Containing Polydentate Groups. XIV. The Stability of the Complexes Formed between the Nickel(1) Ion and Tetraethylenepentamine, *J. Am. Chem. Soc.* 79 (1957) 4275-4279.
- [109] R.B. Merrifield, Solid Phase Peptide Synthesis. I. The Synthesis of a Tetrapeptide, *J. Am. Chem. Soc.* 85 (1963) 2149-2154.
- [110] Y. Liu, S. Xu, L. Teng, B. Yung, J. Zhu, H. Ding, R.J. Lee, Synthesis and evaluation of a novel lipophilic folate receptor targeting ligand, *Anticancer Res.* 31 (2011) 1521-1525.
- [111] A. Kichler, C. Leborgne, E. Coeytaux, O. Danos, Polyethylenimine-mediated gene delivery: a mechanistic study, *J. Gene Med.* 3 (2001) 135-144.
- [112] A. Akinc, M. Thomas, A.M. Klibanov, R. Langer, Exploring polyethylenimine-mediated DNA transfection and the proton sponge hypothesis, *J. Gene Med.* 7 (2005) 657-663.
- [113] M.L. Forrest, J.T. Koerber, D.W. Pack, A degradable polyethylenimine derivative with low toxicity for highly efficient gene delivery, *Bioconjug. Chem.* 14 (2003) 934-940.
- [114] M. Breunig, U. Lungwitz, R. Liebl, A. Goepferich, Breaking up the correlation between efficacy and toxicity for nonviral gene delivery, *Proc. Natl. Acad. Sci. U.S.A.* 104 (2007) 14454-14459.
- [115] V. Russ, M. Günther, A. Halama, M. Ogris, E. Wagner, Oligoethylenimine-grafted polypropylenimine dendrimers as degradable and biocompatible synthetic vectors for gene delivery, *J. Control. Release* 132 (2008) 131-140.
- [116] K. Miyata, M. Oba, M. Nakanishi, S. Fukushima, Y. Yamasaki, H. Koyama, N. Nishiyama, K. Kataoka, Polyplexes from poly(aspartamide) bearing 1,2-diaminoethane side chains induce pH-selective, endosomal membrane destabilization with amplified transfection and negligible cytotoxicity, *J. Am. Chem. Soc.* 130 (2008) 16287-16294.
- [117] C. Lin, C.J. Blaauboer, M.M. Timoneda, M.C. Lok, M. van Steenberg, W.E. Hennink, Z. Zhong, J. Feijen, J.F. Engbersen, Bioreducible poly(amido amine)s with oligoamine side chains: synthesis, characterization, and structural effects on gene delivery, *J. Control. Release* 126 (2008) 166-174.
- [118] H. Yu, V. Russ, E. Wagner, Influence of the molecular weight of bioreducible oligoethylenimine conjugates on the polyplex transfection properties, *AAPS J.* 11 (2009) 445-455.
- [119] H. Wei, L.R. Volpatti, D.L. Sellers, D.O. Maris, I.W. Andrews, A.S. Hemphill, L.W. Chan, D.S. Chu, P.J. Horner, S.H. Pun, Dual responsive, stabilized nanoparticles for efficient in vivo plasmid delivery, *Angew. Chem. Int. Ed. Engl.* 52 (2013) 5377-5381.

References

- [120] L. Hartmann, Polymers for Control Freaks: Sequence-Defined Poly(amidoamine)s and Their Biomedical Applications, *Macromol. Chem. Phys.* 212 (2011) 8-13.
- [121] U.K. Laemmli, Characterization of DNA condensates induced by poly(ethylene oxide) and polylysine, *Proc. Natl. Acad. Sci. U.S.A.* 72 (1975) 4288-4292.
- [122] E. Wagner, M. Ogris, W. Zauner, Polylysine-based transfection systems utilizing receptor-mediated delivery, *Adv. Drug Deliv. Rev.* 30 (1998) 97-113.
- [123] N.J. Baumhover, J.T. Duskey, S. Khargharia, C.W. White, S.T. Crowley, R.J. Allen, K.G. Rice, Structure-Activity Relationship of PEGylated Polylysine Peptides as Scavenger Receptor Inhibitors for Non-Viral Gene Delivery, *Mol. Pharm.* 12 (2015) 4321-4328.
- [124] E. Wagner, K. Zatloukal, M. Cotten, H. Kirlappos, K. Mechtler, D.T. Curiel, M.L. Birnstiel, Coupling of adenovirus to transferrin-polylysine/DNA complexes greatly enhances receptor-mediated gene delivery and expression of transfected genes, *Proc. Natl. Acad. Sci. U.S.A.* 89 (1992) 6099-6103.
- [125] E. Wagner, C. Plank, K. Zatloukal, M. Cotten, M.L. Birnstiel, Influenza virus hemagglutinin HA-2 N-terminal fusogenic peptides augment gene transfer by transferrin-polylysine-DNA complexes: toward a synthetic virus-like gene-transfer vehicle, *Proc. Natl. Acad. Sci. U.S.A.* 89 (1992) 7934-7938.
- [126] S. Uchida, K. Itaka, Q. Chen, K. Osada, T. Ishii, M.-A. Shibata, M. Harada-Shiba, K. Kataoka, PEGylated polyplex with optimized PEG shielding enhances gene introduction in lungs by minimizing inflammatory responses, *Mol. Ther.* 20 (2012) 1196-1203.
- [127] H. Dautzenberg, Polyelectrolyte complex formation in highly aggregating systems. 1. Effect of salt: polyelectrolyte complex formation in the presence of NaCl, *Macromolecules* 30 (1997) 7810-7815.
- [128] F.J. Verbaan, C. Oussoren, I.M. van Dam, Y. Takakura, M. Hashida, D.J. Crommelin, W.E. Hennink, G. Storm, The fate of poly(2-dimethyl amino ethyl)methacrylate-based polyplexes after intravenous administration, *Int. J. Pharm.* 214 (2001) 99-101.
- [129] J. Sudimack, R.J. Lee, Targeted drug delivery via the folate receptor, *Adv. Drug Deliv. Rev.* 41 (2000) 147-162.
- [130] G. Toffoli, C. Cernigoi, A. Russo, A. Gallo, M. Bagnoli, M. Boiocchi, Overexpression of folate binding protein in ovarian cancers, *Int. J. Cancer* 74 (1997) 193-198.
- [131] P.S. Low, W.A. Henne, D.D. Doorneweerd, Discovery and development of folic-acid-based receptor targeting for imaging and therapy of cancer and inflammatory diseases, *Acc. Chem. Res.* 41 (2008) 120-129.

References

- [132] D. He, K. Müller, A. Krhac Levacic, P. Kos, U. Lächelt, E. Wagner, Combinatorial optimization of sequence-defined oligo (ethanamino) amides for folate receptor-targeted pDNA and siRNA delivery, *Bioconjug. Chem.* (2016).
- [133] C. Dohmen, D. Edinger, T. Fröhlich, L. Schreiner, U. Lächelt, C. Troiber, J. Rädler, P. Hadwiger, H.-P. Vornlocher, E. Wagner, Nanosized multifunctional polyplexes for receptor-mediated siRNA delivery, *ACS Nano* 6 (2012) 5198-5208.
- [134] S.D. Weitman, R.H. Lark, L.R. Coney, D.W. Fort, V. Frasca, V.R. Zurawski, Jr., B.A. Kamen, Distribution of the folate receptor GP38 in normal and malignant cell lines and tissues, *Cancer Res.* 52 (1992) 3396-3401.
- [135] H.S. Choi, W. Liu, F. Liu, K. Nasr, P. Misra, M.G. Bawendi, J.V. Frangioni, Design considerations for tumour-targeted nanoparticles, *Nat. Nanotechnol.* 5 (2010) 42-47.
- [136] F. Yuan, M. Dellian, D. Fukumura, M. Leunig, D.A. Berk, V.P. Torchilin, R.K. Jain, Vascular permeability in a human tumor xenograft: molecular size dependence and cutoff size, *Cancer Res.* 55 (1995) 3752-3756.
- [137] B. Smrekar, L. Wightman, M.F. Wolschek, C. Lichtenberger, R. Ruzicka, M. Ogris, W. Rödl, M. Kurasa, E. Wagner, R. Kircheis, Tissue-dependent factors affect gene delivery to tumors in vivo, *Gene Ther.* 10 (2003) 1079-1088.
- [138] H. Cabral, Y. Matsumoto, K. Mizuno, Q. Chen, M. Murakami, M. Kimura, Y. Terada, M. Kano, K. Miyazono, M. Uesaka, Accumulation of sub-100 nm polymeric micelles in poorly permeable tumours depends on size, *Nat. Nanotechnol.* 6 (2011) 815-823.
- [139] J. Rejman, V. Oberle, I.S. Zuhorn, D. Hoekstra, Size-dependent internalization of particles via the pathways of clathrin- and caveolae-mediated endocytosis, *Biochem. J.* 377 (2004) 159-169.
- [140] P. Midoux, M. Monsigny, Efficient gene transfer by histidylated polylysine/pDNA complexes, *Bioconjug. Chem.* 10 (1999) 406-411.
- [141] K. Itaka, A. Harada, Y. Yamasaki, K. Nakamura, H. Kawaguchi, K. Kataoka, In situ single cell observation by fluorescence resonance energy transfer reveals fast intra-cytoplasmic delivery and easy release of plasmid DNA complexed with linear polyethylenimine, *J. Gene Med.* 6 (2004) 76-84.
- [142] M. Ramamoorth, A. Narvekar, Non viral vectors in gene therapy-an overview, *J. Clin. Diagn. Res.* 9 (2015) GE01.
- [143] V. Šubr, C. Konák, R. Laga, K. Ulbrich, Coating of DNA/poly (L-lysine) complexes by covalent attachment of poly [N-(2-hydroxypropyl) methacrylamide], *Biomacromolecules* 7 (2006) 122-130.

References

- [144] C.M. Ward, M. Pechar, D. Oupicky, K. Ulbrich, L.W. Seymour, Modification of pLL/DNA complexes with a multivalent hydrophilic polymer permits folate-mediated targeting in vitro and prolonged plasma circulation in vivo, *J. Gene Med.* 4 (2002) 536-547.
- [145] A.E. Nel, L. Mädler, D. Velegol, T. Xia, E.M. Hoek, P. Somasundaran, F. Klaessig, V. Castranova, M. Thompson, Understanding biophysicochemical interactions at the nano–bio interface, *Nat. Mater.* 8 (2009) 543-557.
- [146] C. Masson, M. Garinot, N. Mignet, B. Wetzler, P. Mailhe, D. Scherman, M. Bessodes, pH-sensitive PEG lipids containing orthoester linkers: new potential tools for nonviral gene delivery, *J. Control. Release* 99 (2004) 423-434.
- [147] K. Müller, E. Kessel, P.M. Klein, M. Hoehn, E. Wagner, Post-PEGylation of siRNA lipo-oligoamino amide polyplexes using tetra-glutamylated folic acid as ligand for receptor-targeted delivery, *Mol. Pharm.* (2016) DOI: 10.1021/acs.molpharmaceut.6b00102.
- [148] S.K. Jones, V. Lizzio, O.M. Merkel, Folate Receptor Targeted Delivery of siRNA and Paclitaxel to Ovarian Cancer Cells via Folate Conjugated Triblock Copolymer to Overcome TLR4 Driven Chemotherapy Resistance, *Biomacromolecules* 17 (2015) 76-87.
- [149] M. Barz, F. Canal, K. Koynov, R. Zentel, M.a.J. Vicent, Synthesis and in vitro evaluation of defined HPMA folate conjugates: influence of aggregation on folate receptor (FR) mediated cellular uptake, *Biomacromolecules* 11 (2010) 2274-2282.

Appendix

7. Appendix

7.1. Abbreviations

AA	Amino acid
ACN	Acetonitrile
APS	Ammonium persulfate
AzMMMan	3-(azidomethyl)-4-methyl-2,5-furandione
Boc	<i>tert</i> -Butoxycarbonyl protecting group
BrMMMan	3-(bromomethyl)-4-methyl-2,5-furandione
DAPI	4',6-diamidino-2-phenylindole
DBCO	Dibenzocyclooctyl
DBCO-NH ₂	3-amino-1-(11,12-didehydrodibenzo[b,f]azocin-5(6H)-yl)propan-1-one
DBU	1,8-diazabicyclo[5.4.0]undec-7-en
DCC	<i>N,N'</i> -Dicyclohexylcarbodiimide
DCM	Dichloromethane
DMMAN	2,3-dimethylmaleic anhydride
DiBrMMMan	3,4-bis(bromomethyl)furan-2,5-dione
DIPEA	<i>N,N</i> -Diisopropylethylamine
DLS	Dynamic light scattering
DMEM	Dulbecco's Modified Eagle's Medium - high glucose
DMF	<i>N,N</i> -Dimethylformamide
DMSO	Dimethyl sulfoxide
EDTA	Ethylenediaminetetraacetic acid
EtBr	Ethidium bromide
EtOH	Ethanol
eq	Equivalent
FACS	Fluorescence-activated cell sorting
FCS	Fetal calf serum
Fmoc	Fluorenylmethoxycarbonyl protecting group
FolA	Folic acid
FR	Folic acid receptor
HBG	Hepes-buffered glucose
HBTU	2-(1H-benzotriazole-1-yl)-1,1,3,3-tetramethyluronium hexafluorophosphate
HCl	Hydrochloric acid
HEPES	<i>N</i> -(2-hydroxyethyl)piperazine- <i>N'</i> -(2-ethanesulfonic acid)
H ₂ O	water
HOBt	1-hydroxybenzotriazole
HPLC	High-performance liquid chromatography
HPMA	<i>N</i> -(2-Hydroxypropyl)methacrylamide
KCN	Potassium cyanide
LPEI	Linear polyethylenimine
LSM	Laser-scanning microscopy
MeOH	Methanol
M _n	Number-average molecular weight
MTBE	Methyl <i>tert</i> -butylether
MTT	3-(4,5-dimethylthiazol-2-yl)-2,5-diphenyltetrazolium bromide

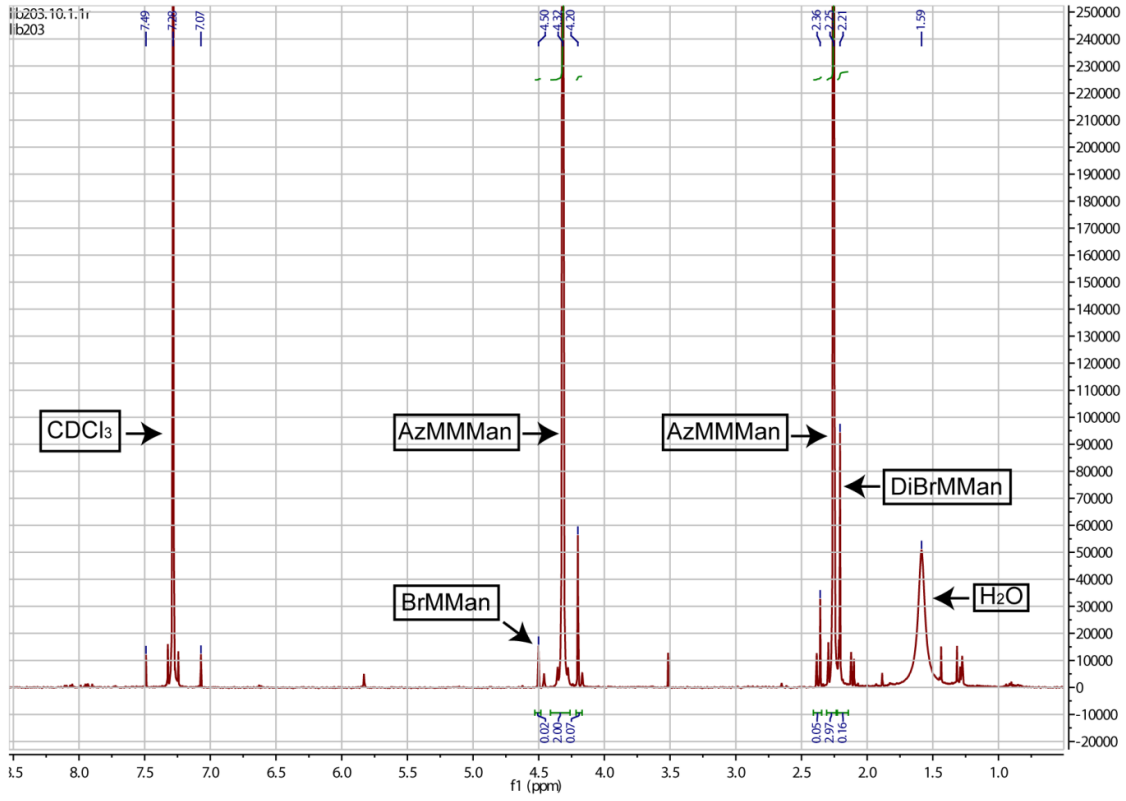
Appendix

Mw	Weight-average molecular weight
N/P	(Protonatable) nitrogen to phosphates ratio
Na ₂ SO ₄	Sodium sulfate
NaCl	Sodium chloride
NaOH	Sodium hydroxide
NBS	<i>N</i> -Bromosuccinimide
NHS	<i>N</i> -Hydroxysuccinimide
NMP	<i>N</i> -Methyl-2-pyrrolidone
NMR	Nuclear magnetic resonance
OPSS	Ortho-pyridyl disulfide
PBS	Phosphate-buffered saline
pCMVL	Plasmid encoding for firefly luciferase under the control of the cytomegalie virus (CMV) promoter
pDNA	Plasmid DNA
PEG	Polyethylene glycol
PEHA	Pentaethylenhexamine
PyBOP	Benzotriazol-1-yloxy-tripyrrolidinophosphonium hexafluorophosphate
RNA	Ribonucleic acid
RT	Room temperature
SDS	Sodium dodecyl sulfate
SEC	Size-exclusion chromatography
SPH	Succinyl-pentaethylene hexamine
SPPS	Solid-phase assisted peptide synthesis
TEMED	<i>N,N,N',N'</i> -Tetramethylethylenediamin
TFA	Trifluoroacetic acid
THF	Tetrahydrofuran
TIS	Triisopropylsilane
Tris	Tris(hydroxymethyl)aminomethane
TT	Thiazolidine-2-thione

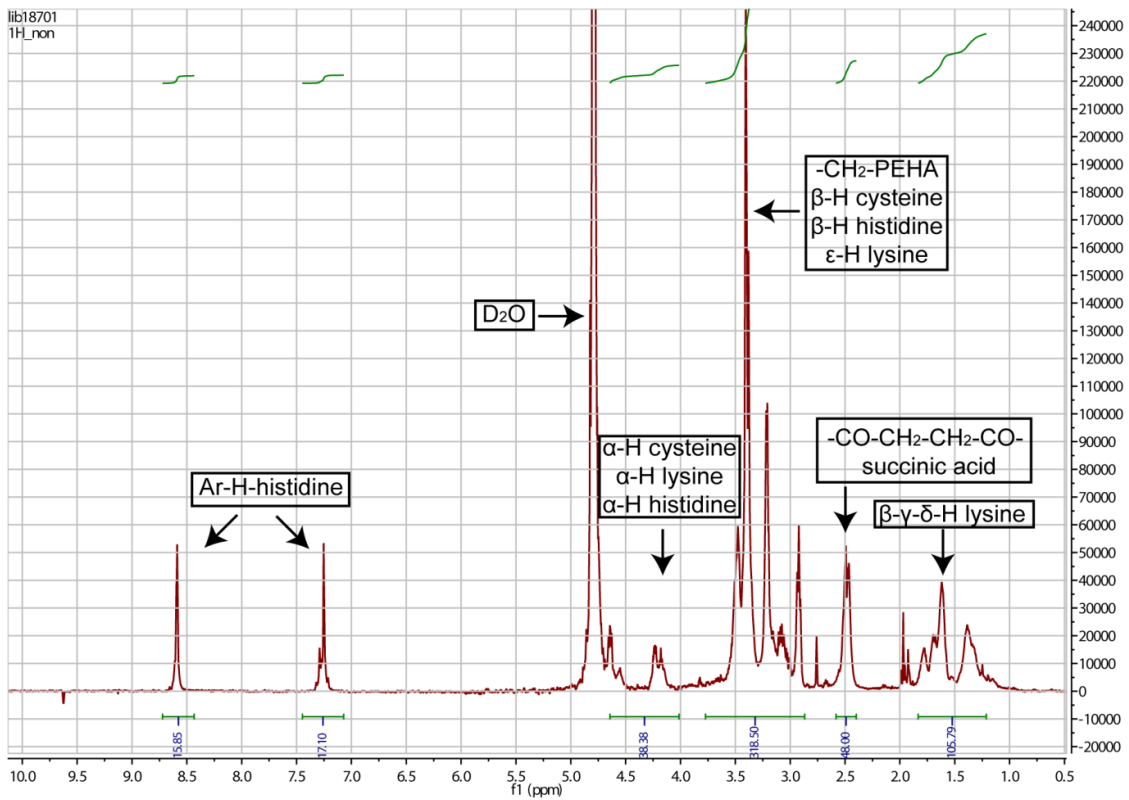
Appendix

7.2. Analytical data

$^1\text{H-NMR}$ spectra of the pH-sensitive linker AzMMMan (400MHz; CDCl_3)



$^1\text{H-NMR}$ spectra of key oligomer 784 (400MHz; D_2O)



Appendix

7.3. Summarized spectral data

Oligomer 497 – Sequence C→N: AK[K(SPH₃-C)₂]₂

¹H-NMR (400 MHz, D₂O) δ= 1.2-1.5 (m, 21H, β-H alanine, β-γ-δ-H lysine), 2.3-2.7 (m, 48H, -CO-CH₂-CH₂-CO-succinic acid), 2.8-3.9 (m, 254H, -CH₂-PEHA, β-H cysteine, ε-H lysine), 4.0-4.3 (m, 8H, α-H alanine, α-H cysteine, α-H lysine)

Oligomer 606– Sequence C→N: AK[HK[(H-SPH)₃-HC]₂]₂

¹H-NMR (400 MHz, D₂O) δ= 1.2-1.5 (m, 21H, β-H alanine, β-γ-δ-H lysine), 2.3-2.7 (m, 48H, -CO-CH₂-CH₂-CO-succinic acid), 2.8-3.9 (m, 290H, -CH₂-PEHA, β-H cysteine, β-H histidine, ε-H lysine), 4.0-4.3 (m, 8H, α-H alanine, α-H cysteine, α-H lysine), 4.6-4.7 (m, 18H α-H histidine), 7.0-7.5 (s, 18H, Ar-H-histidine), 8.59 (s, 18H, Ar-H histidine)

Oligomer 748– Sequence C→N: AK[HK[(H-SPH)₃-HKC]₂]₂

¹H-NMR (400 MHz, D₂O) δ= 1.2-1.5 (m, 45H, β-H alanine, β-γ-δ-H lysine), 2.3-2.7 (m, 48H, -CO-CH₂-CH₂-CO-succinic acid), 2.8-3.9 (m, 298H, -CH₂-PEHA, β-H cysteine, β-H histidine, ε-H lysine), 4.0-4.7 (m, 30H, α-H alanine, α-H cysteine, α-H lysine, α-H histidine), 7.0-7.5 (s, 18H, Ar-H-histidine), 8.59 (s, 18H, Ar-H histidine)

Oligomer 749– Sequence C→N: AK[HK[(H-SPH)₃-HKKC]₂]₂

¹H-NMR (400 MHz, D₂O) δ= 1.2-1.5 (m, 69H, β-H alanine, β-γ-δ-H lysine), 2.3-2.7 (m, 48H, -CO-CH₂-CH₂-CO-succinic acid), 2.8-3.9 (m, 306H, -CH₂-PEHA, β-H cysteine, β-H histidine, ε-H lysine), 4.0-4.7 (m, 34H, α-H alanine, α-H cysteine, α-H lysine, α-H histidine), 7.0-7.5 (s, 18H, Ar-H-histidine), 8.59 (s, 18H, Ar-H histidine)

Appendix

Oligomer 784 – Sequence C→N: KK[HK[(H-SPH-K)₃-HC]₂]₂

¹H-NMR (400 MHz, D₂O) δ= 1.2-1.5 (m, 96H, β-γ-δ-H lysine), 2.4-2.6 (m, 48H, -CO-CH₂-CH₂-CO-succinic acid), 2.8-3.9 (m, 316H, -CH₂-PEHA, β-H cysteine, β-H histidine, ε-H lysine), 4.0-4.7 (m, 38H, α-H cysteine, α-H lysine, α-H histidine) 7.253 (s, 18H, Ar-H-histidine), 8.588 (s, 18H, Ar-H histidine)

Oligomer 785 – Sequence C→N: KK[HK[(H-SPH-K)₄-HC]₂]₂

¹H-NMR (400 MHz, D₂O) δ= 1.2-1.5 (m, 120H, β-γ-δ-H lysine), 2.4-2.6 (m, 64H, -CO-CH₂-CH₂-CO-succinic acid), 2.8-3.9 (m, 412H, -CH₂-PEHA, β-H cysteine, β-H histidine, ε-H lysine), 4.0-4.7 (m, 46H, α-H cysteine, α-H lysine, α-H histidine) 7.253 (s, 22H, Ar-H-histidine), 8.588 (s, 22H, Ar-H histidine)

Oligomer 797 – Sequence C→N: KK[HK(H-SPH-K-H-H-K-H-H-SPH-K-H-SPH-K-H-C)₂]₂

¹H-NMR (400 MHz, D₂O) δ= 1.2-1.5 (m, 120H, β-γ-δ-H lysine), 2.4-2.6 (m, 48H, -CO-CH₂-CH₂-CO-succinic acid), 2.8-3.9 (m, 348H, -CH₂-PEHA, β-H cysteine, β-H histidine, ε-H lysine), 4.0-4.7 (m, 54H, α-H cysteine, α-H lysine, α-H histidine) 7.253 (s, 30H, Ar-H-histidine), 8.588 (s, 30H, Ar-H histidine)

Oligomer 935 – Sequence C→N: KK[K[(SPH-K)₃-C]₂]₂

¹H-NMR (400 MHz, D₂O) δ= 1.2-1.5 (m, 96H, β-γ-δ-H lysine), 2.4-2.6 (m, 48H, -CO-CH₂-CH₂-CO-succinic acid), 2.8-3.9 (m, 280H, -CH₂-PEHA, β-H cysteine, β-H histidine, ε-H lysine), 4.0-4.7 (m, 20H, α-H cysteine, α-H lysine)

Appendix

7.4. Publication

Linda Beckert, Libor Kostka, Eva Kessel, Ana Krhac Levacic, Hana Kostkova, Tomas Etrych, Ulrich Lächelt, Ernst Wagner: "Acid-labile pHPMA modification of four-arm oligoaminoamide pDNA polyplexes balances shielding and gene transfer activity *in vitro* and *in vivo*." Eur. J. Pharm. Biopharm., doi:10.1016/j.ejpb.2016.05.019 (2016)

Linda Beckert, Alexander Philipp and Ernst Wagner: "Receptor-Targeted Polyplexes for pDNA and siRNA delivery."; Gene and Cell Therapy Forth Edition; page 287-314

7.5. Poster presentation

Linda Beckert und Ruth Röder: " Traceless pH-sensitive coating of viral and non-viral vectors." Interact Munich 2015, Poster prize (2nd place)

Libor Kostka, Linda Beckert, Ana Krhac Levacic, Tomas Etrych, Ernst Wagner: "Traceless pH sensitive coating of polyplexes prepared from well-defined polycations."; SIPCD 2014

Linda Beckert und Ruth Röder: " Traceless pH-sensitive coating of viral and non-viral vectors." 2014 CeNS/SFB workshop, Venice, Italy

Acknowledgements

8. Acknowledgements

The presented thesis was prepared under the supervision of Prof. Dr. Ernst Wagner at the facilities at the Department of Pharmacy, Pharmaceutical Biotechnology at the Ludwig-Maximilians-University in Munich, Germany.

Foremost, I am grateful to my doctoral supervisor Professor Ernst Wagner for the possibility to join his research group and for his professional guidance.

My sincere gratitude is expressed to Dr. Libor Kostka from the Academy of Sciences of the Czech Republic, Prague, Czech Republic, for the very close corporation, scientific input, personal support and proof reading of the publication.

I would also like to express my gratitude to Ruth for spending countless hours with me in the lab to synthesize the AzMMMan. I really appreciated her scientific as well as personal support. Furthermore, I want to thank Uli for very helpful advices concerning scientific work, proof reading of the manuscript and his enthusiasm and never-fading encouragement in my work. Additionally, I would like to thank Eva for conducting animal experiences. Many thanks also to Dr. Lars Allmendinger for his excellent advice and support in NMR analysis. I also want to thank Ursula, Anna, Markus, Miriam and Olga for their help in keeping everything running. In that concern, my special thanks go to Wolfgang for solving any imaginable technical issue/problem in the lab and for fixing my computer.

My deepest gratitude goes to Annika for a great time, the enrichment of my lunch as well as coffee breaks and the best office atmosphere ever. Additionally, I would like to express my deepest thankfulness to Joana for introducing me into scientific writing and being the best reviewer I can imagine. Furthermore, I would like to thank Andi for always having an open ear and helpful advices.

Finally, I would like to thank my family for their continuously encouragement and their trust and support during all periods of my life. A special thanks goes to my friends for the fun and laughs we share. Last but not least, thank you Kenneth, for your great support and your love!